CO_2 STORAGE CAPACITY ESTIMATION IN DEPLETED GAS RESERVOIRS WITH WATER DRIVE USING MATERIAL BALANCE AND CONVECTION DIFFUSION MODEL

A Thesis

by

SETIAWAN

Submitted to the Office of Graduate and Professional Studies of
Texas A&M University
in partial fulfillment of the requirements for the degree of

MASTER OF SCIENCE

Chair of Committee,	Maria A. Barrufet
Committee Members,	Jenn-Tai Liang
	Thomas A. Blasingame
Head of Department,	Jeff Spath

December 2019

Major Subject: Petroleum Engineering

ABSTRACT

CO_2 sequestration in depleted gas reservoir is an option to reduce the CO_2 emissions. It is specifically good because of data availability, safe trap mechanism, and high ratio of CO_2 storage capacity per pore volume. One method to estimate the CO_2 storage capacity is using a material balance model. However, previous studies have not included the effect of CO_2 solubility in water in the calculations. It is an important variable to consider because CO_2 dissolved in water changes water properties affecting the estimation especially for gas reservoirs with water drive.

In this study, the effect of CO_2 solubility in water to the CO_2 storage capacity in depleted gas reservoir with water drive is analyzed. A method to estimate the CO_2 storage capacity considering the CO_2 solubility in water is developed. The method is an iterative method based on material balance model which is divided into production and injection stages, Van Everdingen-Hurst aquifer model, and a modified convection diffusion model. The CO_2 storage capacities are estimated using conventional material balance and this iterative method. The results are compared to analyze the effect of CO_2 solubility in water.

Generally, CO_2 solubility in water changes the water properties which makes the storage capacity lower compared to the result from conventional material balance estimation. The difference between the results are a function of several variables including aquifer and reservoir properties, such as: radial aquifer-reservoir ratio; aquifer permeability; temperature; salinity, and injection rate. Moreover, because CO_2 dissolves in water, some of the CO_2 is stored in the aquifer through convection and diffusion. The

amount of CO_2 stored in the aquifer is far smaller than the amount of CO_2 stored in the gas reservoir, but the absolute value is still significant.

I developed a method to estimate CO_2 storage capacity in depleted gas reservoir with water drive while considering CO_2 solubility in water. It is important because it may help avoiding storage capacity over-estimation by the conventional method. The estimation is also one of important parameters necessary to design CO_2 storage facilities.

DEDICATION

This thesis is dedicated to:

My mother, *Metta Carolin*

My father, *Gunady Setyanto*

My brother, *Vonny Anggelina*

ACKNOWLEDGEMENTS

I would like to thank my committee chair, Dr. Maria Barrufet, and my committee members, Dr. Jenn-Tai Liang, and Dr. Thomas Blasingame, for their guidance and support throughout the course of this research.

Thanks also go to my friends and colleagues and the department faculty and staff for making my time at Texas A&M University a great experience. I would also like to thank Pribadi Agung Sulistyadi, Farid Bakti, Tubagus Maqdisi, Aldo, Johnsen Kosman, and Rayten Tiano for being such great roommates during my entire stay in College Station.

Finally, thanks to my mother, father, and sister for their encouragement.

CONTRIBUTORS AND FUNDING SOURCES

Contributors

This work was supervised by a thesis committee consisting of Professor Maria Barrufet as research advisor and committee chair and Professor Jenn-Tai Liang of the Department of Petroleum Engineering and Professor Thomas Blasingame of the Department of Petroleum Engineering and Geology.

All work conducted for the thesis was completed by the student independently.

Funding Sources

Graduate study was supported by a scholarship from Indonesia Endowment Fund for Education.

This works and its contents are solely the responsibility of the authors and do not necessarily represent the official views of Indonesia Ministry of Finance.

NOMENCLATURE

B_g	Gas formation volume factor, ft^3/SCF
B_{g_i}	Initial gas formation volume factor, ft^3/SCF
B_w	Water formation volume factor, bbl/STB
c	Compressibility, psi^{-1}
c_e	Total compressibility, psi^{-1}
c_f	Formation compressibility, psi^{-1}
c_w	Water compressibility, psi^{-1}
C_i	Mass concentration of component 'i'
C_{I_i}	Mass concentration of component 'i' in reservoir
C_{J_i}	Mass concentration of component 'i' in injected fluid
$C_{J_{CO_2@res}}$	Mass concentration of CO_2 in gas reservoir
C_{wi}	Coefficient to calculate cumulative water influx from Van Everdingen-Hurst solution, STB/psi
$C^j_{CO_2}$	CO_2 concentration at j-th iteration step
G	Original gas in place, SCF
G_{inj}	Cumulative injected gas, SCF
G_p	Cumulative produced gas, SCF
$G_{p,abd}$	Cumulative produced gas at abandonment condition, SCF
k	Permeability, mD

K_l	Longitudinal dispersion coefficient, ft^2/s
L	Reservoir length, ft
N_{pe}	Peclet number
p	Pressure, psia
p_D	Dimensionless pressure
p_i	Initial reservoir pressure, psia
$p_{r_{owc}}$	Pressure at boundary between reservoir and aquifer, psia
p_{sc}	Pressure at standard condition, psia
$\bar{p}$	Average reservoir pressure, psia
$\bar{p}^j$	Average reservoir pressure at j-th iteration step, psia
Δp	Pressure difference, psi
Q	Fluid flow rate, ft^3/day
r	Radius, ft
r_D	Dimensionless radius
r_{owc}	Radius of boundary between reservoir and aquifer, ft
RF	Recovery factor, fraction
R_{s_w}	Gas solubility in water, SCF/STB
$R_{s_{CO_2}}$	CO_2 solubility in water, SCF/STB
S_{w_i}	Initial water saturation
t	Time or duration, day
t_D	Dimensionless time for Material Balance model

t_D^*	Dimensionless time for Convection Diffusion model
$t_{D,final}^*$	Dimensionless time for Modified Convection Diffusion model at final pressure after injection stage
$t_{D_n}^*$	Dimensionless time for Modified Convection Diffusion model at step n-th
T	Temperature, ^oF
T_{sc}	Temperature at standard condition, ^oF
u	Fluid velocity, ft/s
V_g	Gas reservoir volume, ft^3
V_{g_i}	Initial gas reservoir volume, ft^3
V_{aq}	Aquifer volume, bbl
$V_{CO_2@aq}$	CO_2 volume in aquifer, SCF
$V_{CO_2@res}$	CO_2 volume in gas reservoir, SCF
$V_{CO_2@res}^g$	CO_2 volume as gas phase in gas reservoir, SCF
$V_{CO_2@res}^l$	CO_2 volume dissolved in water in gas reservoir, SCF
V_{DP}	Dykstra-Parson variable
W_e	Water influx, bbl
W_e^j	Water influx at j-th iteration step, bbl
W_p	Cumulative produced water, STB
x	Position, ft
x_C	Molar ratio of dissolved CO_2 in water

x_{CS}	Molar ratio of dissolved CO_2 in fully saturated water
z	Gas deviation factor
z_i	Initial gas deviation factor
μ	Fluid viscosity, cP
μ_{w,CO_2}	Water with dissolved CO_2 viscosity, cP
μ_w	Water viscosity, cP
ϕ	Formation porosity
ρ	Fluid density, lb/ft^3
ρ_{aq}	Aquifer fluid density, lb/ft^3
$\rho_{CO_2@sc}$	CO_2 density at standard condition, lb/ft^3

TABLE OF CONTENTS

Page

Page

LIST OF FIGURES

Page

Page

LIST OF TABLES

Page

Page

CHAPTER I

INTRODUCTION

Background

Global warming, which increased the average earth's surface temperature by 0.85^{o}C between 1880 and 2012, is dominantly caused by human influences (IPCC, 2013). The increasing temperature has profound effects to the natural systems, including droughts, floods, extreme weathers, rising sea levels, and biodiversity loss which also impact human populations (IPCC, 2012) (IPCC, 2014) (Mysiak, et al., 2016). Of all the greenhouse gases, CO_2 gives the largest contribution from human activities (IPCC, 2005).

Several options that can be made to reduce the level of CO_2 emissions including: reducing the use of fossil fuel; using less carbon-intensive fuel; replacing fossil fuel technologies with near-zero-carbon alternatives; enhancing atmospheric carbon absorption by natural systems; and carbon capture and storage (IPCC, 2005). Carbon capture and storage is done by capturing the carbon emissions from fuel combustion or industrial processes and store it away from the atmosphere (IPCC, 2005). The capture approach is more appropriate for large sources than small dispersed sources, and the storage can be in depleted oil and gas fields, deep saline formations, and in the ocean (IPCC, 2001). The technology is influenced by several factors such as relative cost, storage time, CO_2 transport, environmental concerns, and the acceptability of this approach (IPCC, 2005).

As mentioned before, CO_2 storage in depleted gas reservoir is one of the options. The reservoir is a good choice for CO_2 sequestration because of its data availability and safety (Bachu, et al., 2007) (Mamora & Seo, 2002) (Oldenburg & Benson, 2002). It is also favorable because of the high ratio of CO_2 mass storage capacity per pore volume due to its high overall compressibility, which can reach 13 times higher storage capacity compared to an aquifer with the same pore volume (Barrufet, et al., 2010).

The estimation of CO_2 storage capacity in oil and gas reservoirs is straightforward because of better reservoir characterization. The capacity is estimated on the basis of reservoir properties and fluid characteristics (Bachu, et al., 2007). Material balance is one of methods that can be used to estimate the storage capacity with or without water drive (Tseng, et al., 2012) (Bachu & Shaw, 2003) (Lawal & Frailey, 2002) (Sobers & Frailey, 2004). Reservoirs with water drive, depending on the strength of the aquifers, have reduced theoretical storage capacities because of the water invasions (Bachu & Shaw, 2003). Their study showed that it is important to model the water influx since it is essential to estimate the volume of water that occupies the reservoir at the end of the injection period. However, the models used in the previous studies did not incorporate the CO_2 solubility in the water in the estimation.

The CO_2 solubility in water will change the water properties, so it is important to investigate whether the underlying assumptions following the water influx model are still valid. The next step is to incorporate the solubility into the aquifer model and material balance model during the CO_2 injection period. Moreover, taking diffusion into account, the storage capacity of the reservoirs and aquifer can be differentiated.

Research Objectives

The main objective of this research is to estimate the CO_2 storage capacity in a depleted gas reservoir with water drive while incorporating the changing water properties due to CO_2 solubility in water. This is done using material balance model with Van Everdingen-Hurst aquifer model and convection diffusion model including the solubility of CO_2 in pure water and saline aquifer as a function of pressure and temperature. Specific tasks of this research included:

- Modifying convection diffusion model to estimate the amount of dissolved CO_2 in the aquifer with changing pressure and composition
- Modifying the material balance model for production and injection stages.
- Incorporating changing water properties due to CO_2 solubility in the aquifer model
- Developing an algorithm to combine the models to estimate the CO_2 storage capacity in gas reservoir and aquifer.

Outline of the Thesis

This thesis starts with Introduction in the first chapter. The introduction chapter includes background to this thesis, and research objectives.

The second chapter presents the concepts and fundamentals used in this thesis. It includes the derivations and assumptions of the material balance model, Van Everdingen-Hurst aquifer model and the convection diffusion model.

The third chapter presents the methodology used to achieve the research objectives. The models discussed in the second chapter are modified and the modification is described in this chapter.

The fourth chapter shows the results of the calculation using the modified models and algorithms introduced in chapter three. The results are discussed in this chapter. Finally, the fifth chapter contains conclusions and recommendations for future research based on discussion in chapter four.

CHAPTER II

LITERATURE REVIEW

Material Balance for CO_2 Storage

Material balance model for dry gas is an equation that tracks down initial gas reservoir mass and gas reservoir mass at certain pressures with an assumption that the temperature is constant.

The initial gas reservoir volume is defined as:

$$V_{g_i} = GB_{g_i} \tag{1}$$

While the general gas reservoir volume at certain pressure includes water produced, gas injection, and water influx is defined as:

$$V_g = \left(G - G_p + G_{inj}\right)B_g - W_p R_{s_w} B_g - 5.615\left(W_p B_w - W_e\right) \tag{2}$$

At the right-hand side, the $G - G_p + G_{inj}$ terms are current gas in place, and the B_g is a function of current pressure, temperature, and composition. The second term, $W_p R_{s_w}$, is the produced gas which is dissolved in water. The third term, $5.615\left(W_p B_w - W_e\right)$, is the amount of water currently occupying the pore space in reservoir, and W_e is water influx, which is the amount of water invading the reservoir from the aquifer.

Assuming constant pore and water compressibility, the change of pore volume filled by gas is:

$$\frac{V_g}{V_{g_i}} = \frac{e^{c_f \Delta p} - S_{w_i}\, e^{-(c_w \Delta p)}}{1 - S_{w_i}} \tag{3}$$

Using Taylor series, equation 3 can be approximated by:

$$\frac{V_g}{V_{g_i}} \approx 1 - \left(\frac{c_f + S_{w_i} c_w}{1 - S_{w_i}} \Delta p\right) = 1 - (c_e \Delta p) \tag{4}$$

Substituting equation 4 into equation 1 and 2, the general material balance for dry gas can be made (Dake, 1978) (Craft & Hawkins, 1991):

$$G B_{g_i}\big(1 - (c_e \Delta p)\big) = \big(G - G_p + G_{inj}\big) B_g - W_p R_{s_w} B_g - 5.615\big(W_p B_w - W_e\big) \tag{5}$$

The gas formation volume factor can be expressed as:

$$B_g = \frac{p_{sc}}{T_{sc}} \frac{z}{p} T \tag{6}$$

Substituting Equation 6 into Equation 5 and re-arranging it results in material balance equation in p/z form.

$$\frac{\bar{p}}{z}[1 - c_e(p_i - \bar{p})] = \frac{p_i}{z_i} - \frac{p_i}{z_i} \frac{1}{G}\left[G_p - G_{inj} + W_p R_{s_w} + 5.615 \frac{1}{B_g}\big[W_p B_w - W_e\big]\right] \tag{7}$$

Material balance model has been used to study the effect of aquifers to the CO_2 storage capacity. A study of estimating CO_2 storage capacity at gas and oil reservoirs at Alberta has been done (Bachu & Shaw, 2003). Their study showed that as hydrocarbons are produced, the water from aquifer permeates the reservoir which occupies the pore space and may not be available for the injected CO_2. Additional capacity may eventually become available if the reservoir pressure is allowed to increase to more than the original reservoir pressure. However, it may or may not be allowed or possible. Their study also states that the storage capacity is affected by the strength of the aquifer. For strong aquifer support, the average storage capacity is reduced by 28% for gas reservoir and 60% for oil

reservoir compared to the theoretical capacity. On the other hand, for weak aquifer support, the storage capacity of both oil and gas reservoirs is similar to the theoretical capacity (Bachu & Shaw, 2003). The theoretical capacity assumes that all of the pore spaces left by the produced gas, are filled with CO_2, and is expressed as (Bachu & Shaw, 2003):

$$M_{CO_2} = RF\left(Ah\phi\left(1 - S_{w_i}\right)\right)\rho_{CO2@sc} \tag{8}$$

Material balance model has also been used with Fetkovich aquifer model to analyze storage capacity of depleted gas reservoir with and without water drive (Tseng, et al., 2012). Their study corroborates the results of Bachu et al.'s study. Their study states that for a gas reservoir with water drive, the amount of CO_2 injected to increase the reservoir pressure back to the original pressure is less than the amount of produced gas and that the single effective capacity coefficient for gas reservoir with water drive is less than one depending on the strength of aquifer. On the other hand, for gas reservoir without water drive, the amount of CO_2 injected to increase the reservoir pressure back to the original pressure is more than the amount of produced gas, and that the single effective capacity coefficient is one. The single capacity coefficient is a multiplier to the theoretical storage capacity which is used in Bachu et al.'s study to calculate the reduced storage capacity due to water influx.

Van Everdingen-Hurst Aquifer Model

To estimate the water influx in the material balance, an independent model is required. The model is referred to as aquifer model. The aquifer model that will be used is Van Everdingen-Hurst Model. It is an unsteady-state model for edge-water drive. Van Everdingen and Hurst started with radial flow Darcy's Equation (Van Everdingen & Hurst, 1949):

$$v = \frac{k}{\mu}\frac{\partial P}{\partial r} \tag{9}$$

The difference in weight of fluid flowing past a surface with distance ∂r from another surface (Figure 1) is

$$\frac{2\pi k}{\mu}\frac{\partial\left(\rho r\frac{\partial P}{\partial r}\right)}{\partial r}\partial r \tag{10}$$

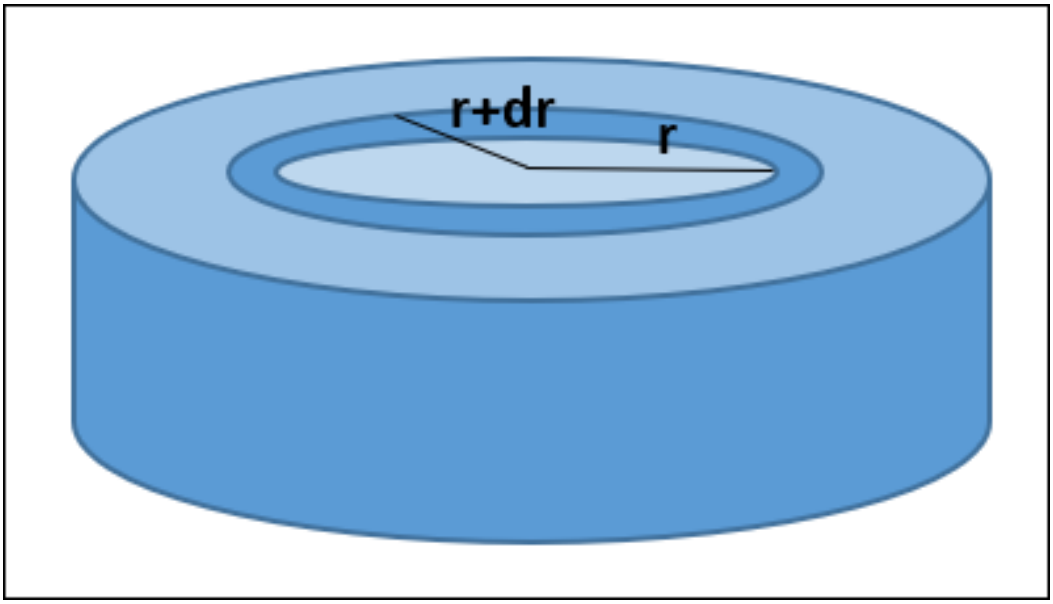

Figure 1. Ilustrations of 2 Surfaces with Distance dr

The weight of fluid lost between those surfaces is

$$2\pi\phi r\frac{\partial(\rho)}{\partial t}\partial r \tag{11}$$

Note that Eq. 9 is equal to Eq. 10

$$\frac{k}{\mu}\frac{\partial\left(\rho r\frac{\partial P}{\partial r}\right)}{\partial r} = \phi r\frac{\partial(\rho)}{\partial t} \tag{12}$$

Using the relationship between pressure and density with compressibility

$$\rho = \rho_i e^{-c(P_i - P)} \tag{13}$$

We can rewrite Eq. 12 to

$$\left(\frac{\partial^2\rho}{\partial r^2} + \frac{1}{r}\frac{\partial P}{\partial r}\right)\frac{k}{\phi\mu c} = \frac{\partial\rho}{\partial t} \tag{14}$$

Moreover, using the first order Taylor estimation with an assumption that liquid is slightly compressible, water or aquifer density can be approximated by:

$$\rho \cong \rho_i\left(1 - c(P_i - P)\right) \tag{15}$$

And substituting Eq. 15 to 14 gives

$$\left(\frac{\partial^2 P}{\partial r^2} + \frac{1}{r}\frac{\partial P}{\partial r}\right)\frac{k}{\phi\mu c} = \frac{\partial P}{\partial t} \tag{16}$$

Introducing dimensionless parameters

$$t_D = 0.00633\frac{kt}{\mu\phi c r_{owc}^2} \tag{17}$$

Note that for Eq. 17, the time variable, t, is in days.

$$r_D = \frac{r}{r_{owc}} \tag{18}$$

$$P_D = \frac{P_i - P}{P_i - P_{r_{owc}}} \tag{19}$$

Eq. 16 becomes

$$\left(\frac{\partial^2 P_D}{\partial r_D^2} + \frac{1}{r_D}\frac{\partial P_D}{\partial r_D}\right) = \frac{\partial P_D}{\partial t_D} \tag{20}$$

The solutions to the differential equation are made using Laplace transforms, which were presented in graphical form. An approximation using a polynomial correlation was developed to make the model easier to be re-used in different functions (Fanchey, 1985).

To calculate the cumulative water influx, the principle superposition is used for different values of pressure. The equation is expressed as:

$$W_e = C_{wi} \sum W_{eD} \Delta p \tag{21}$$

$$C_{wi} = \frac{1.119 r_{owc}^2 h \phi c_t}{B_w}\left(\frac{\theta}{360}\right) \tag{22}$$

C_{wi} is defined as water influx coefficient which is dependent upon reservoir and aquifer.

Convection Diffusion Model

CO_2 dissolved in water changes water properties. The water properties affected by the solubility are density and viscosity. The change in density changes water formation volume factor and also water compressibility. Changes in all of these properties affect the calculations in the aquifer model and the material balance model. Therefore, convection diffusion model needs to be used to analyze the water flow after the CO_2 injection. Moreover, our modified model can also be used to differentiate the amount of CO_2 stored in the gas reservoir and the amount of CO_2 dissolved in the water in the aquifer.

Consider isothermal one-dimensional homogeneous miscible displacement of a component by another component, the conservation of mass of component 'i' with mass concentration C_i is defined by (Lake, 1989):

$$\phi \frac{\partial C_i}{\partial x} + u \frac{\partial C_i}{\partial t} - \phi K_l \frac{\partial^2 C_i}{\partial x^2} = 0 \tag{23}$$

In dimensionless form, Equation 23 can be expressed as:

$$\frac{\partial C_{D_i}}{\partial x_D} + \frac{\partial C_{D_i}}{\partial t_D^*} - N_{pe} \frac{\partial^2 C_{D_i}}{\partial x_D^2} = 0 \tag{24}$$

Where:

$$x_D = \frac{x}{L} \tag{25}$$

$$t_D^* = \int_0^t \frac{u dt}{\phi L} \approx \sum_0^t \frac{Qt}{V_{aq}} \tag{26}$$

$$C_{D_i} = \frac{C_i - C_{I_i}}{C_{J_i} - C_{I_i}} \tag{27}$$

The solution for the equation can be derived using Laplace transform and is given by (Marle, 1981):

$$C_D = \frac{1}{2} erfc \frac{x_D - t_D^*}{2\sqrt{\frac{t_D^*}{N_{pe}}}} + \frac{e^{-x_D N_{pe}}}{2} erfc \frac{x_D + t_D^*}{2\sqrt{\frac{t_D^*}{N_{pe}}}} \tag{28}$$

Where $erfc$ is complementary error function which is defined as:

$$erfc(x) = 1 - erf\,(x) = \frac{2}{\sqrt{\pi}} \int_z^\infty e^{-z} dz \tag{29}$$

There is an approximation to the analytical solution, Eq. 27, which is the same as analytical solution but without its second term on the right-hand side of the equation (Lake, 1989). Note that the second term approaches 0 exponentially when the Peclet Number, N_{pe}, grows. For example, the second term approaches 0.001 when the Peclet Number is 25 for $t_D^* = x_D = 0.1$. This means that the approximation can be used when the Peclet Number is high.

Peclet Number is defined as ratio of convective transport to dispersive transport (Lake, 1989). It can be written as:

$$N_{pe} = \frac{uL}{\phi K_l} \tag{30}$$

K_l is defined as longitudinal dispersion coefficient. The Peclet Number is influenced by heterogeneity, autocorrelation, and aspect ratio (Arya, et al., 1988). In the study done by Arya et al., the Peclet Number decreases as the heterogeneity increases, which is quantified by Dykstra-Parson Variable (V_{DP}).

For aspect ratio (system dimension parallel to bulk flow – system dimension normal to bulk flow ratio) equals to 1, at $V_{DP} \leq 0.6$, the value of Peclet Number is relatively constant for changing dimensionless time. However, for $V_{DP} > 0.6$, the Peclet Number is relatively decreasing as the dimensionless time increases. For $V_{DP} = 0.6$, which can be categorized as a homogeneous reservoir, the Peclet Number is around 50. While for $V_{DP} = 0.8$, which can be categorized as heterogeneous reservoir, the Peclet Number is relatively constant at 18.18 for dimensionless time between 0.3 to 0.8. The Peclet Number is decreasing as the dimensionless time decreases below 0.3, approaching 27 as the dimensionless time approaches 0.1. It increases as the dimensionless time increases above 0.8, approaching 11 as the dimensionless time approaches 1 (Figure 2) (Arya, et al., 1988).

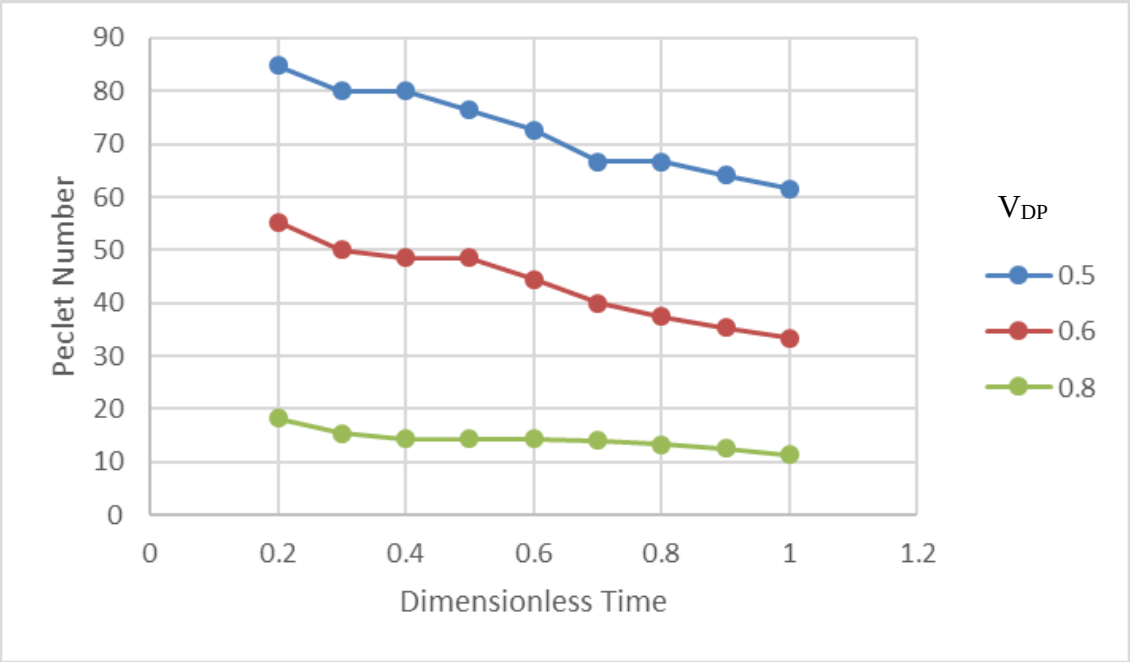

Figure 2. Dimensionless time vs. Peclet Number as a function of V_{DP} for Aspect Ratio = 1. Adapted from (Arya, et al., 1988).

CHAPTER III

METHODOLOGY TO ESTIMATE CO_2 STORAGE CAPACITY IN THE DEPLETED GAS RESERVOIR WITH WATER DRIVE

The change in water properties due to CO_2 solubility may affect the Van Everdingen-Hurst aquifer model calculation. The properties are water compressibility, water formation volume factor and viscosity. In this study, the water properties are obtained using PVTsim Nova (Calsep, 2019) as a function of pressure, temperature, CO_2 composition and salinity.

Moreover, the underlying assumption in the model that may be affected is that the liquid flowing (i.e. water) is slightly compressible. To validate that the assumption still holds, PVTsim Nova is used to determine the water compressibility at different pressures and different solubilities of CO_2 in water.

Based on Figure 3, the assumption that the water is slightly compressible still holds because the gradient is similar to the gradient of water compressibility without dissolved gas. For the viscosity, according to PVTsim Nova, the viscosity of water with and without dissolved CO_2 does not change (Table 1). Note that the results shown are using 200^oF as temperature and no salt dissolved in water. Increasing the amount of CO_2 more than 5% of the fluid composition is not going to change anything since at the pressure and temperature there is a certain maximum amount of CO_2 that can dissolve in the water. In the case of 200^oF temperature, the maximum amount is less than 3% of CO_2 (Table 2) (Figure 4). The value is even less for saline water.

However, based on experiments which were done at low temperatures, the viscosity of water with dissolved CO_2 is different than water without any dissolved CO_2 (Kumagai & Yokohama, 1999) (Bando, et al., 2004). According to a review by Li et al., the experimental data about properties of CO_2/H_2O(/NaCl) mixtures are only available at low temperatures (<140^oF) (Li, et al., 2011). Therefore, it is hard to determine the change of water viscosity due to CO_2 solubility in water at reservoir condition (high temperature).

In this study, I assume that dissolved CO_2 in water changes the density properties (i.e. density, compressibility and formation volume factor) only. The water viscosity is assumed to be constant in most cases. Later, in one case, the impact of changing water viscosity will also be discussed.

Table 1 Viscosity at Different Pressures and Molar Ratios of CO_2 and Water from PVTsim Nova

Pressure (psia)	Viscosity (cP)		
	98% H2O	95% H2O	100% H2O
1500.00	0.308	0.308	0.308
2052.63	0.309	0.309	0.309
2605.26	0.310	0.310	0.310
3157.89	0.311	0.311	0.311
3710.53	0.312	0.312	0.312
4263.16	0.313	0.313	0.313
5000.00	0.314	0.314	0.314

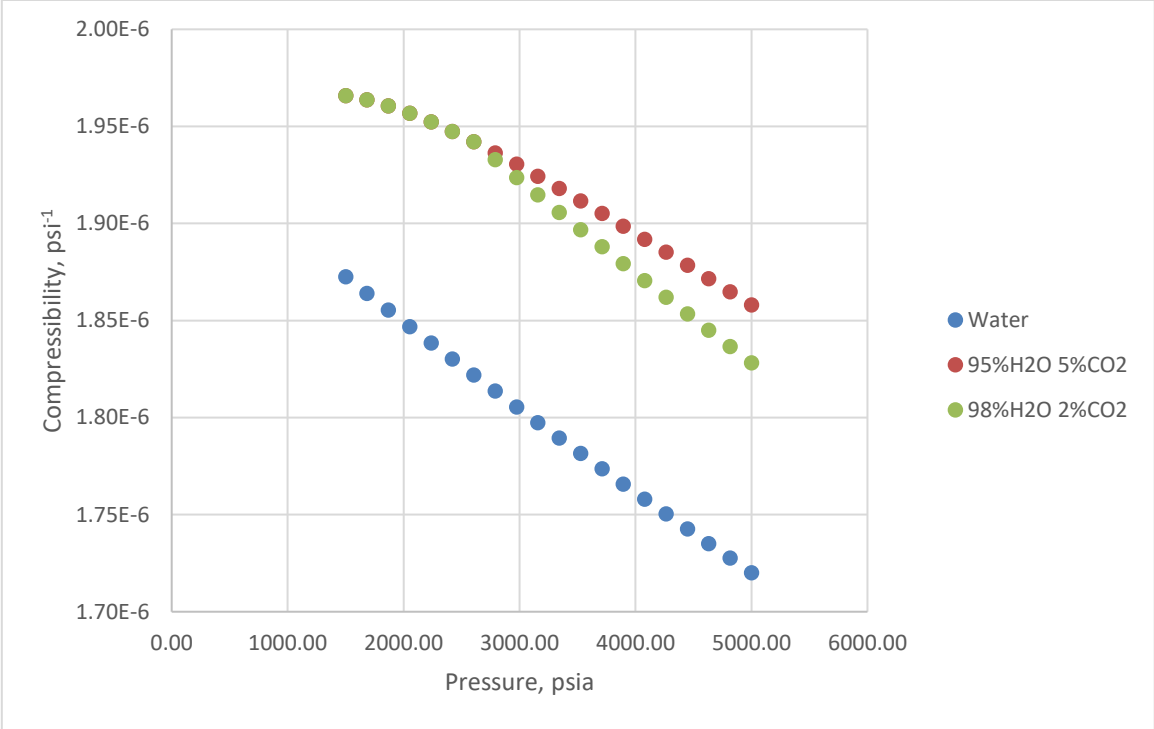

Figure 3. Compressibility at Different Pressures and Molar Ratios of CO_2 at 200°F and Water from PVTsim Nova

Table 2 Molar fraction of Dissolved CO_2 in Water at Different CO_2 Molar Compositions and Pressures for T=200°F from PVTsim Nova

	CO_2 Dissolved in Water for CO_2 %						
Pressure	**0%**	**1%**	**2%**	**3%**	**4%**	**5%**	**10%**
500	0.000	0.006	0.006	0.006	0.006	0.006	0.006
1000	0.000	0.010	0.011	0.011	0.011	0.011	0.011
1500	0.000	0.010	0.015	0.015	0.015	0.015	0.015
2000	0.000	0.010	0.018	0.018	0.018	0.018	0.018
2500	0.000	0.010	0.020	0.020	0.020	0.020	0.020
3000	0.000	0.010	0.020	0.021	0.021	0.021	0.021
3500	0.000	0.010	0.020	0.022	0.022	0.022	0.022
4000	0.000	0.010	0.020	0.023	0.023	0.023	0.023
4500	0.000	0.010	0.020	0.024	0.024	0.024	0.024
5000	0.000	0.010	0.020	0.025	0.025	0.025	0.025

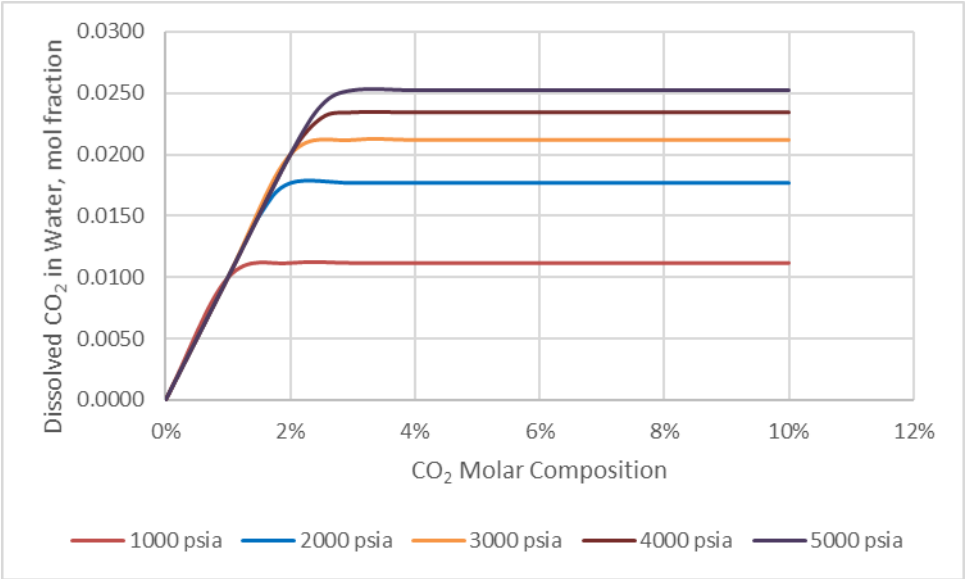

Figure 4. Molar fraction of Dissolved CO_2 in Water at Different CO_2 Molar Compositions and Pressures for T=200ºF

To estimate the changes in water properties, we first need to know the amount of dissolved CO_2 in water. It can be estimated using the convection diffusion model. The dimensionless composition in convection diffusion model is a function of initial composition in the reservoir fluid and the initial composition of injected fluid. In our case, the injected fluid is assumed to be the water with dissolved CO_2 inside the gas reservoir, and the reservoir fluid is the water in the aquifer. The model can be modified to:

$$C_{D_{CO_2}} = \frac{C_{CO_2} - C_{I_{CO_2}}}{C_{J_{CO_2@res}} - C_{I_{CO_2}}} = \frac{1}{2} erfc \frac{x_D - t_D^*}{2\sqrt{\frac{t_D^*}{N_{pe}}}} + \frac{e^{-x_D N_{pe}}}{2} erfc \frac{x_D + t_D^*}{2\sqrt{\frac{t_D^*}{N_{pe}}}} \quad (31)$$

Moreover, as time goes by, the amount of CO_2 in the gas reservoir is increasing because of the injection. This means that the amount of CO_2 dissolved in the water in the

gas reservoir is also increasing as long as it has not reached the limit determined by solubility. The maximum value of the dissolved CO_2 in the water is affected by pressure and temperature. Therefore, the amount of dissolved CO_2 in the water inside the gas reservoir is a function of time, pressure, and temperature. In this case, because we assume an isothermal reservoir, the concentration of CO_2 dissolved in water within the gas reservoir, $C_{J_{CO_2@res}}$, is a function of pressure and time. Later, we also included the effect of salts.

The principle of superposition will be used to consider the changing concentration of CO_2 dissolved in the water inside the gas reservoir. For each pressure step (and thus time step), the solution for CO_2 concentration inside the aquifer will be added to the solutions from the previous steps. It is presented graphically in Figure 5.

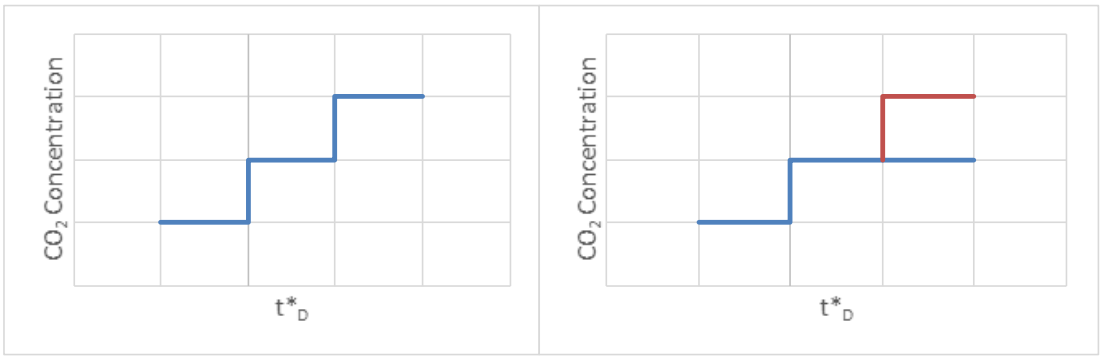

Figure 5. Left: Continuous Solution for CO_2 Concentration inside the Aquifer; Right: Superposition of CO_2 Concentration inside the Aquifer.

The model can be modified to:

$$\left(C_{CO_2}\right)_{t^*_{D_n}} = \left(C_{CO_2}\right)_{t^*_{D_{n-1}}} + \left(\left(C_{J_{CO_2@res}}\right)_{t^*_{D_n}} - \left(C_{J_{CO_2@res}}\right)_{t^*_{D_{n-1}}}\right)\left[\frac{1}{2}erfc\frac{x_D - t^*_{D_n}}{2\sqrt{\frac{t^*_{D_n}}{N_{pe}}}} + \frac{e^{-x_D N_{pe}}}{2}erfc\frac{x_D + t^*_{D_n}}{2\sqrt{\frac{t^*_{D_n}}{N_{pe}}}}\right] \quad (32)$$

Using the equation above, the concentration of CO_2 inside the aquifer can be calculated. After calculating the composition of CO_2 inside the aquifer, and using the average pressure, we can determine the water properties inside the aquifer which can be used in the aquifer model calculation. As previously mentioned, the water viscosity is assumed to be constant, so the only property that will be estimated using this method is water density. Note that we can calculate water compressibility and water formation volume factor using water density.

To get the parameters needed to run the convection diffusion model, material balance calculation needs to be done. After we get the new water properties, the material balance model can be run again with new water properties, therefore, making this an iterative method.

The Material Balance equations will be divided into 2 stages, before injection (during production) and during injection. The first part will be used to characterize the aquifer. Since this study focuses on a depleted gas reservoir, it means that we have complete production data. The second part of the equation will be used to estimate the carbon storage capacity. The first equation is the general gas material balance without water injection and gas injection.

$$\frac{\bar{p}}{z}[1 - c_e(p_i - \bar{p})] = \frac{p_i}{z_i} - \frac{p_i}{z_i}\frac{1}{G}\left[G_p + W_p R_{sw} + 5.615\frac{1}{B_g}\left[W_p B_w - W_e\right]\right] \quad (33)$$

The second equation is the general gas material balance without water injection, but the cumulative gas production and cumulative water production terms are constant and the values are the maximum values from the end of production stage, which are the values at abandonment condition. Note that the subscript 'abd' in Eq. 33 means abandonment condition.

$$\frac{\bar{p}}{z}[1 - c_e(p_i - \bar{p})] = \frac{p_i}{z_i} - \frac{p_i}{z_i}\frac{1}{G}\left[G_{p,abd} - G_{inj} + \left(W_p R_{sw}\right)_{abd} + 5.615\frac{1}{B_g}\left[\left(W_p R_{sw}\right)_{abd} - W_e\right]\right] \quad (34)$$

The changes in water properties due to CO_2 solubility occur only in the Eq. 34. The changes affect the water influx term. In this case, the water properties change as the ratio of CO_2 and water changes and the pressure increases. The water properties are determined using PVTsim combined with the convection diffusion model.

The problem with this approach is that to determine the water properties, the pressure is needed, and the pressure is one of the results from calculation using Eq. 34. Therefore, iterations are needed to calculate the pressure and water influx incorporating the changes in water properties. The iteration procedures are:

1. Build the material balance model (Eq. 33)
2. History match with production data to characterize the water influx and aquifer
3. Run prediction with the material balance model (Eq. 34) to determine time, gas injected, pressure, and water influx.
4. Determine the change in water properties using the prediction results due to CO_2 solubility
5. Run prediction with the material balance model (Eq. 34) and new water properties
6. Repeat steps 4 and 5 until pressure and water influx converge. In this case, I used <0.5% as convergence criteria.

The flowchart can be found in Figure 6.

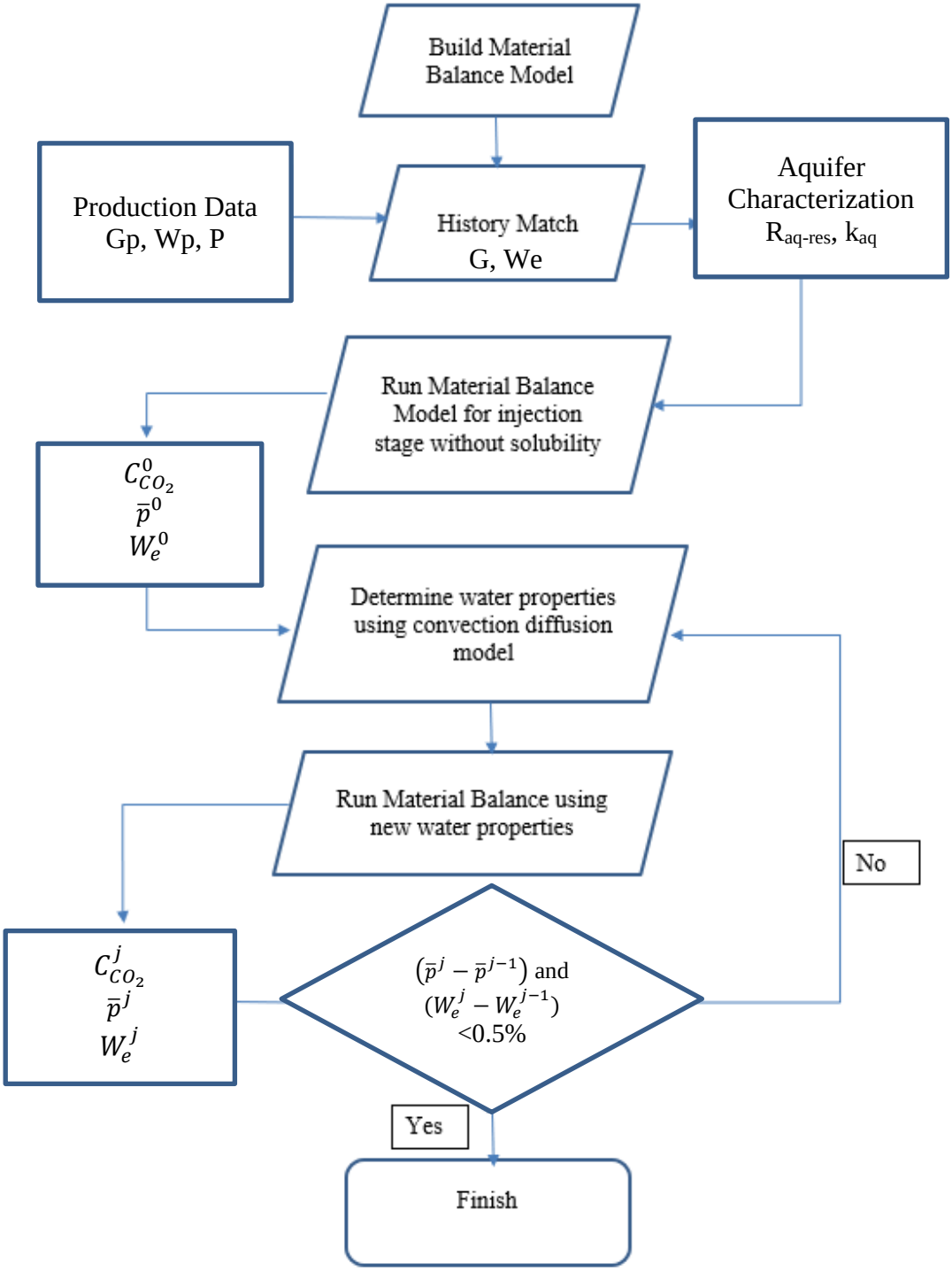

Figure 6. Flowchart for Material Balance Calculation to Incorporate the CO_2 Solubility

Determination of CO_2 Storage in the Gas Reservoir and the Aquifer

To determine the CO_2 Storage in the gas reservoir and the aquifer, the combination of material balance and convection diffusion model are used. The cumulative gas injected from the iteration results of material balance model is the total CO_2 storage inside the gas reservoir and aquifer. Using the modified convection diffusion model, we can estimate the concentration of CO_2 inside the aquifer. Thus, we can calculate the mass of CO_2 stored in the gas reservoir by subtracting the mass of CO_2 in aquifer from the total CO_2 storage from material balance.

The estimated value of concentration of CO_2 inside the aquifer from convection diffusion model is used to calculate the amount of CO_2 stored inside the aquifer. The equation below can be used to calculate the amount of CO_2 stored inside the aquifer in standard condition:

$$V_{CO_2@aq} = \frac{\bar{C}_{CO_2}\rho_{aq}V_{aq}}{\rho_{CO_2@sc}} \tag{32}$$

Where:

$$\bar{C}_{CO_2} = \frac{\int_0^1 C_{CO_2}dx_D}{\int_0^1 dx_D} = \int_0^1 C_{CO_2}dx_D \approx \sum_{x_D=0}^{x_D=1} C_{CO_2}\left(x_D, t^*_{D,final}\right) \tag{33}$$

Finally, the amount of CO_2 stored inside the gas reservoir can be calculated using:

$$V_{CO_2@res} = G_{inj} - V_{CO_2@aq} \tag{34}$$

Note that all the volume variables in Eq. 32 and 34 are in standard conditions.

Moreover, the amount of CO_2 stored in the gas reservoir can also be differentiated between gas phase (first term in Eq. 35) and dissolved CO_2 in water (second term in Eq. 35):

$$V_{CO_2@res} = V^g_{CO_2@res} - V^l_{CO_2@res} V_{CO_2@res} = V^g_{CO_2@res} - W_e R_{s_{CO_2}} \quad (35)$$

Synthetic Reservoir Data

The data used is created arbitrary. For the sake of simplicity, the gas is assumed to be a dry gas consisting of CH_4 only. There is no water production during the production stage. The reservoir and fluid characterization data for base case to be run can be found in Table 3.

Table 3 Reservoir and Fluid Data for Base Case

Reservoir Pressure	3000	psia
Temperature	200	F
OGIP	94007.6	MMSCF
Porosity	0.25	
Aquifer-reservoir Ratio	7.5	
Aquifer Permeability	100	mD
Reservoir Thickness	30	ft
Salinity	0	ppm
Peclet Number	50	
Gas Production rate	15	MMSCFD
Gas Injection Rate	15	MMSCFD
Abandonment Pressure	500	psia

A sensitivity analysis will be done only by changing one variable for each case. The variables considered are aquifer-reservoir ratio, aquifer permeability, injection rate, temperature, salinity, and Peclet Number. This is done to analyze the effect of each variable to the results and also to compare the results between the estimation considering and without considering CO_2 solubility in water.

The data for the sensitivity analysis can be found in Table 4. Note that other than the data listed in the table, we use the same value as the base case data in Table 3.

Table 4 Data for Sensitivity Analysis

Case	Aquifer-Reservoir Ratio	Aquifer Permeability (mD)	Injection Rate (MMSCFD)	Temperature (°F)	Salinity (ppm)	Peclet Number
Base Case	7.5	100	15	200	0	50
Case 1	5	100	15	200	0	50
Case 2	10	100	15	200	0	50
Case 3	7.5	50	15	200	0	50
Case 4	7.5	200	15	200	0	50
Case 5	7.5	100	10	200	0	50
Case 6	7.5	100	20	200	0	50
Case 7	7.5	100	15	300	0	50
Case 8	7.5	100	15	350	0	50
Case 9	7.5	100	15	200	5000	50
Case 10	7.5	100	15	200	15000	50
Case 11	7.5	100	15	200	25000	50
Case 12	7.5	100	15	200	0	10
Case 13	7.5	100	15	200	0	25

In addition to the sensitivity analysis mentioned above, I also ran the case of changing viscosity using a correlation created from experiment results from Bando et al. (Bando, et al., 2004). The correlation is based on a linear relationship between viscosity and CO_2 composition in water. The intercept for the linear correlation is the water viscosity without any dissolved CO_2, and the slope is a linear function of temperature (Bando, et al., 2004). The correlation is expressed as:

$$\mu_{w,CO_2} = \mu_w \left\{1 + \left(-4.069\ (10^{-3})(T - 32)\left(\frac{5}{9}\right) + 0.2531\right)\frac{x_C}{x_{CS}}\right\} \qquad (36)$$

The correlation was originally created for 86-140^{o}F temperature range (Bando, et al., 2004), which is smaller to most of the reservoir temperatures. Therefore, the analysis done in this study will only be a qualitative analysis.

CHAPTER IV

RESULTS AND DISCUSSION

Comparison between the Estimations Considering and Neglecting CO_2 Solubility in Water

For the estimation without considering CO_2 solubility, the total stored CO_2 is 135615.064 MMSCF (Table 5). This is equivalent with 4.7% reduction from the theoretical capacity calculated using Eq. 8, which is lower compared to the average value of 28% reduction for strong aquifer support according to Bachu et al.'s study (Bachu & Shaw, 2003). However, for aquifer-reservoir ratio = 13, the reduction reaches 26% which is close to the average value that Bachu et al. states. Furthermore, the result from this study is in line with Tseng et al.'s study, which states that the single capacity coefficient is less than one (Tseng, et al., 2012). Single capacity coefficient is a coefficient to calculate the reduction of CO_2 storage capacity compared to the theoretical capacity.

The material balance iteration procedure converges in 3 iterations for the base case. The difference in total CO_2 storage between the model without solubility (i.e. conventional material balance) and the model with solubility reaches 9.4% (Table 5). When we consider the changing water properties due to CO_2 solubility in water, the pressure reaches the initial pressure faster during the injection stage compared to when we do not consider the change in water properties (Figure 7) (Figure 10) (Table 5).

The pressure reaches the initial pressure faster when considering CO_2 solubility in water because the changing in water properties affects the water influx in the reservoir

during the injection stage. Based on the water influx trend observed in Figure 8, the water influx in gas reservoir is higher compared to the result without considering CO_2 solubility. A higher amount of water in the gas reservoir means that the pore spaces available to be occupied by the CO_2 are smaller, thus the amount of CO_2 stored is smaller. Water saturation trends also follow the same trend as the water influx (Figure 9). The estimated water saturation at the end of injection stage considering CO_2 solubility in water results in higher water saturation compared to the estimated value without considering the solubility.

The amount of CO_2 stored in the reservoir as gas phase is far more significant compared to the amount of CO_2 dissolved in water inside the gas reservoir and the aquifer as can be seen at Table 5. The amount of stored CO_2 inside the aquifer at the end of injection period is only 0.41% of the total amount of CO_2 stored. However, if we are looking at absolute value of the amount of CO_2 stored inside the aquifer, it almost reaches 2 million tones. It is a significant value and cannot be neglected. For a comparison, let us consider 200MW power plant with 998.4 lb/MWh average CO_2 emission rates (EPA, 2016). The annual emission for said power plant is almost 800000 tons of CO_2.

Based on this exercise, we can see that the small amount of CO_2 dissolved in the water, which changes the water properties, can have quite significant effect on the storage capacity. The changes in water properties accelerate the increase in reservoir pressure, and thus reduce the amount of CO_2 that can be stored, even though some of the CO_2 goes into the aquifer through the water flow and diffusion.

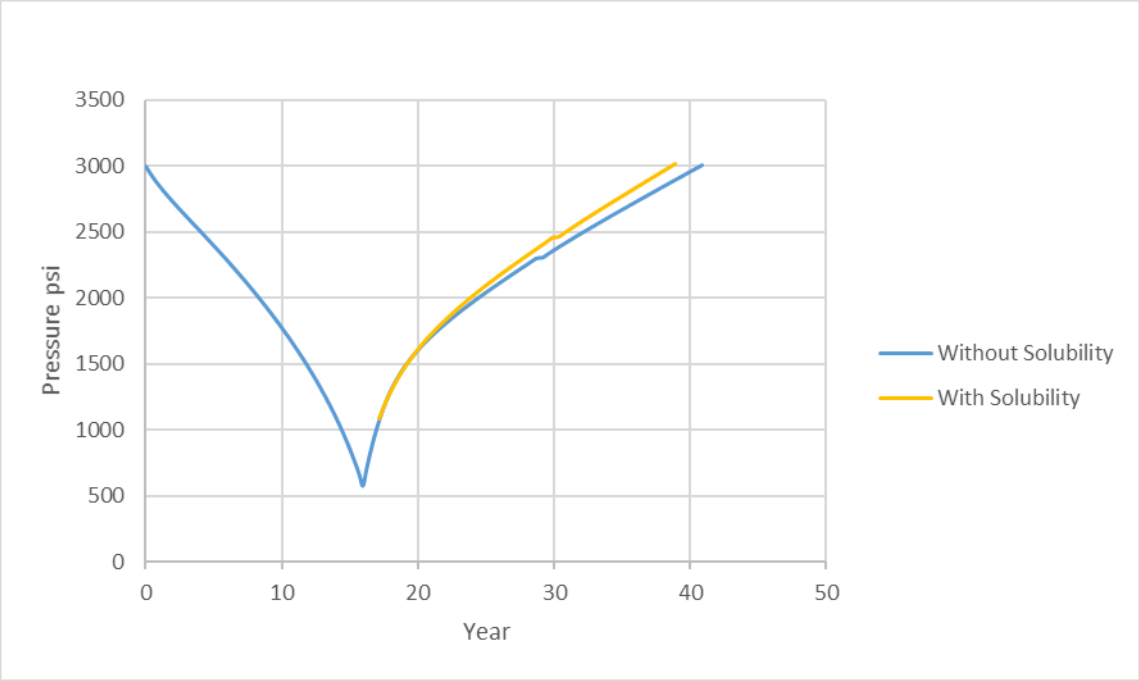

Figure 7. Pressure Trend of Base Case Considering or Neglecting CO_2 Solubility in Water

Table 5 Cumulative Gas Injected of Base Case Considering or Neglecting CO_2 Solubility in Water

	Without Solubility	With Solubility	% Difference
Total CO_2 Stored (MMSCF)	135615.064	123983.718	9.38%
Total CO_2 Stored (MMtones)	539.5956836	493.3159879	9.38%
Aquifer Storage (MMSCF)	0	504.352	
Aquifer Storage (MMtones)	0	2.007	
Gas Reservoir Storage Gas Phase (MMSCF)	135615.064	121349.796	11.75%
Gas Reservoir Storage Gas Phase (MMtones)	539.5956836	482.836	11.75%
Gas Reservoir Storage Dissolved (MMSCF)	0	2129.57044	
Gas Reservoir Storage Dissolved (MMtones)	0	8.473	
Time to reach initial pressure (years)	24.75	22.63	9.38%

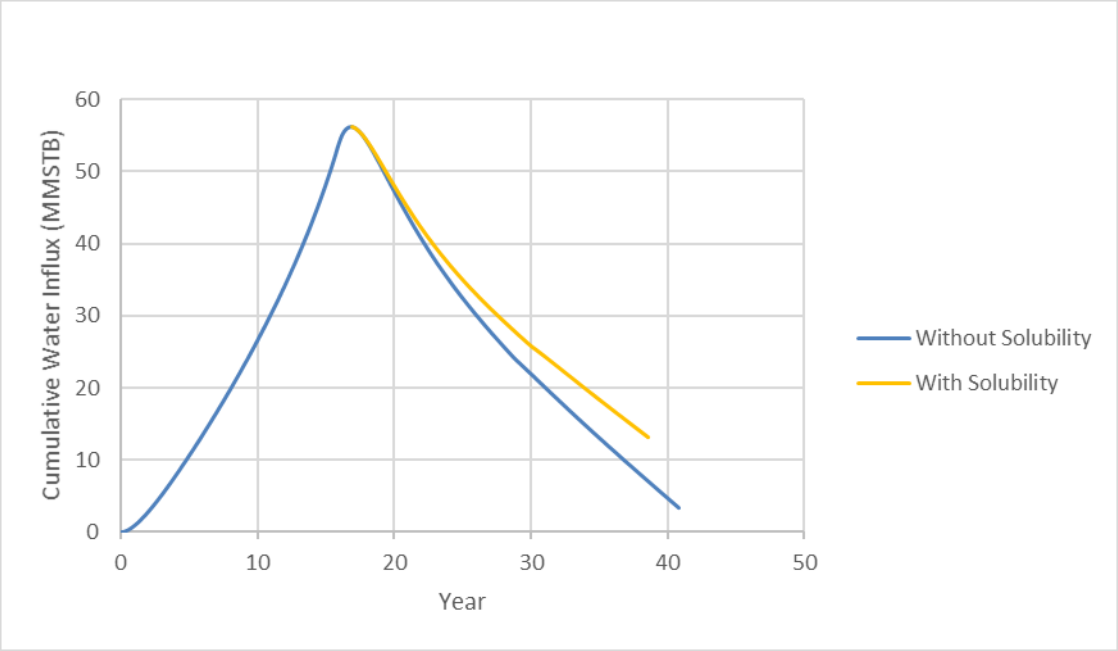

Figure 8. Water Influx Trend of Base Case Considering or Neglecting CO_2 Solubility in Water

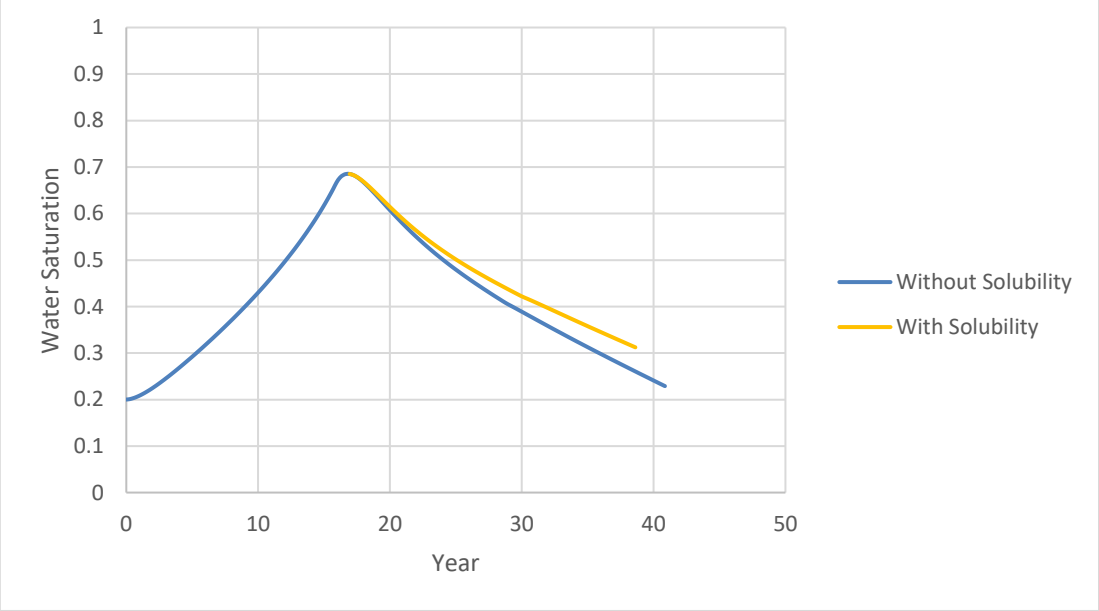

Figure 9. Water Saturation Trend of Base Case Considering or Neglecting CO_2 Solubility in Water

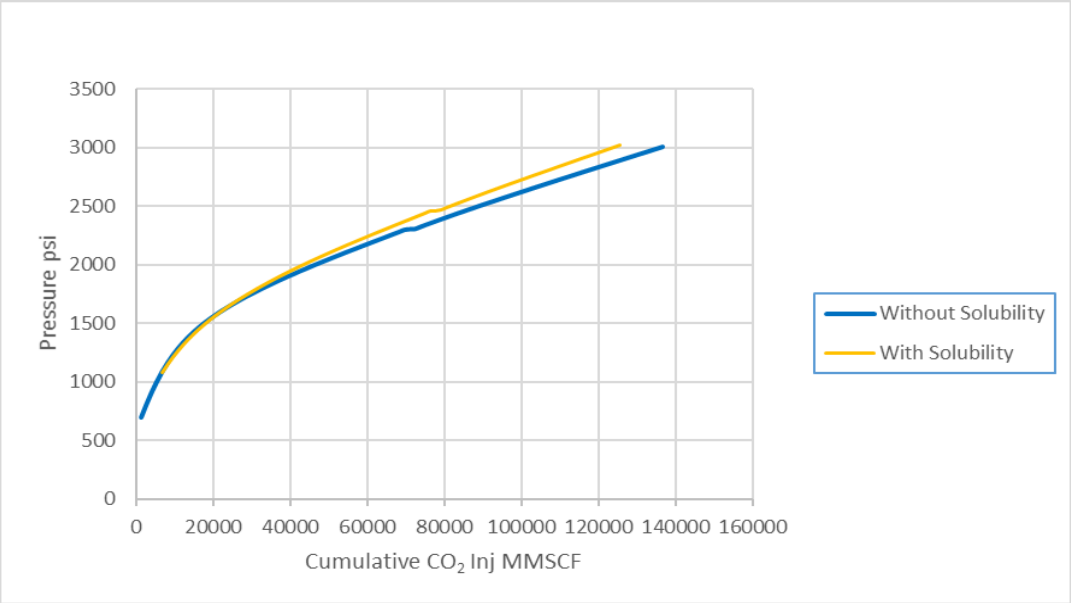

Figure 10. Pressure vs Cumulative Injected CO_2 of Base Case Considering or Neglecting CO_2 Solubility in Water

The Impact of Aquifer-Reservoir Ratio to the CO_2 Storage Capacity

Aquifer-reservoir Ratio value may be obtained from aquifer characterization during production history matching using the production stage material balance model. The bigger the Aquifer-reservoir Ratio is, the bigger the aquifer size and therefore, pressure support and the amount of water influx into the gas reservoir during production stage are also higher.

Similar to the base case, various other values of Aquifer-reservoir Ratio also result in lower amount of total gas stored because the pressures increase faster compared to the case without solubility (Table 6). As can be seen in Figure 11, lower value of Aquifer-reservoir Ratio gives smaller deviations in the results Considering or Neglecting solubility of CO_2 in water, while higher value of Aquifer-reservoir Ratio gives higher deviation in

the results. This can be explained by the water influx into the gas reservoir before the injection begins. The amount of water influx is lower for the smaller Aquifer-reservoir Ratio because of lower pressure support. This leads to lower water flows towards the aquifer, which is the only parameter affected by the changing water properties in the material balance model. On the other hand, higher ratio means that the amount of water influx inside the reservoir before the injection stage is also higher, which makes the difference between the results Considering or Neglecting the CO_2 solubility in water greater. The water influx trends and pressure trends can be found in Appendix A.

Considering the CO_2 solubility in water, a higher Aquifer-reservoir Ratio provides a lower value of total CO_2 stored (Figure 11). This is can be explained by the delay in the water flowing into the aquifer due to stronger pressure support (Bachu & Shaw, 2003) in addition to the effect of changing water properties which accelerates the pressure increase during the injection stage. For higher ratio, the effect of water properties is bigger because the water influx during injection stage is higher.

Table 6 Time Needed to Reach Initial Pressure since the Start of Injection Considering or Neglecting CO_2 Solubility in Water for Various Aquifer-reservoir Ratios

Reservoir-aquifer Ratio	Time Needed to reach Initial Pressure (Years)		% difference
	Without Solubility	With Solubility	
5	24.24	23.72	2.2%
7.5	24.75	22.63	9.4%
10	24.06	18.40	30.8%

The amounts of CO_2 stored in the aquifer for all three Aquifer-reservoir Ratios are still smaller compared to the amounts of CO_2 inside the gas reservoir as can be seen at (Table 7). In line with increasing water influx after the injection stage at higher aquifer-reservoir ratio, the stored CO_2 in gas phase decreases while the dissolved CO_2 in gas reservoir increases (Table 7). The difference between the amount of CO_2 stored inside the aquifer and gas reservoir decreases for higher value of Aquifer-reservoir Ratio. The absolute value of CO_2 stored inside the aquifer is increasing for higher value of Aquifer-reservoir Ratio.

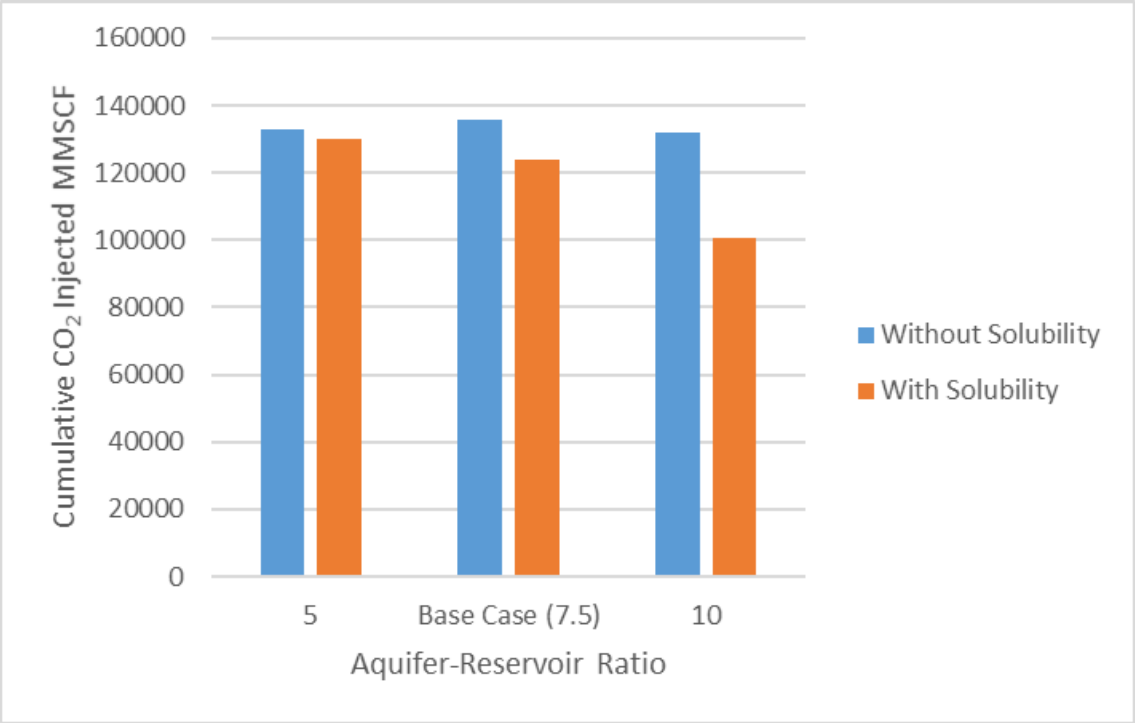

Figure 11. Cumulative CO_2 Injected Considering or Neglecting CO_2 Solubility in Water for Various Aquifer-reservoir Ratios

Table 7 CO_2 Stored inside Gas Reservoir and Aquifer for Various Aquifer-reservoir Ratio

Reservoir-aquifer Ratio	Aquifer		Gas Reservoir Gas Phase		Gas Reservoir Dissolved	
	MMSCF	MMtonnes	MMSCF	MMtonnes	MMSCF	MMtonnes
5	224.530	0.893	128744.028	512.257	970.712	3.862
7.5	504.352	2.007	121349.796	482.836	2129.570	8.473
10	896.578	3.567	95658.520	380.614	4260.847	16.953

The Impact of Aquifer Permeability to the CO_2 Storage Capacity

Similar to Aquifer-reservoir Ratio, aquifer permeability may also be obtained from aquifer characterization during production history matching. Usually, higher value of aquifer permeability also gives better pressure support and thus, higher water influx.

However, unlike the Aquifer-reservoir Ratio, the higher the aquifer permeability, the total stored CO_2 is increasing (Figure 12). The aquifer permeability dictates the "easiness" of the water flowing out of and into the aquifer, therefore, higher aquifer permeability results in higher water influx before the injection period and lower water influx after the injection period. Moreover, the increase in reservoir pressure is slower as the aquifer permeability increases (Table 8). Pressure trends and water influx trends can be found in Appendix A.

Consistently, by considering CO_2 solubility in water, the amount of CO_2 stored is decreased compared to the results without considering CO_2 solubility in water. The percent difference between results with and without CO_2 solubility is greater in higher value of aquifer permeability because of the faster pressure increase when we consider CO_2 solubility in water (Table 8).

Differentiating between the amount of CO_2 stored inside the aquifer and gas reservoir for various aquifer permeabilities results in increasing amount of CO_2 stored both inside the aquifer and gas reservoir (Table 9). The increase in the amount of CO_2 stored inside of the gas reservoir is higher compared to the increase in the amount of CO_2 stored inside the aquifer. This implies that the increase in the total amount of CO_2 stored for higher aquifer permeability is actually mostly contributed by the storage in gas reservoir instead of aquifer. In line with the water influx trend, the dissolved CO_2 in gas reservoir decreases as the aquifer permeability decreases (Table 9). This means that the increasing storage in the gas reservoir is from the storage in gas phase.

Table 8 Time Needed to Reach Initial Pressure since the Start of Injection Considering or Neglecting CO_2 Solubility in Water for Various Aquifer Permeabilities

Aquifer perm (mD)	Time Needed to reach Initial Pressure (Years)		% difference
	Without Solubility	With Solubility	
50	23.10	21.83	5.8%
100	24.75	22.63	9.4%
200	25.78	23.30	10.7%

Table 9 CO_2 Stored inside Gas Reservoir and Aquifer for Various Aquifer Permeabilities

Aquifer perm (mD)	Aquifer		Gas Reservoir Gas Phase		Gas Reservoir Dissolved	
	MMSCF	MMtonnes	MMSCF	MMtonnes	MMSCF	MMtonnes
50	503.991	2.005	116826.926	464.840	2248.806	8.948
100	504.352	2.007	121289.796	482.597	2189.570	8.712
200	504.677	2.008	124996.706	497.347	2136.293	8.500

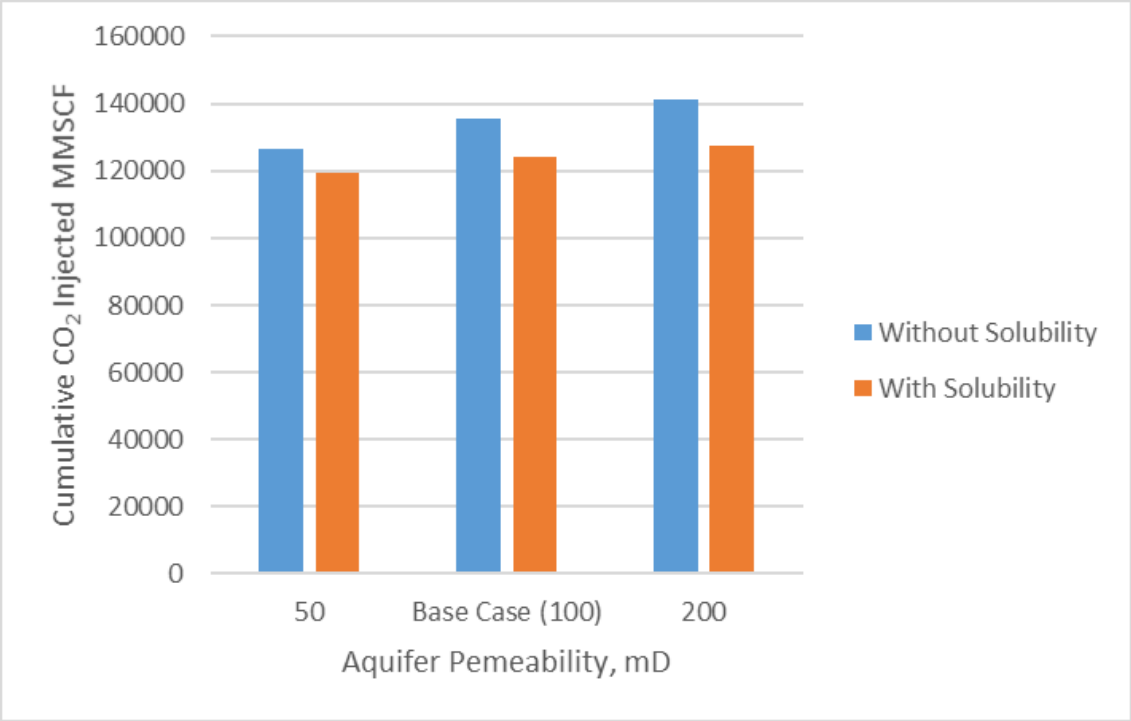

Figure 12. Cumulative CO_2 Injected Considering or Neglecting CO_2 Solubility in Water for Various Aquifer Permeabilities

The Impact of Injection Rate to the CO_2 Storage Capacity

Sensitivity analysis for various injection rate can be used to determine optimum injection rate to maximize CO_2 storage. Several other considerations should be made to determine the optimum injection rate in addition to the maximum CO_2 storage, for example economic considerations, surface facilities, etc.

As can be seen at Figure 13, the increase in injection rate decreases the amount of CO_2 stored with or without considering the CO_2 solubility in water. Low injection rate increases the storage because at low injection rates the pressure increases slowly, which means more injection duration and more amount of stored CO_2 (Table 10).

On the other hand, increasing injection rate slightly increases the amount of CO_2 stored inside the aquifer (Table 11). In general, similar to the previous cases, the changing water properties decreases the amount of CO_2 stored because of faster pressure increase in the gas reservoir. Increasing injection rate increases the water influx after the injection stage (see Appendix A for pressure and water influx trends). In line with this, the dissolved CO_2 stored in gas reservoir increases as the injection rate increases (Table 11). Therefore, the total decreasing storage is mostly contributed by decreasing storage capacity as free gas in gas reservoir for increasing rate.

Based on this result, we can argue that injecting at low injection rate maximizes the amount of CO_2 stored. Barrufet et al. made the same observation from reservoir simulation using several injection rates (Barrufet, et al., 2010). Their study state that the increasing injection rate decreases the storage efficiency. Injecting at low injection rate, however, is not favorable because it takes longer time to fill in the reservoir. Based on this argument, there is an optimum point of gas injection rate with high storage capacity and efficiency in terms of injection time. Further analysis using real field data, in addition to economic considerations and surface facilities considerations can be made as future research.

Table 10 Time Needed to Reach Initial Pressure since the Start of Injection Considering or Neglecting CO_2 Solubility in Water for Various Injection Rates

Injection Rate (MMSCFD)	Time Needed to reach Initial Pressure (Years)		% difference
	Without Solubility	With Solubility	
10	25.13	22.87	9.9%
15	24.75	22.63	9.4%
20	24.37	22.44	8.6%

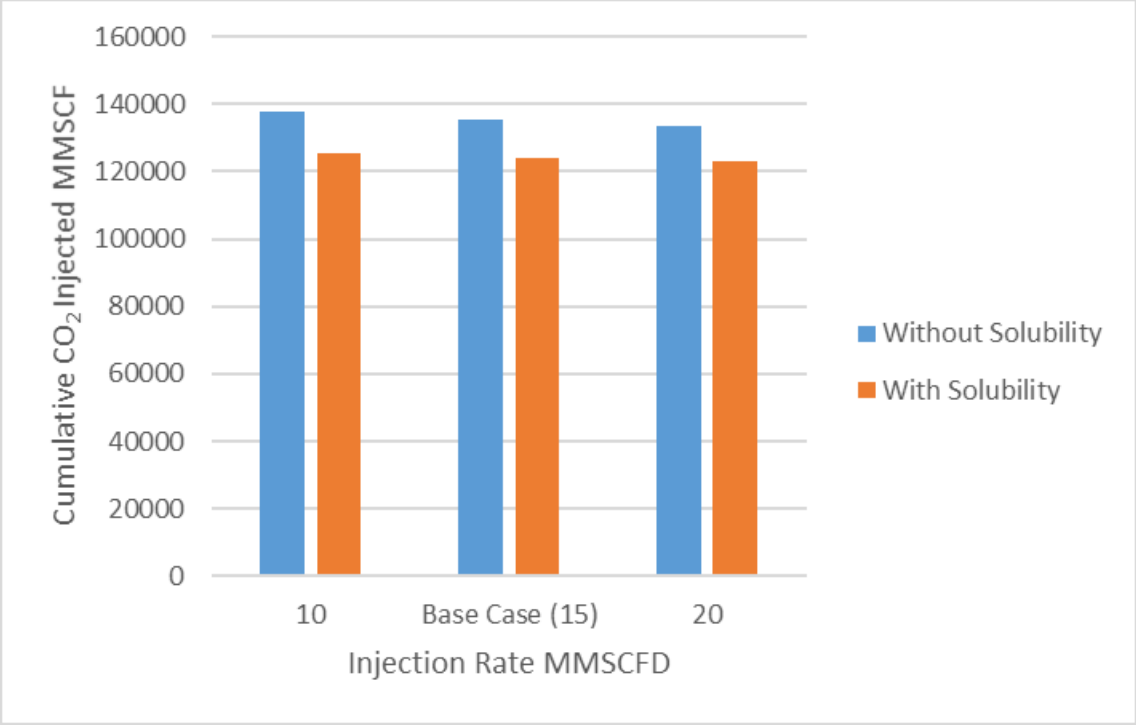

Figure 13. Cumulative CO_2 Injected Considering or Neglecting CO_2 Solubility in Water for Various Injection Rates

Table 11 CO_2 Stored inside Gas Reservoir and Aquifer for Various Injection Rates

Injection Rate (MMSCFD)	Aquifer		Gas Reservoir Gas Phase		Gas Reservoir Dissolved	
	MMSCF	MMtonnes	MMSCF	MMtonnes	MMSCF	MMtonnes
10	504.022	2.005	122756.316	488.432	2023.014	8.049
15	504.352	2.007	121349.796	482.836	2129.570	8.473
20	504.796	2.009	120162.146	478.110	2252.362	8.962

The Impact of Reservoir Temperature to the CO_2 Storage Capacity

The results for the temperature sensitivity analysis can be found at Figure 14. As expected, total **CO_2** stored decreases as the temperature increases because of the increasing pressure due to increasing temperature. During the injection period, for higher reservoir temperature, the reservoir pressure increases faster (Table 12).

Furthermore, the difference between the results with and without solubility diminishes as the temperature increases because the CO_2 solubility in water decreases as the temperature increases. This means the amount of CO_2 dissolved in water decreases and therefore the water properties are similar to the water properties without dissolved CO_2. For initial reservoir pressure at 3000 psi, at high temperature (i.e. >350^oF), we can estimate the CO_2 storage without considering the CO_2 solubility in water. The amount of CO_2 stored inside the aquifer also diminishes as the temperature increases because of the same reason in addition to reduced injection duration due to faster increase in reservoir pressure (Table 13).

Table 12 Time Needed to Reach Initial Pressure since the Start of Injection Considering or Neglecting CO_2 Solubility in Water for Various Temperatures

Temperature (°F)	Time Needed to reach Initial Pressure (Years)		% difference
	Without Solubility	With Solubility	
200	24.75	22.63	9.4%
300	19.78	18.77	5.4%
350	18.61	18.33	1.5%

Table 13 CO_2 Stored inside Gas Reservoir and Aquifer for Various Temperatures

Temperature (°F)	Aquifer		Gas Reservoir Gas Phase		Gas Reservoir Dissolved	
	MMSCF	MMtonnes	MMSCF	MMtonnes	MMSCF	MMtonnes
200	504.352	2.007	121349.796	482.836	2129.570	8.473
300	347.022	1.381	100873.685	401.364	1638.398	6.519
350	197.872	0.787	99202.042	394.713	999.644	3.977

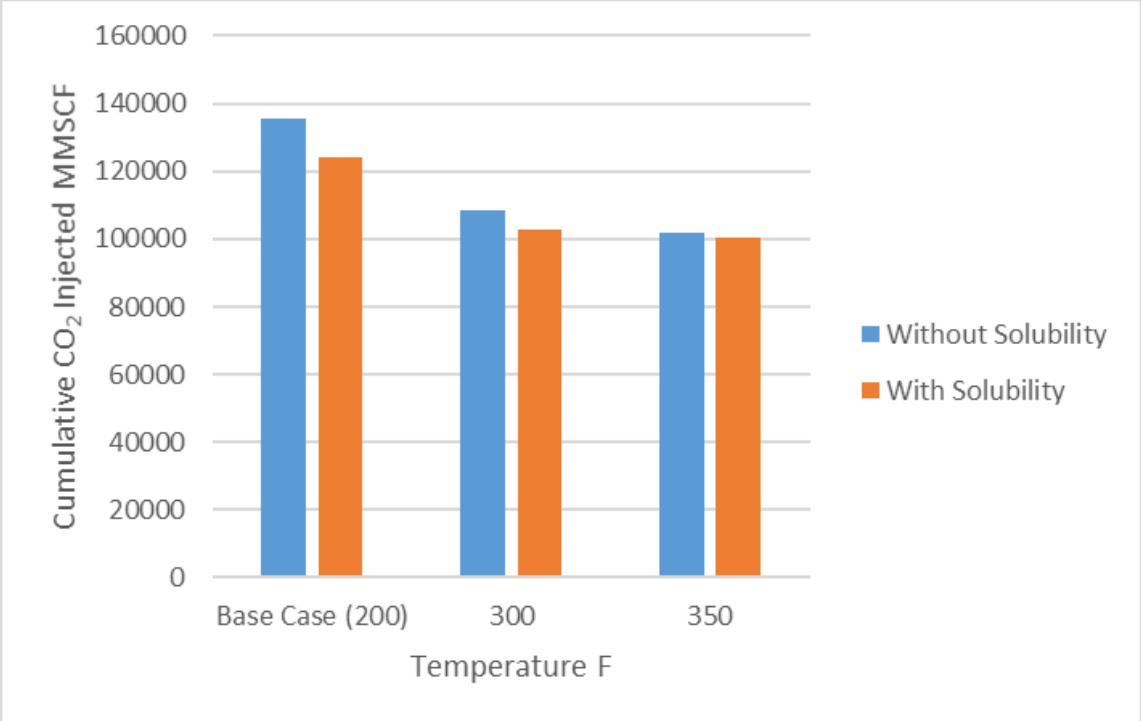

Figure 14. Cumulative CO_2 Injected Considering or Neglecting CO_2 Solubility in Water for Various Temperatures

The Impact of Water Salinity to the CO_2 Storage Capacity

Similar to temperature, increasing salinity decreasing the solubility of CO_2 in water. The results for salinity sensitivity can be found in Figure 15. Compared to increasing temperature, increasing salinity does not change the amount of stored CO_2 that significant. The decrease in difference between the results of with and without CO_2 solubility in water is observable. As the salinity increases, the result with CO_2 solubility approaches the result without CO_2 solubility.

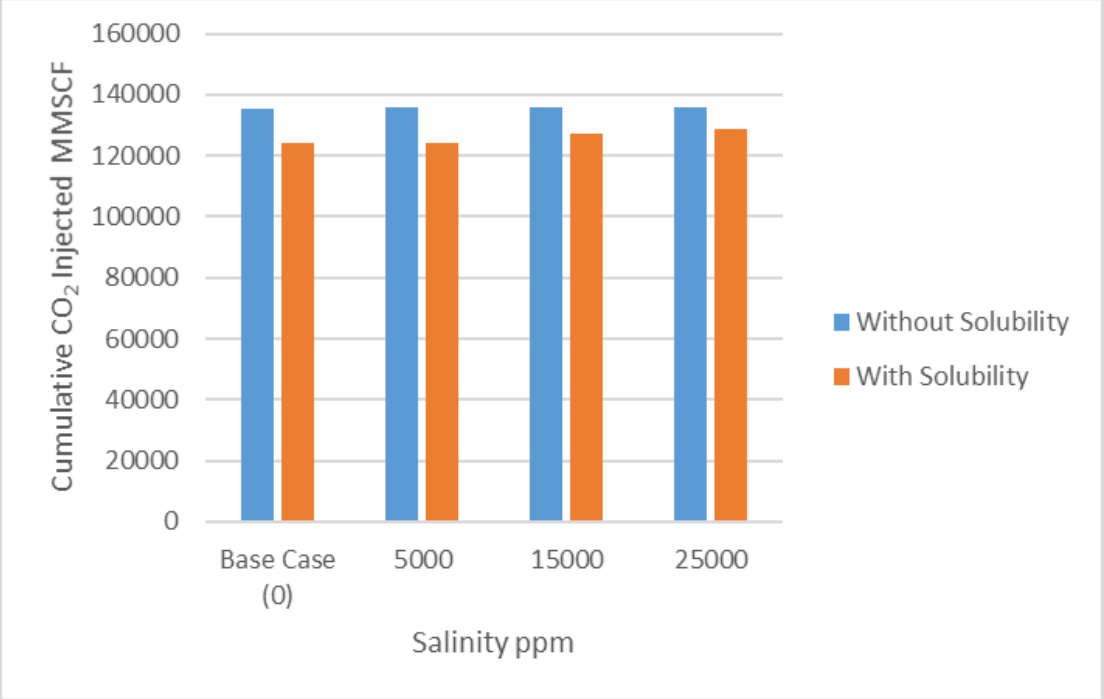

Figure 15. Cumulative CO_2 Injected Considering or Neglecting CO_2 Solubility in Water for Various Salinities

Consistent with previous results, considering CO_2 solubility in water reduces the injection duration due to faster pressure increase (Table 14). However, as the salinity increases, the increase in injection duration is not that significant.

In line with that, the amount of CO_2 stored inside the aquifer also decreases as the salinity increases. This is caused by the decreasing solubility in water which makes the amount of CO_2 flowing through water convection and diffusion decreases as well. The dissolved CO_2 in gas reservoir is also decreasing due to decreasing solubility (Table 15).

Table 14 Time Needed to Reach Initial Pressure since the Start of Injection Considering or Neglecting CO_2 Solubility in Water for Various Salinities

Salinity (ppm)	Time Needed to reach Initial Pressure (Years)		% difference
	Without Solubility	With Solubility	
0	24.75	22.63	9.4%
5000	24.77	22.69	9.1%
15000	24.79	23.25	8.5%
25000	24.81	23.51	7.4%

Table 15 Stored inside Gas Reservoir and Aquifer for Various Salinities

Salinity (ppm)	Aquifer		Gas Reservoir Gas Phase		Gas Reservoir Dissolved	
	MMSCF	MMtonnes	MMSCF	MMtonnes	MMSCF	MMtonnes
0	504.352	2.007	121349.796	482.836	2129.570	8.473
5000	488.243	1.943	121757.412	484.458	2068.269	8.229
15000	469.051	1.866	124974.599	497.259	1915.605	7.622
25000	405.652	1.614	126687.671	504.075	1702.419	6.774

The Impact of Peclet Number to the CO_2 Storage Capacity

To consider aquifer heterogeneity in the convection-diffusion calculation, Peclet Number 25 and 10 are used. Peclet Number = 25 corresponds to V_{DP} around 0.8 at small

value of dimensionless time, while Peclet Number = 10 corresponds to V_{DP} around 0.8 at high value of dimensionless time (Arya, et al., 1988). Note that for the base case, the Peclet Number 50 is used, and it corresponds to V_{DP} around 0.6. A reservoir with V_{DP} around 0.6 is considered a homogeneous reservoir, while a reservoir with VDP around 0.8 is considered a heterogeneous reservoir.

Comparing the Peclet Numbers estimation results in Figure 16, there is no observable difference between the CO_2 storage estimations. The times needed for the pressure to increase to initial pressure for both cases also have little to no difference (Table 16). We can argue that the change in Peclet Number does not have significant effect for this case.

Looking at Table 17, the amount of CO_2 stored in the aquifer is slightly higher for the heterogeneous aquifer. The difference is caused by the change in Peclet Number. Low Peclet Number results in higher CO_2 concentration. As can be seen in Eq. 32, as the Peclet Number decreases, the results from the complementary error function increases, and therefore the CO_2 concentration increases. Physically, a smaller Peclet Number means that the contribution of dispersive transport compared to convective transport is more significant. For a same water flow rate towards the aquifer, the amount of CO_2 that goes into the aquifer through diffusion increases, and therefore, for a smaller Peclet Number, the stored CO_2 in aquifer is higher.

Table 16 Time Needed to Reach Initial Pressure since the Start of Injection Considering or Neglecting CO_2 Solubility in Water for Different Peclet Numbers

Peclet Number	Time Needed to reach Initial Pressure (Years)		% difference
	Without Solubility	With Solubility	
10	24.75	22.60	9.5%
25	24.75	22.61	9.5%
50	24.75	22.63	9.4%

Table 17 CO_2 Stored inside Gas Reservoir and Aquifer for Different Peclet Numbers

Peclet Number	Aquifer		Gas Reservoir Gas Phase		Gas Reservoir Dissolved	
	MMSCF	MMtonnes	MMSCF	MMtonnes	MMSCF	MMtonnes
10	515.077	2.049	121141.091	482.006	2163.582	8.609
25	508.168	2.022	121231.360	482.365	2145.081	8.535
50	504.352	2.007	121349.796	482.836	2129.570	8.473

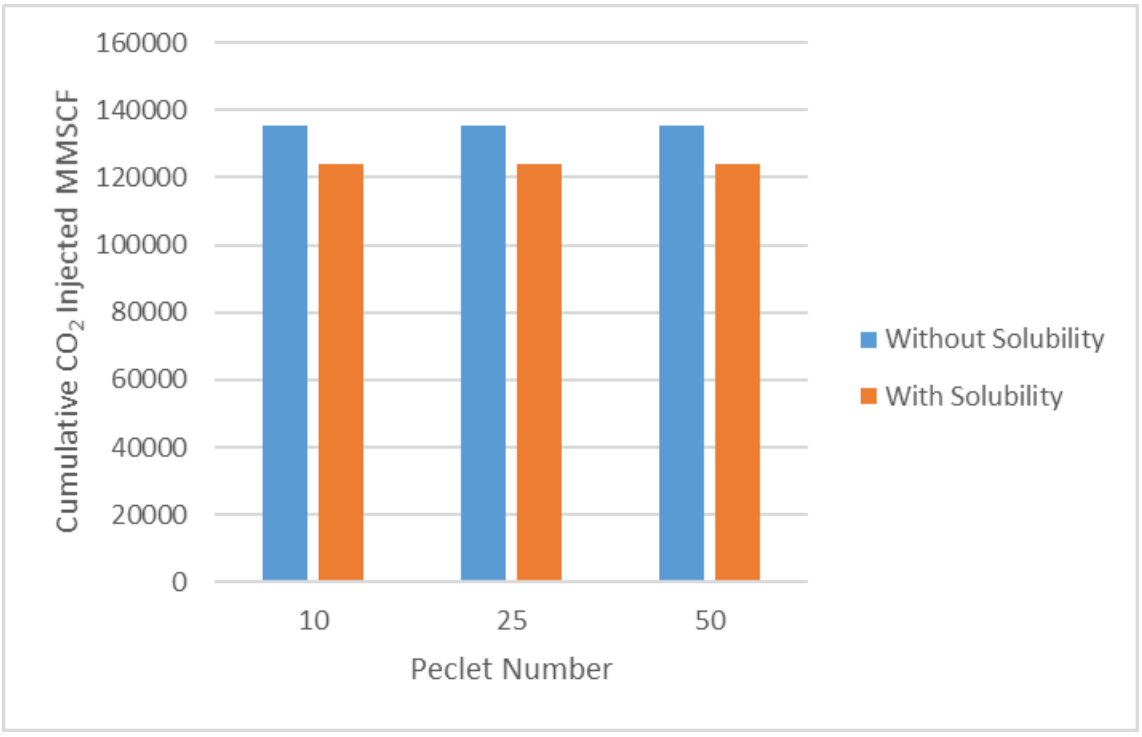

Figure 16. Cumulative CO_2 Injected Considering or Neglecting CO_2 Solubility in Water for Different Peclet Numbers

The Impact of Changing Water Viscosity to the CO_2 Storage Capacity

The change in viscosity is estimated using Eq. 36. The correlation states that increasing dissolved CO_2 in water increases the water viscosity (Bando, et al., 2004). Although the correlation includes temperature as one of the variables, the correlation was developed for low temperatures. Even assuming the correlation can be used in our reservoir temperature, 200^{o}F, the slope ends up being negative which means that the viscosity decreases as the dissolved CO_2 in water decreases, contrary to the experiment results from Bando et al.'s study (Bando, et al., 2004).

To be able to analyze the effect of changing viscosity, I used the same slope as 86^{o}F. The viscosity estimation using such method may not be accurate. However, using this method, we can quantitatively analyze the result of CO_2 storage estimation considering changing viscosity. The CO_2 storage estimation for changing viscosity algorithm is the same as Figure 6, but with water viscosity as an additional water property and iteration parameter.

Based on Table 18, the total CO_2 stored decreases if we consider viscosity change. As expected, this result is in line with the fact that increasing water viscosity decreases the flow rate of water towards the aquifer, therefore, water influx in gas reservoir is higher and the pressure increases faster. Aquifer storage also decreases because of the same reason.

In the end, to be able to analyze the effect of changing viscosity, lab experiments to measure changing viscosity due to dissolved CO_2 needs to be done at higher temperatures with different pressures and salinities.

Table 18 Cumulative Gas Injected of Base Case Considering or Neglecting Changing Water Viscosity

	Without Viscosity	With Viscosity	% Difference
Total CO_2 Stored (MMSCF)	123983.718	123775.302	0.17%
Total CO_2 Stored (MMtones)	493.316	492.487	0.17%
Aquifer Storage (MMSCF)	504.352	469.930	7.32%
Aquifer Storage (MMtones)	2.007	1.870	7.32%
Gas Reservoir Storage Gas Phase (MMSCF)	121349.796	121171.768	0.15%
Gas Reservoir Storage Gas Phase (MMtones)	482.836	482.128	0.15%
Gas Reservoir Storage Dissolved (MMSCF)	2129.570	2133.604	-0.19%
Gas Reservoir Storage Dissolved (MMtones)	8.473	8.489	-0.19%
Time to reach initial pressure (years)	22.630	22.592	0.17%

CHAPTER V

CONCLUSIONS AND RECOMMENDATIONS

An iterative method to determine CO_2 storage in depleted gas reservoir with water drive has been introduced. The method combines material balance and aquifer model to model the flow and pressure, with convection diffusion model to estimate the amount of CO_2 dissolved in water in the aquifer to finally estimate the changing water properties. The iterative procedure is needed because the water flow is affected by water properties which changes as the amount of CO_2 dissolved in water increases due to pressure increase and increasing mass of CO_2 because of CO_2 injection.

Using the iterative method, a case of gas production and CO_2 injection is analyzed. The result shows that if we consider CO_2 solubility, the amount of CO_2 stored is decreasing. In the base case in this study, the decrease reaches almost 10% of the result without considering CO_2 solubility. Moreover, using convection diffusion model, the amount of CO_2 stored is differentiated between storage inside gas reservoir and aquifer. The storage inside the aquifer is much smaller than the storage in gas reservoir. However, the absolute value is still significant, i.e. reaching 2 million tones.

Sensitivity analysis is also done. High Aquifer-reservoir Ratio results in higher difference between the results Considering or Neglecting the CO_2 solubility. On the other hand, low Aquifer-reservoir Ratio gives result similar to the result without the CO_2 solubility. It is logical because low Aquifer-reservoir Ratio gives low pressure support and

low amount of water influx, thus, the changing water properties is not affecting the results that much.

Other than the Aquifer-reservoir Ratio, aquifer permeability can also be obtained from production history matching. Increasing aquifer permeability increases the amount of stored CO_2 because at higher aquifer permeability the water influx remaining in the reservoir is low. The increase in the amount of CO_2 stored inside of the gas reservoir is higher compared to the increase in the amount of CO_2 stored inside the aquifer. This implies that the increase in the total amount of CO_2 stored for higher aquifer permeability is actually mostly contributed by the storage in gas reservoir instead of aquifer.

Decreasing injection rate increases the amount of CO_2 that can be stored. Low injection rate increases the storage because at low injection rates, the pressure is given time to propagate into the aquifer compared to injecting with higher rate, while injecting using higher rate creates faster pressure build-up which decreases the CO_2 stored. This implies that we can find an optimum rate by considering economic factors, surface facilities, and injection duration while maximizing the amount of CO_2 to be stored.

Increasing temperature and salinity both decreases the CO_2 solubility in water, and thus, in higher temperature and salinity, the results of calculation with CO_2 solubility are approaching the results of calculation without CO_2 solubility. Having said that, increasing salinity gives smaller effect to the difference in the results compared to increasing temperature.

A case for heterogeneous aquifer with V_{DP} around 0.8 has also been analyzed. The comparison between the results for homogeneous and heterogeneous aquifer is made and

there is no observable difference between the amount of CO_2 stored and time needed to reach initial pressure. The amount of CO_2 stored in the aquifer is slightly higher for the heterogeneous case because the calculation from modified convection diffusion model results in higher CO_2 concentration for lower Peclet Number.

Including the effect of changing viscosity in the estimation amplify the reduction of storage capacity due to remaining water in the reservoir. This result is expected, as the dissolved CO_2 in water increases the viscosity also increases. Further researches including laboratory experiments to determine viscosity changes due to CO_2 solubility in water in higher temperatures are needed to be able to accurately determine the effect of changing viscosity in the estimation of CO_2 storage in a depleted gas reservoir with water drive.

Future Recommendations

1. Apply this method to real field data, and combine the results with economic factors, surface facilities, and other data to find optimum injection rates.
2. Conduct laboratory experiments to determine water viscosity as a function of dissolved CO_2 composition, salinity, and pressure at higher temperatures.
3. Apply this method to changing water density, compressibility, formation volume factor, and viscosity due to CO_2 solubility in water to estimate the storage capacity.

REFERENCES

Arya, A., Hewett, T. A., Larson, R. G. & Lake, L. W., 1988. Dispersion and Reservoir Heterogeneity. *SPE Reservoir Engineering,* 3(01), pp. 139-148.

Bachu, S. et al., 2007. CO_2 Storage Capacity Estimation: methodology and gaps. *International Journal of Greenhouse Gas Control,* 1(4), pp. 430-443.

Bachu, S. & Shaw, J., 2003. Evaluation of the CO_2 Sequestration Capacity in Alberta's Oil and Gas Reservoirs at Depletion and the Effect of Underlying Aquifers. *Journal of Canadian Petroleum Technology,* 42(9), pp. 51-61.

Bando, S. et al., 2004. Viscosity of Aqueous NaCl Solutions with Dissolved CO_2 at (30 to 60)oC and (10 to 20) MPa. *Journal of Chemical Engineering Data,* Volume 49, pp. 1328-1332.

Barrufet, M. A., Bacquet, A. & Falcone, G., 2010. Analysis of the Storage Capacity for CO_2 Sequestration of a Depleted Gas Condensate Reservoir and a Saline Aquifer. *Journal of Canadian Petroleum Technology,* 49(8), pp. 23-31.

Calsep, 2019. *PVTsim Nova 3.3.* Lyngby, Denmark: Calsep.

Craft, B. C. & Hawkins, M. F., 1991. *Applied Petroleum Reservoir Engineering.* Englewood Cliffs, NJ, USA: Prentice Hall.

Dake, L. P., 1978. *Fundamentals of Reservoir Engineering.* Amsterdam, The Netherlands: Elsevier Scientific B.V..

EPA, 2016. *eGRID Summary Tables,* USA: United States Environmental Protection Agency.

Fanchey, J. R., 1985. Analytical Representation of the Van Everdingen-Hurst Aquifer Influence Functions for Reservoir Simulation. *SPE Journal,* pp. 405-406.

IPCC, 2001. *Climate Change 2001. The Third Assessment Report of the Intergovernmental Panel on Climate Change,* Cambridge, UK: Cambridge University Press.

IPCC, 2005. *IPCC Special Report on Carbon Dioxide Capture and Storage.,* Cambridge, UK and New York, NY, USA: Cambridge University Press.

IPCC, 2012. *Summary for Policymakers. In: Managing the Risks of Extreme Events and Disasters to Advance Climate Change Adaptation,* Cambridge, UK and New York, NY, USA: Cambridge University Press.

IPCC, 2013. *Summary for Policymakers. In: Climate Change 2013: The Physical Science Basis. ,* Cambridge, UK and New York, NY, USA: Cambridge University Press.

IPCC, 2014. *Summary for Policymakers. In: Climate Change 2014: Impacts, Adaptation, and Vulnerability. Part A: Global and Sectoral Aspects.,* Cambridge, UK and New York, NY, USA: Cambridge University Press.

Kumagai, A. & Yokohama, C., 1999. Viscosity of Aqueous Solutions of CO_2 at high pressures. *International Journal of Thermophysics,* 19(5), pp. 1315-1323.

Lake, L. W., 1989. *Enhanced Oil Recovery.* New Jersey: Prentice Hall.

Lawal, A. S. & Frailey, S. M., 2002. *Material Balance Reservoir Model for* CO_2 *Sequestration in Depleted Gas Reservoirs. SPE 90669.* Houston, TX, USA, Society of Petroleum Engineers. SPE Annual Technical Conference and Exhibition.

Li, H. et al., 2011. Viscosities, Thermal Conductivities and Diffusion Coefficients of CO_2 Mixtures: Review of Experimental Data and Theoretical Models. *International Journal of Greenhouse Gas Control,* Volume 5, pp. 1119-1139.

Mamora, D. D. & Seo, J. G., 2002. *Enhanced Gas Recovery by Carbon Dioxide Sequestration in Depleted Gas Reservoirs. SPE 77347.* Houston, TX, USA, SPE Annual Technical Conference and Exhibition.

Marle, C. M., 1981. *Multiphase Flow in Porous Media.* Houston, TX, USA: Gulf Publishing.

Mysiak, J. et al., 2016. Brief Communication: Sendai Framework for Disaster Risk Reduction - Success of Warning Sign for Paris?. *Natural Hazards and Earth System Sciences,* 16(10), pp. 2189-2193.

Oldenburg, C. M. & Benson, S. M., 2002. CO_2 *Injection for Enhanced Gas Production and Carbon Sequestration. SPE 74367.* Villahermosa, Mexico, SPE International Petroleum Conference and Exhibition in Mexico.

Sobers, L. E. & Frailey, S. M., 2004. *Geological Sequestration of Carbon Dioxide in Depleted Gas Reservoirs. SPE 89345.* Tulsa, OK, USA, Society of Petroleum Engineers. SPE/DOE Symposium on Improved Oil Recovery.

Tseng, C. C., Hsieh, B. Z., Hu, S. T. & Lin, Z. S., 2012. Analytical Approach for Estimating CO_2 Storage Capacity of Produced Gas Reservoirs with or without Water Drive. *International Journal of Greenhouse Gas Control,* Volume 9, pp. 254-261.

Van Everdingen, A. F. & Hurst, W., 1949. The Application of the Laplace Transformation to Flow Problems in Reservoirs. *Trans. AIME,* pp. 305-324.

APPENDIX A

PRESSURE AND WATER INFLUX TREND FROM CALCULATION

CONSIDERING CO_2 SOLUBILITY IN WATER

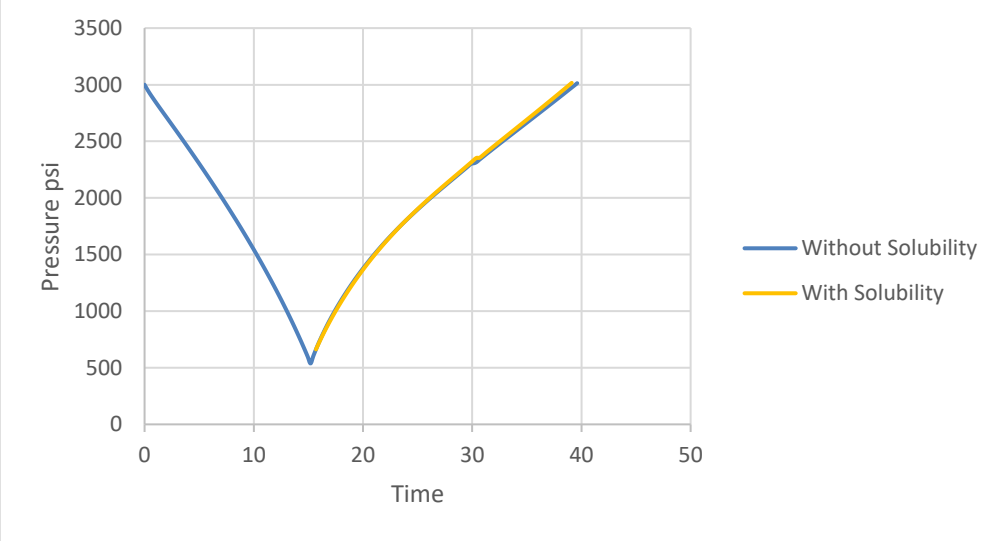

Figure A-1. Pressure Trend for Radial Aquifer-Reservoir Ratio = 5

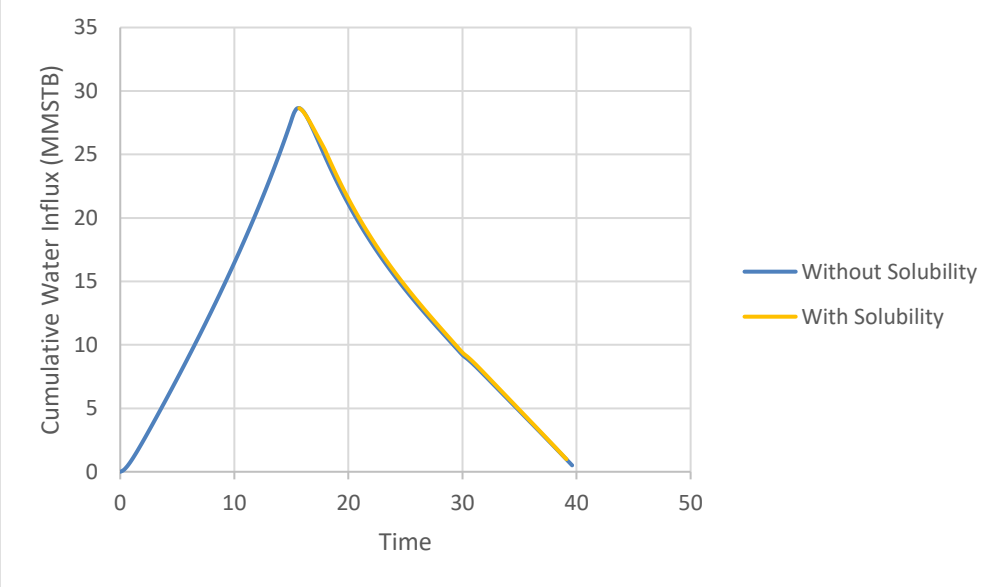

Figure A-2. Water Influx Trend for Radial Aquifer-Reservoir Ratio = 5

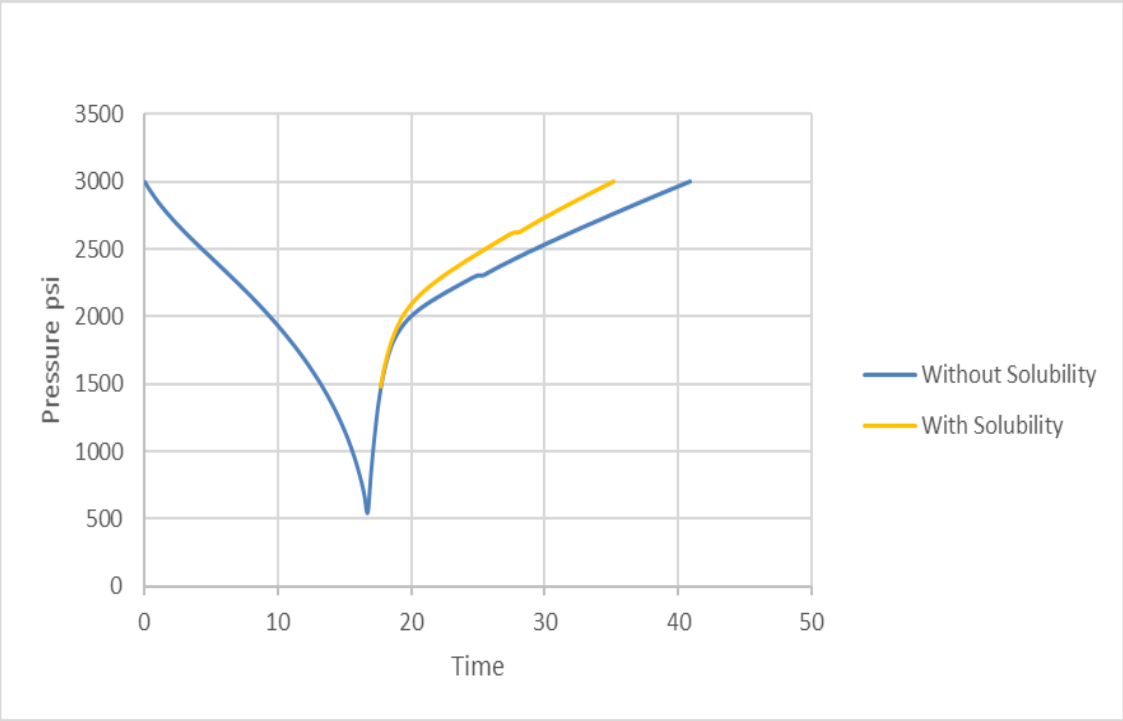

Figure A-3. Pressure Trend for Radial Aquifer-Reservoir Ratio = 10

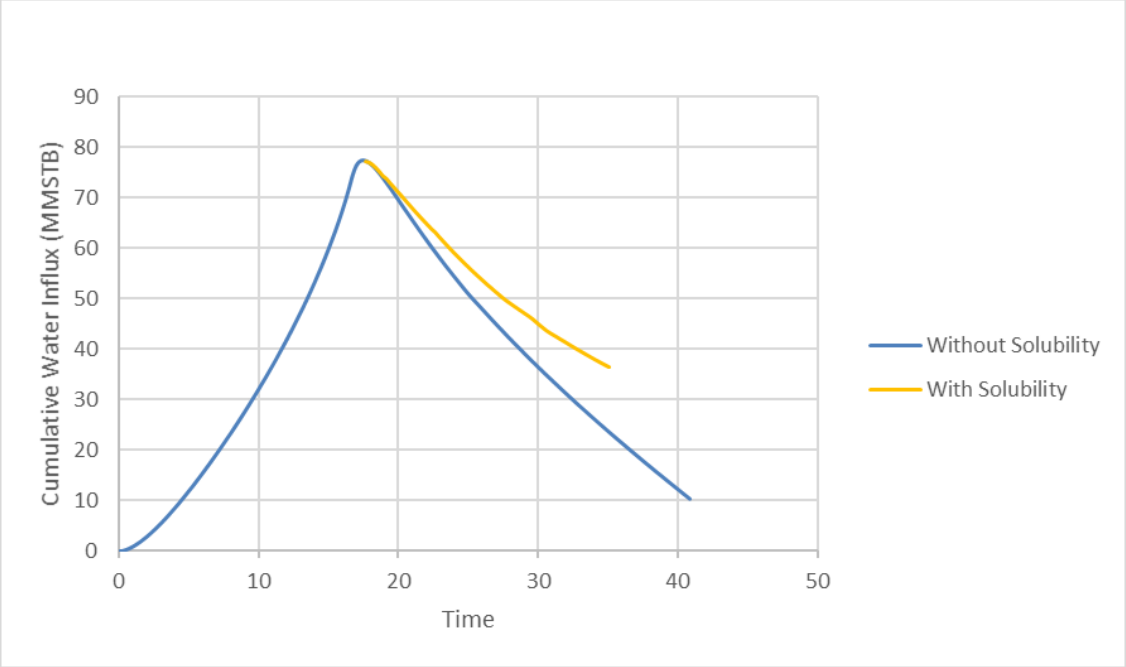

Figure A-4. Water Influx Trend for Radial Aquifer-Reservoir Ratio = 10

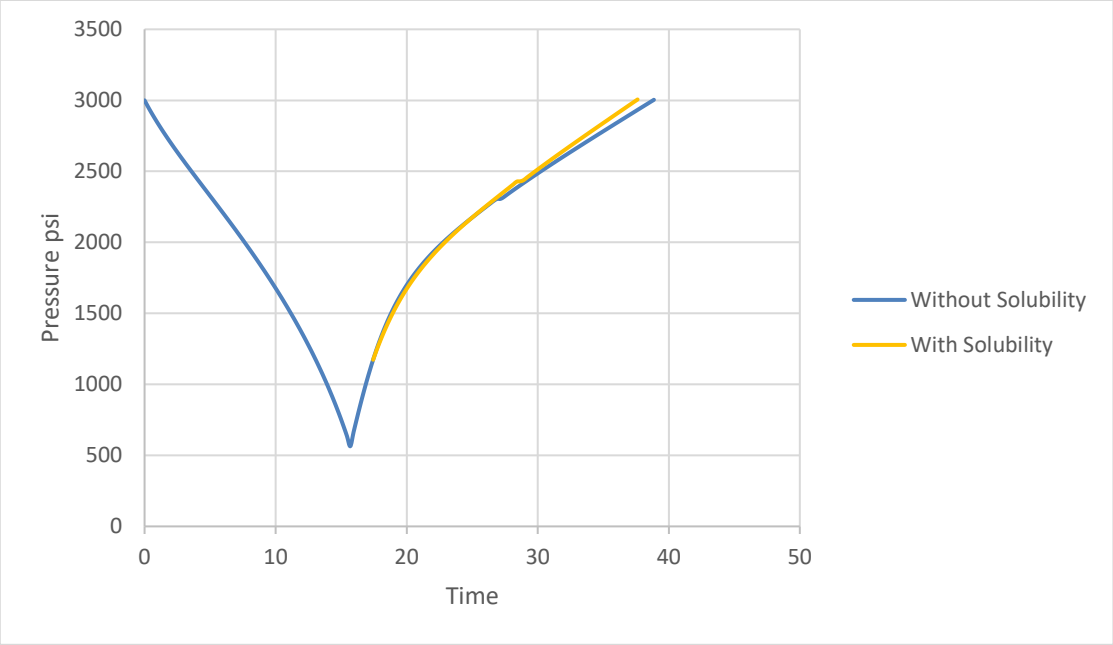

Figure A-5. Pressure Trend for Aquifer Permeability = 50 mD

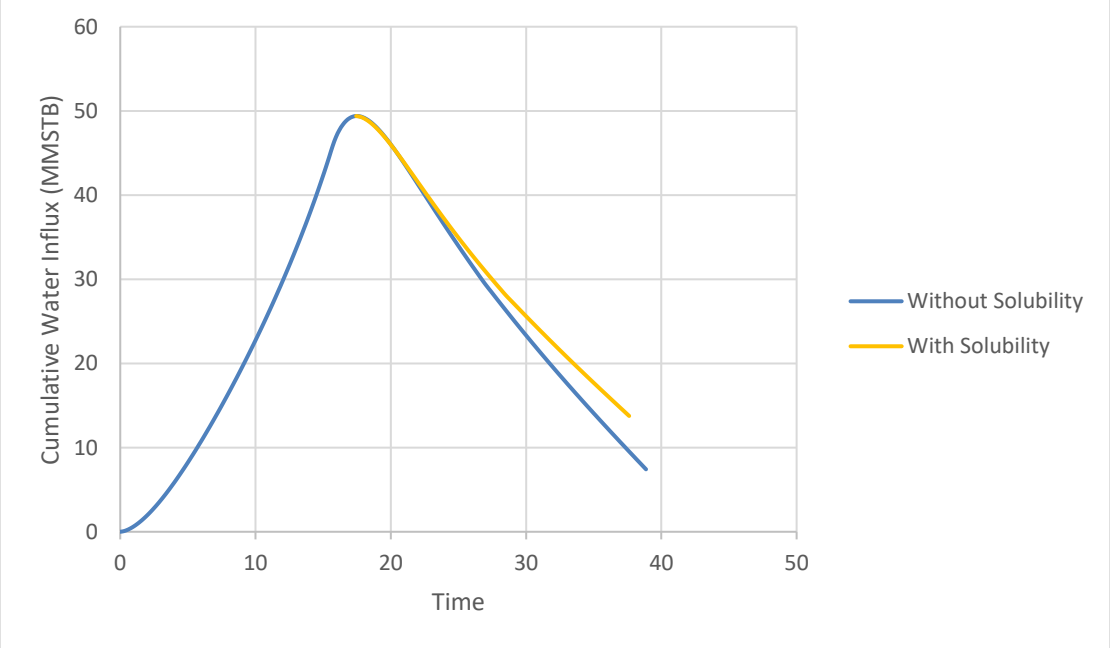

Figure A-6. Water Influx Trend for Aquifer Permeability = 50 mD

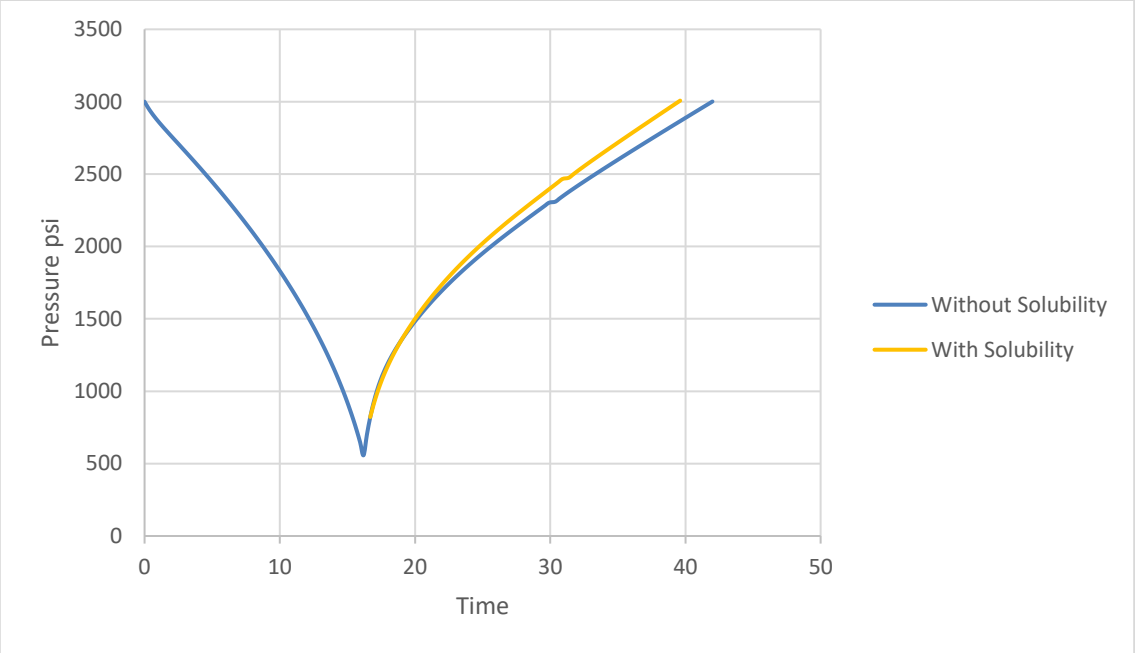

Figure A-7. Pressure Trend for Aquifer Permeability = 200 mD

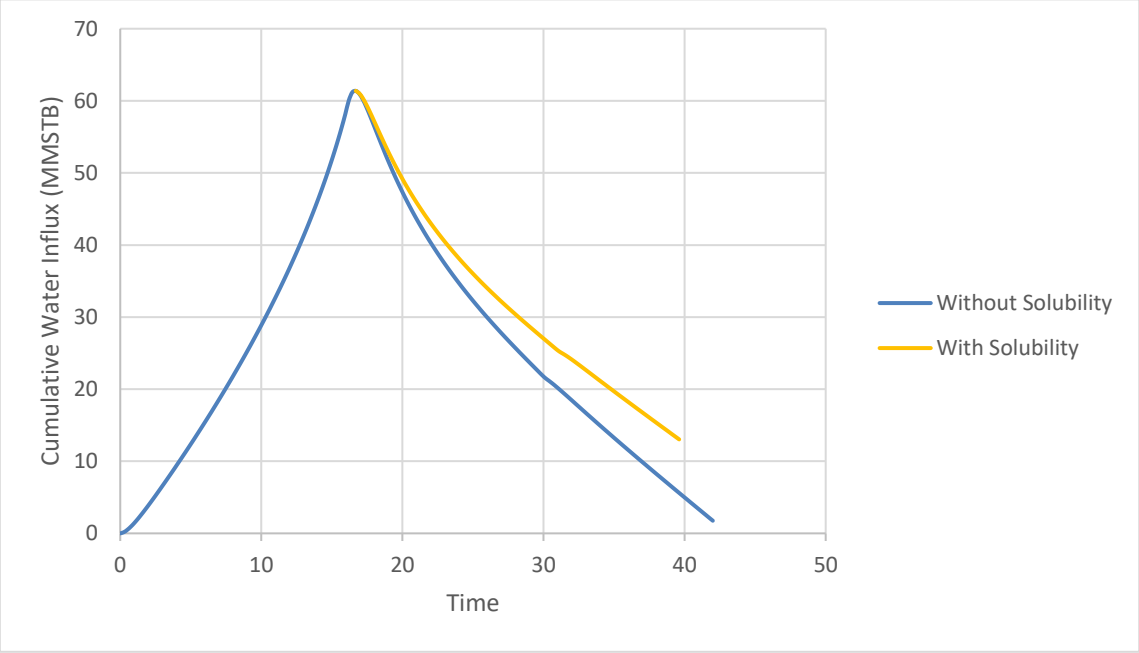

Figure A-8. Water Influx Trend for Aquifer Permeability = 200 mD

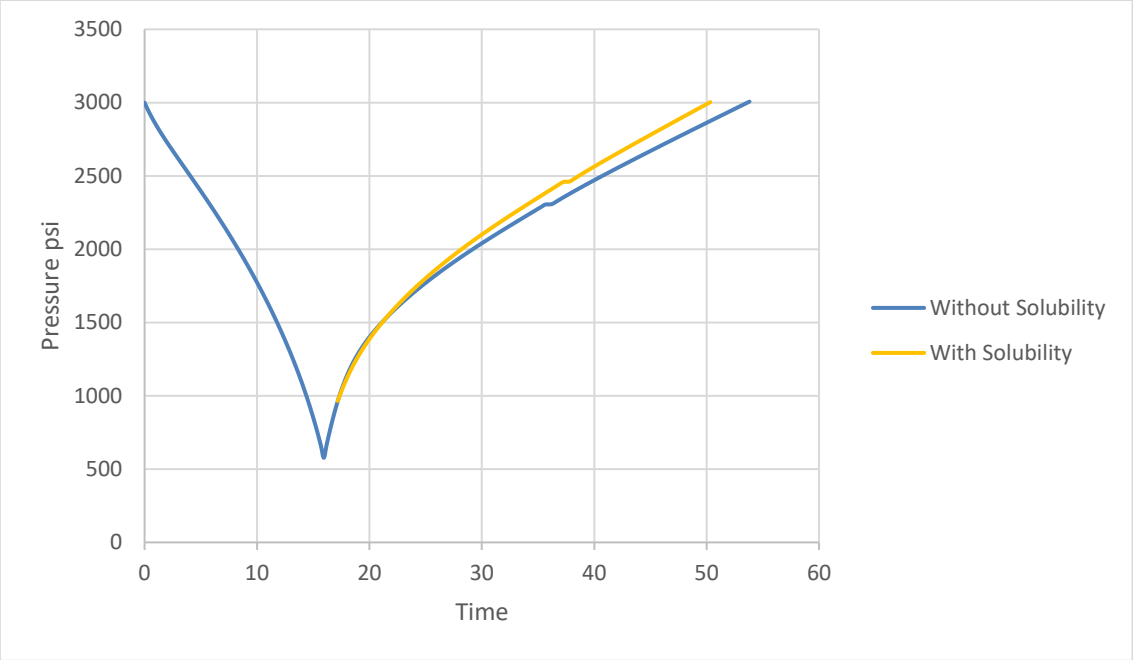

Figure A-9. Pressure Trend for Injection rate = 10 MMSCFD

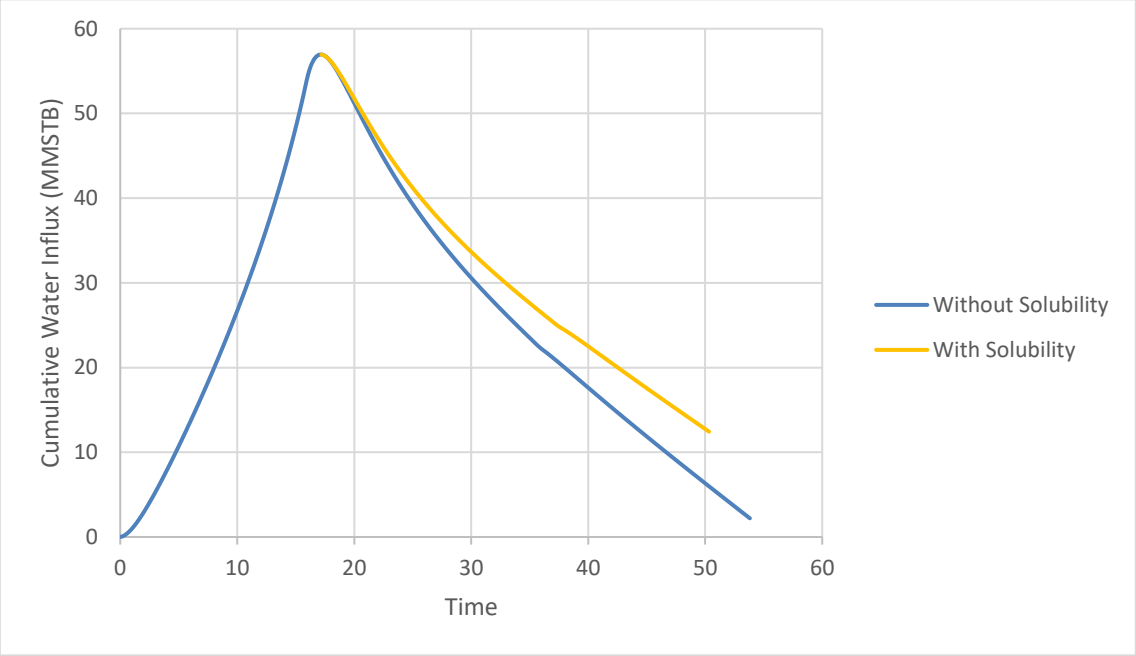

Figure A-10. Water Influx Trend for Injection rate = 10 MMSCFD

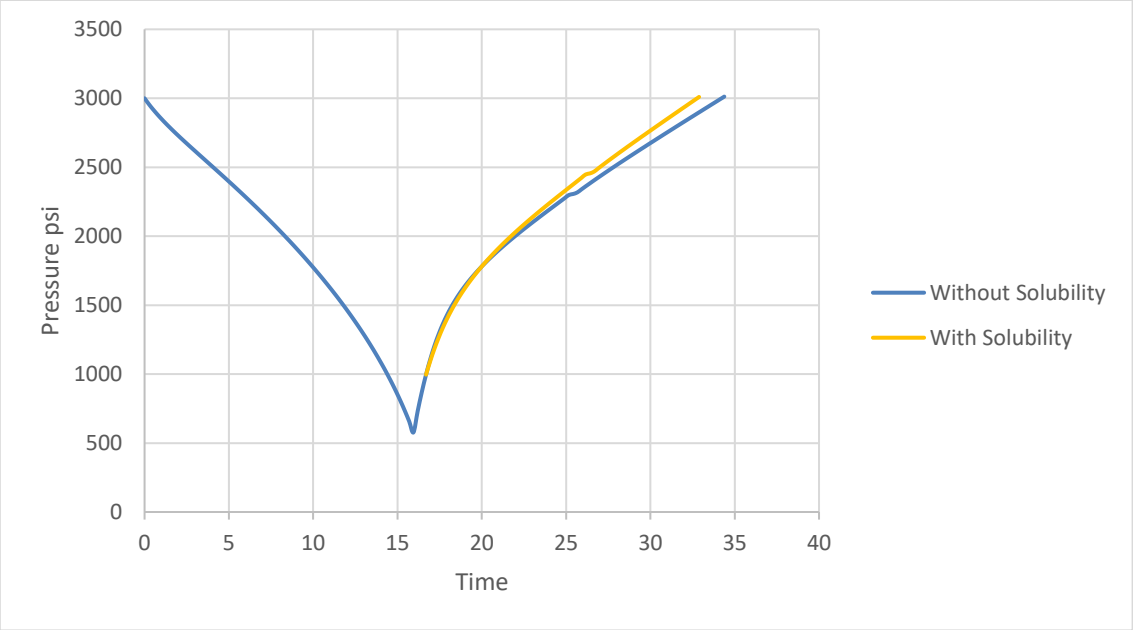

Figure A-11. Pressure Trend for Injection rate = 20 MMSCFD

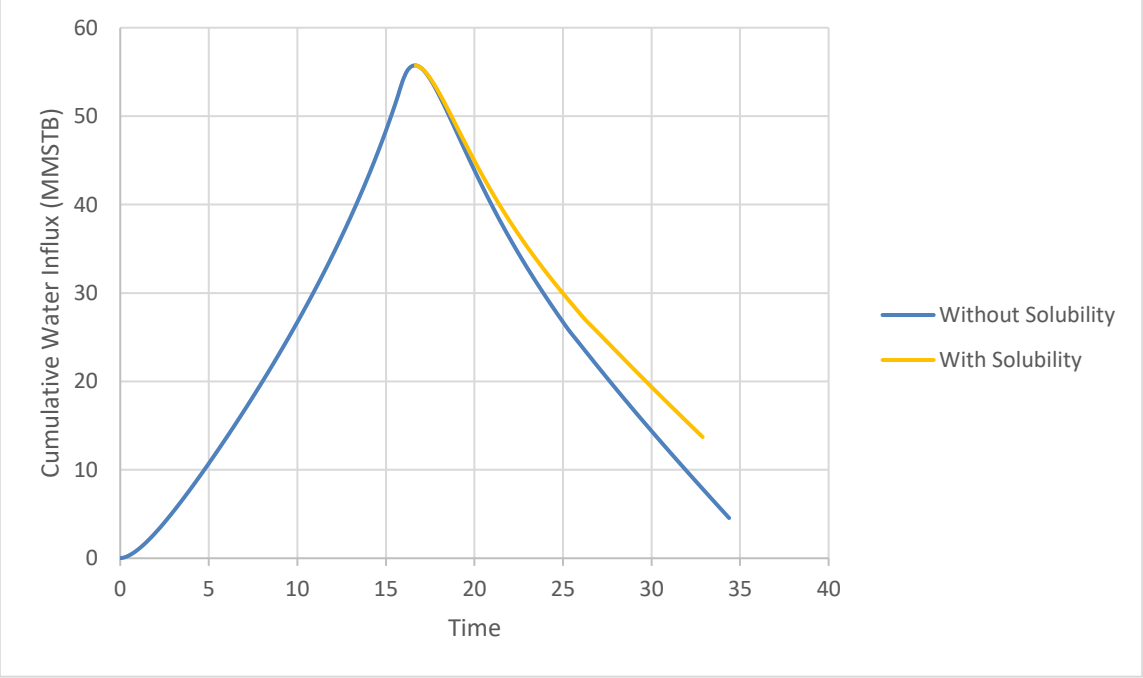

Figure A-12. Water Influx Pressure Trend for Injection rate = 20 MMSCFD

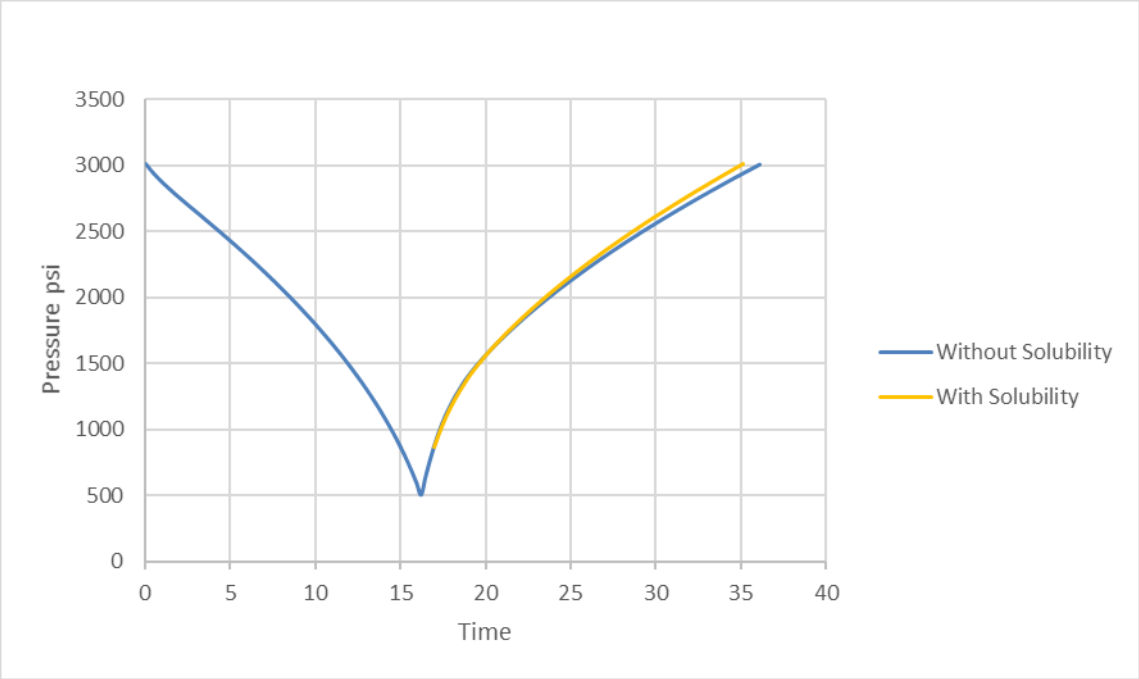

Figure A-13. Pressure Trend for Temperature = 300ºF

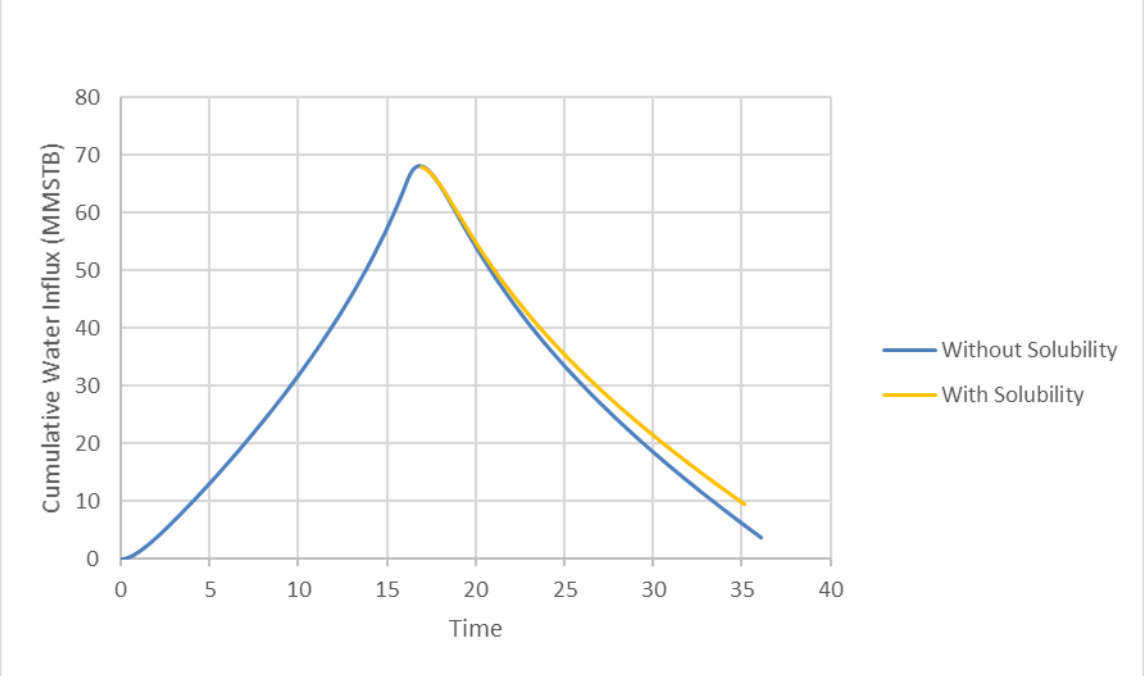

Figure A-14. Water Influx Trend for Temperature = 300ºF

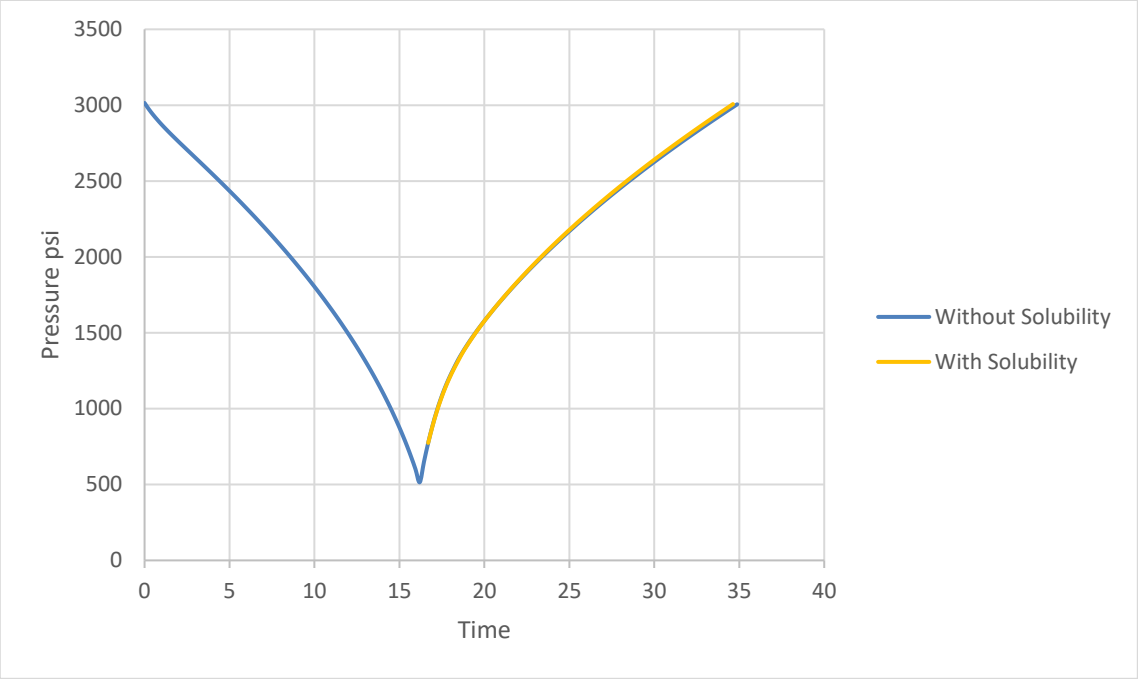

Figure A-15. Pressure Trend for Temperature = 350ºF

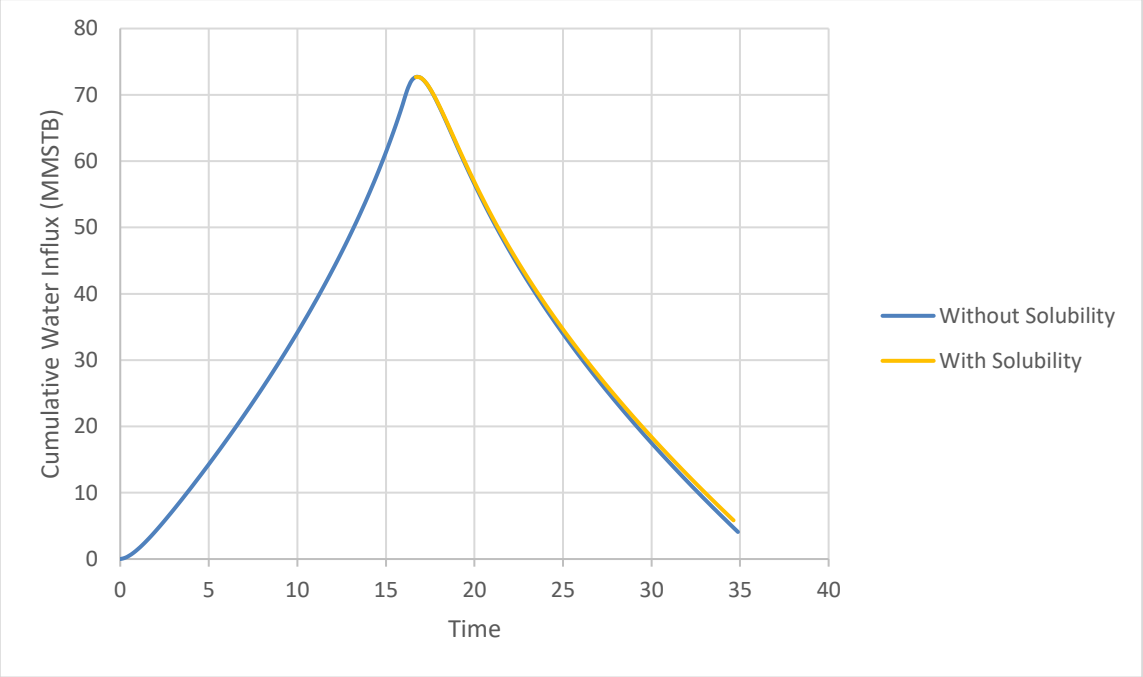

Figure A-16. Water Influx Trend for Temperature = 350ºF

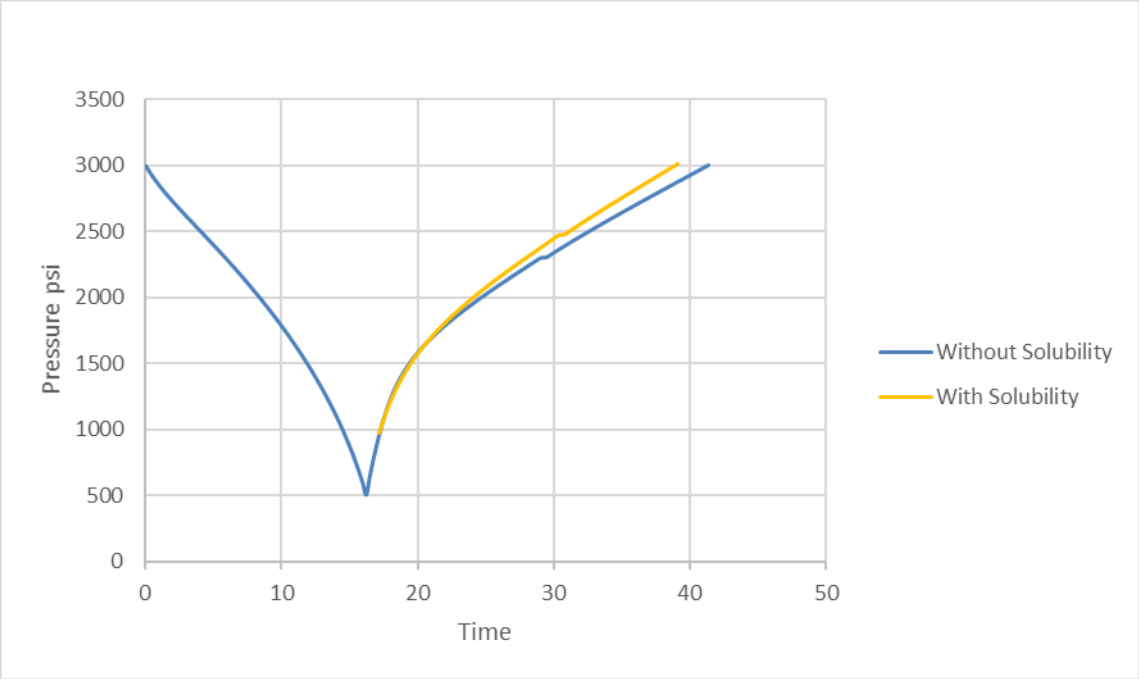

Figure A-17. Pressure Trend for Salinity = 5000 ppm

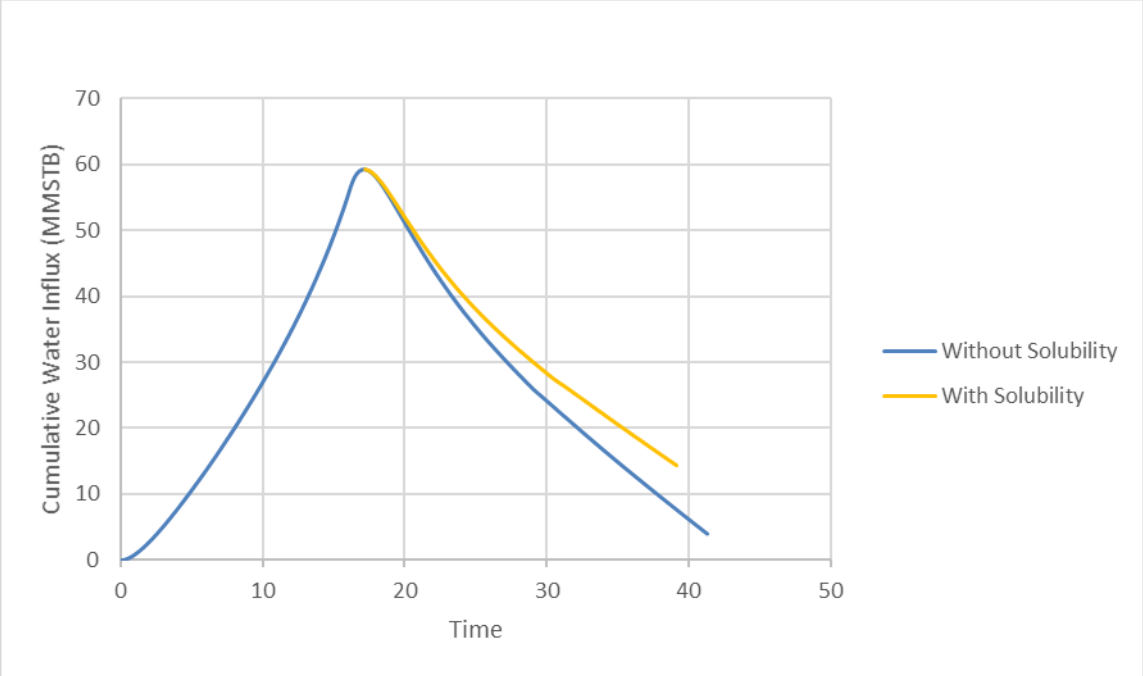

Figure A-18. Water Influx Trend for Salinity = 5000 ppm

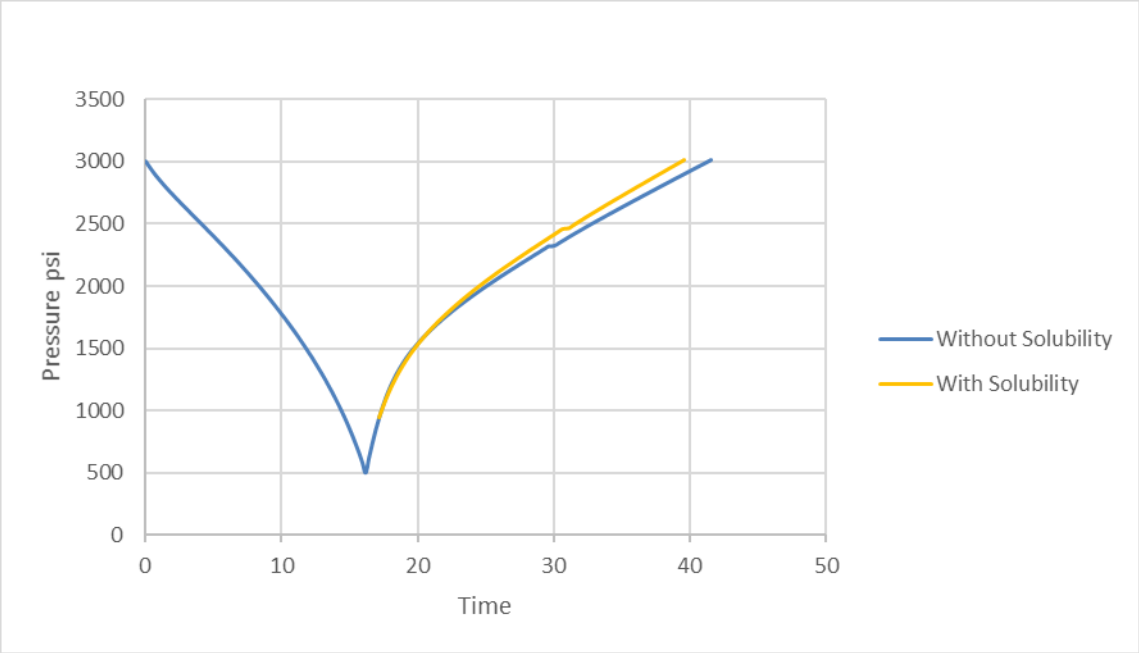

Figure A-19. Pressure Trend for Salinity = 15000 ppm

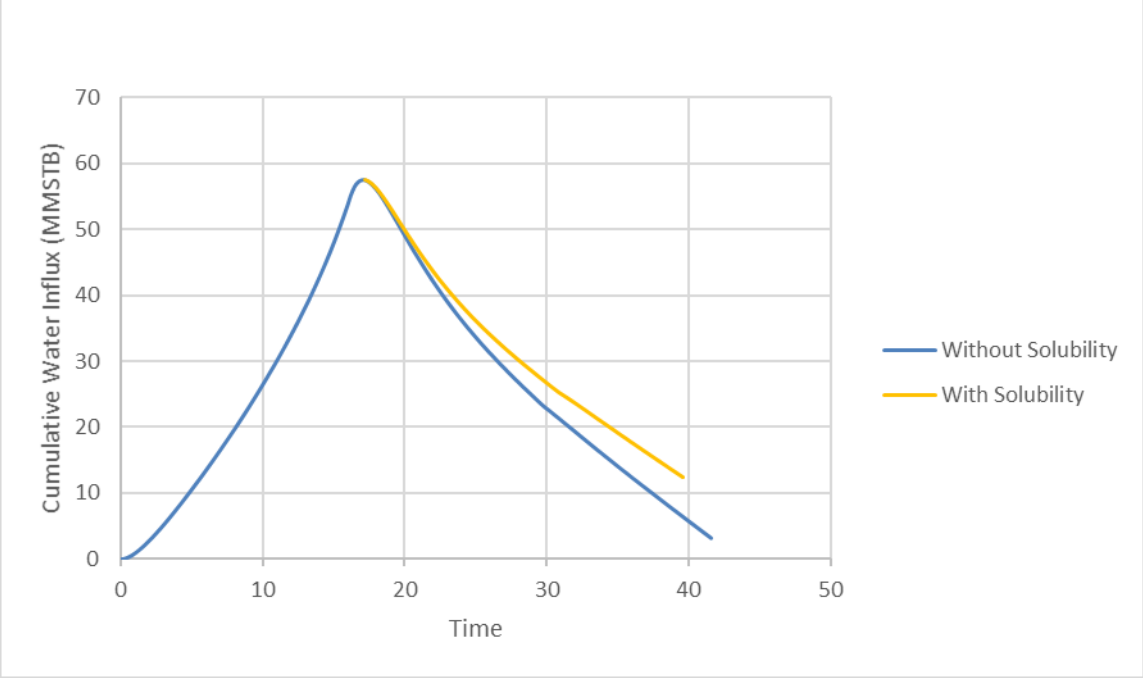

Figure A-20. Water InfluxTrend for Salinity = 15000 ppm

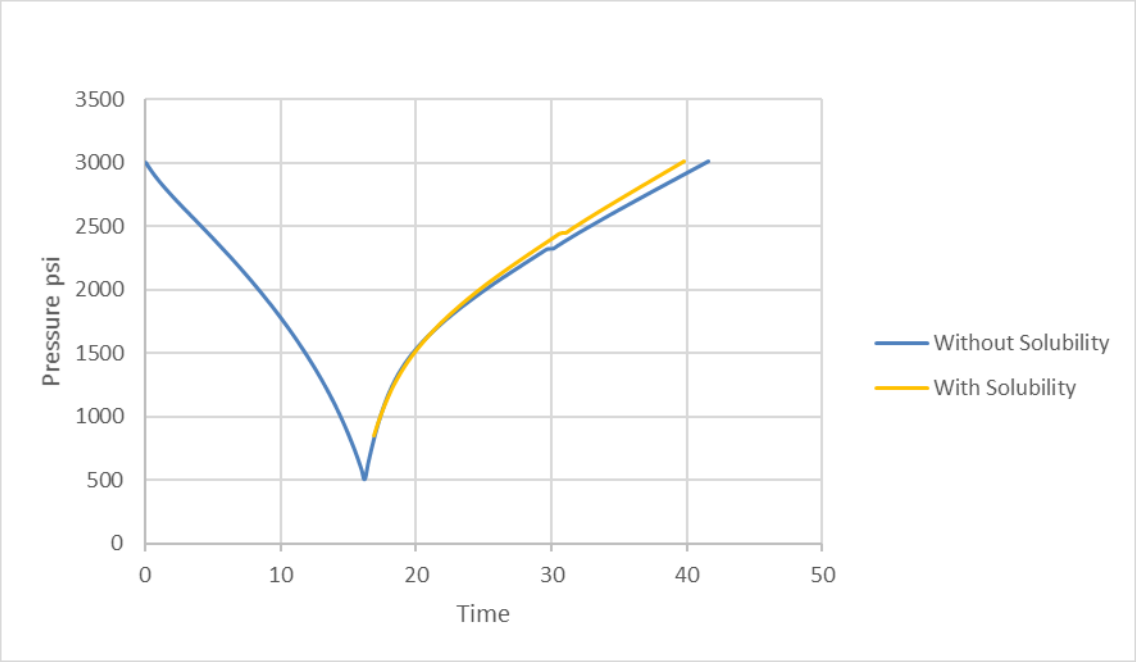

Figure A-21. Pressure Trend for Salinity = 25000 ppm

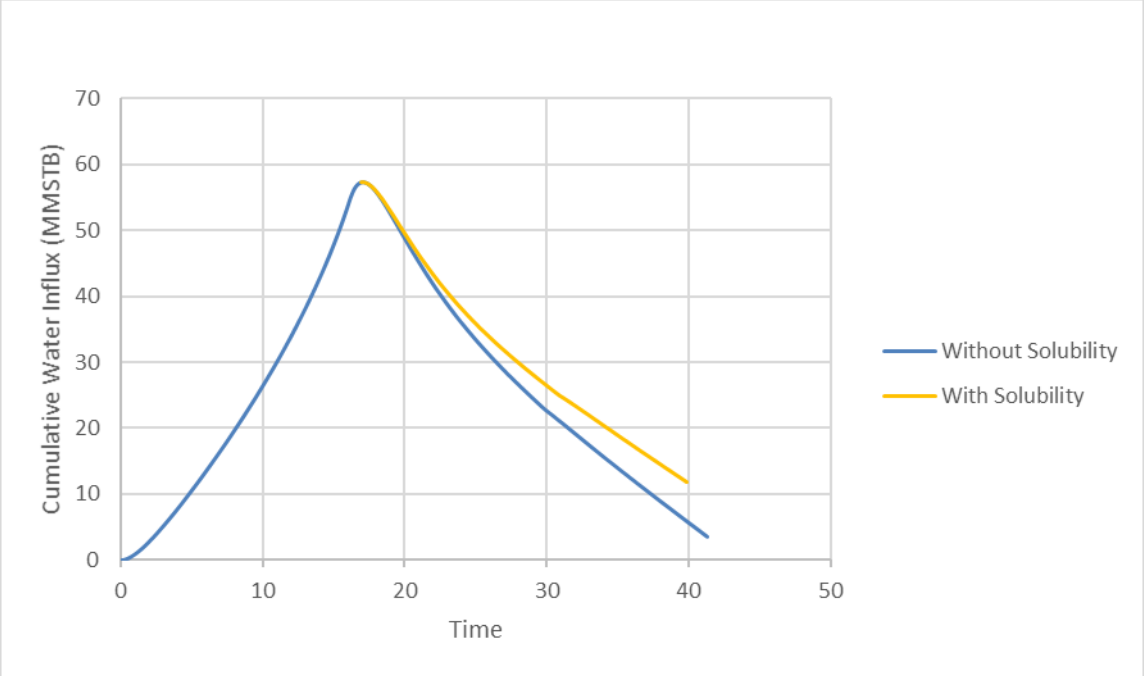

Figure A-22. Water Influx Trend for Salinity = 25000 ppm

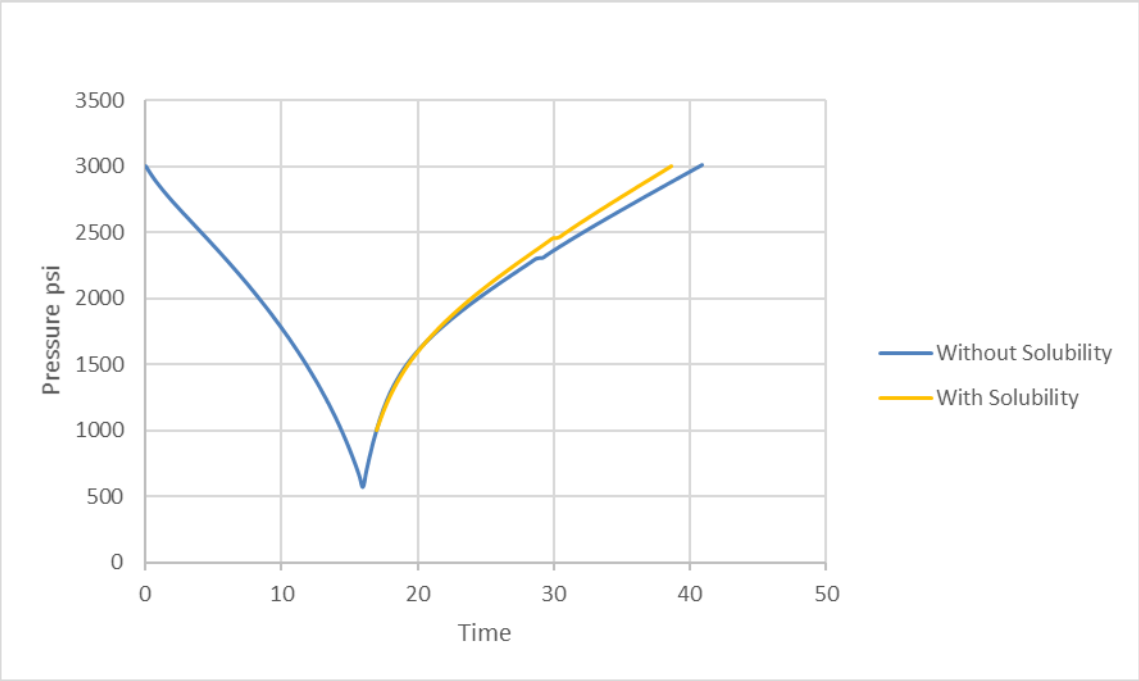

Figure A-23. Pressure Trend for NPE = 10

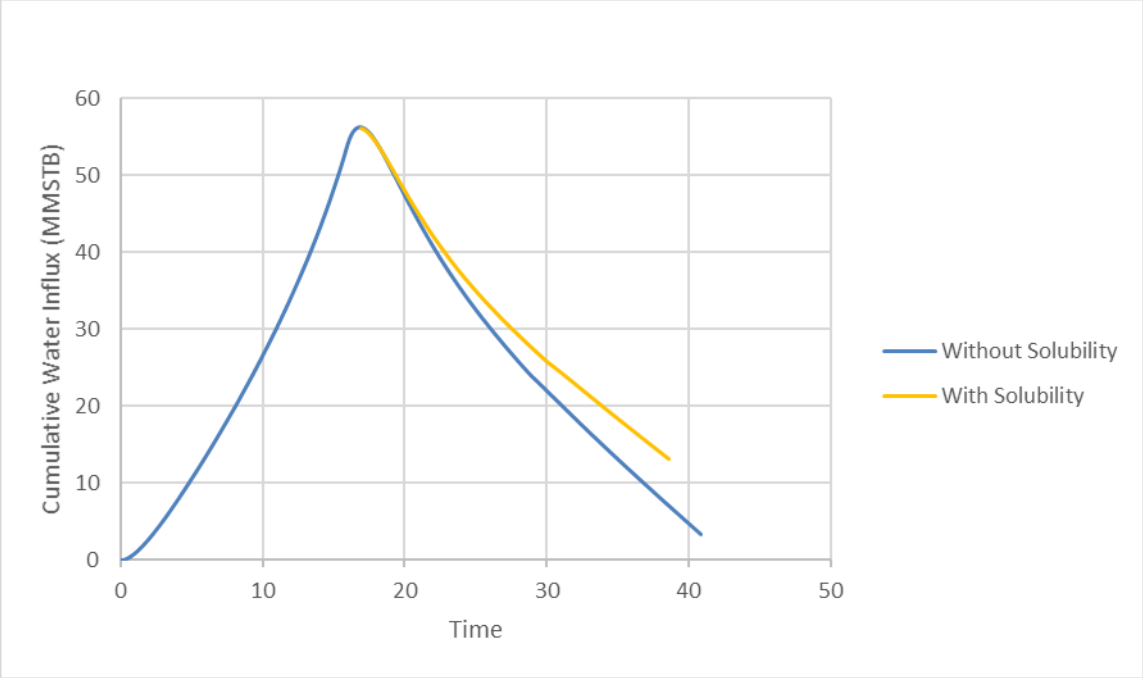

Figure A-24. Water Influx Trend for NPE = 10

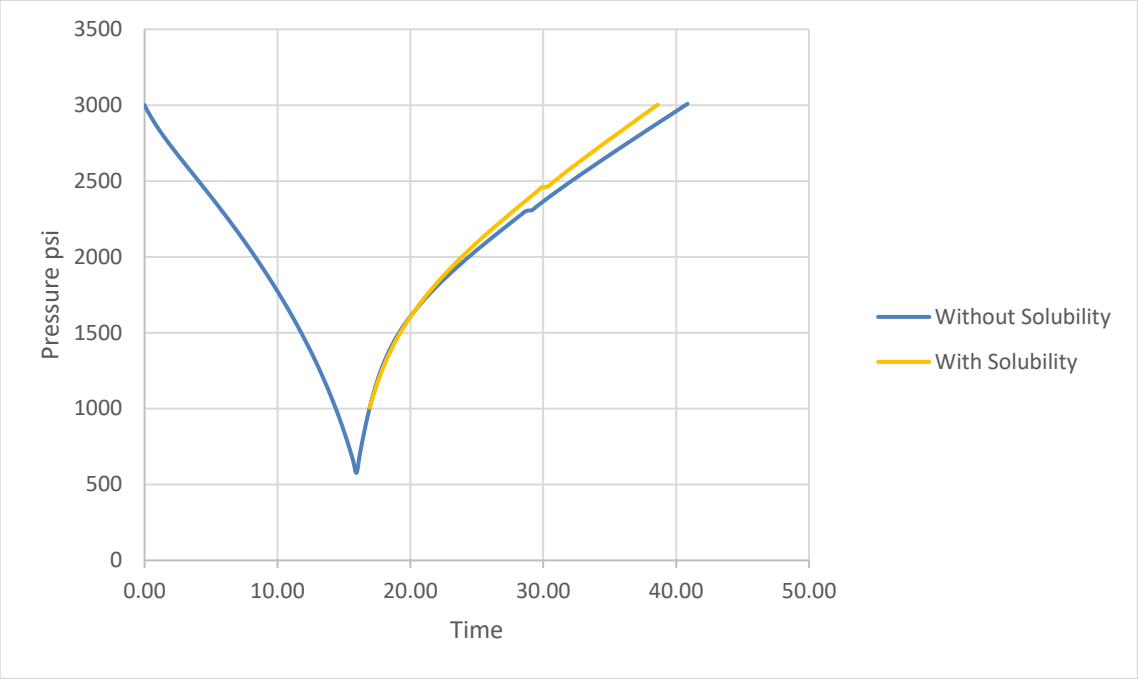

Figure A-25. Pressure Trend for NPE = 25

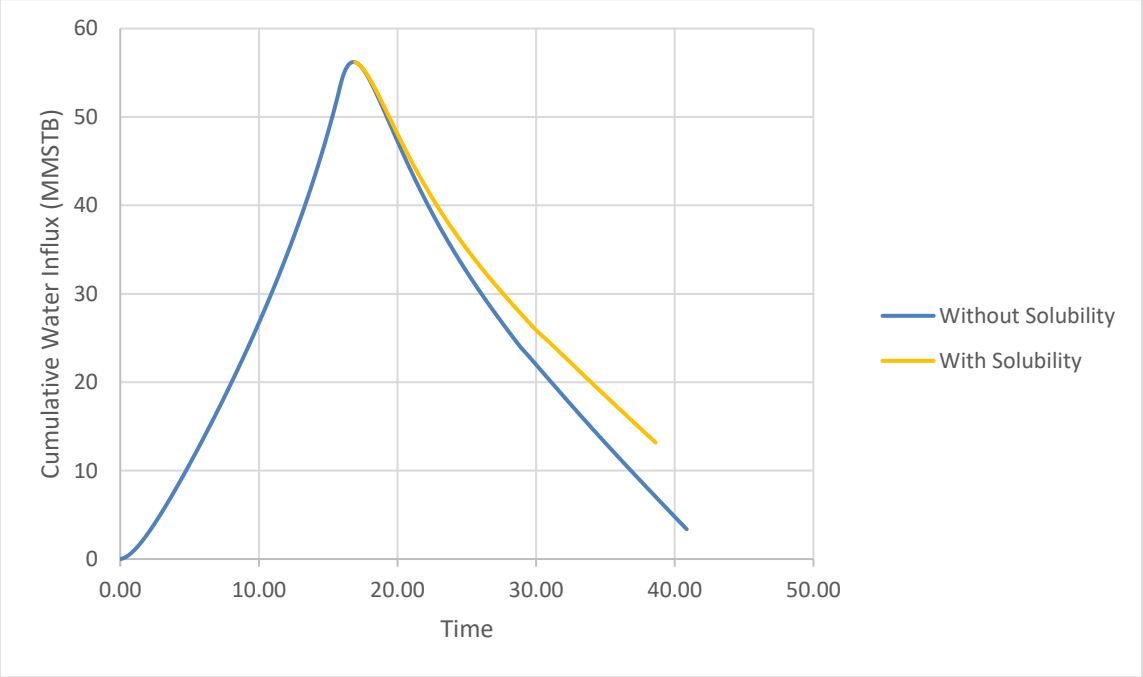

Figure A-26. Water Influx Trend for NPE = 25

APPENDIX B

CODE FOR CO_2 SOLUBILITY, DENSITY, AND VISCOSITY; RESULTS FROM CONVENTIONAL MATERIAL BALANCE AND EACH ITERATION

VBA Code for CO_2 solubility:

```
Sub main()
Dim penunjuk As Range
Dim t As Double
Dim P As Double
Dim C As Double

'Set worksheet
Dim ws As Worksheet
Set ws = Sheets("Sheet1")
ws.Select

Set penunjuk = Range("A15").EntireRow.Find("CO2 %")
Set penunjuk = penunjuk.End(xlDown)

t = 200
While Not (IsEmpty(penunjuk.Value))
P = penunjuk.Offset(0, -13).Value
C = penunjuk.Value
penunjuk.Offset(0, 1).Value = Setiawan(t, P, C)
Set penunjuk = penunjuk.Offset(1, 0)
Wend
ws.Select
End Sub

Function Setiawan(t As Double, P As Double, C As Double) As Double

'1) Gather data
'2) Navigate to the correct cell based on user input
'3) Calculate the appropriate solubility

'Dim temp As Double
'Dim pressure As Double
'Dim composition As Double

Dim result As Double
```

```
Dim pointer As Range
Dim presP As Range
Dim compP As Range

Dim soluIPCC As Double
Dim soluIPPrevC As Double
Dim solu As Double

Dim safetyCounter As Integer

'Set worksheet ke Sheet2 tempat datanya
Dim ws As Worksheet

Set ws = Sheets("Sheet2")
ws.Select
'1)

'Pasang pointer ke cell yang contain word "Temperature"
'Set pointer = Range("A1").EntireColumn.Find("Temperature")

'temp = pointer.Offset(0, 1).Value
'pressure = pointer.Offset(1, 1).Value
'composition = pointer.Offset(2, 1).Value

'2)
Set pointer = Range("A1").Offset(1, 0)

While t > pointer.Value
   Set pointer = pointer.Offset(0, 5)
Wend

If (t <> pointer.Value) Then
   MsgBox ("We can't seem to find the exact temperature for your input: " & temp &
vbNewLine & "We are showing results from temperature of " & pointer.Value & "
instead.")
End If

'If we reached the correct Temp table, we can go through the corresponding pressure and
composition

'Go through each value on the composition (CO2) column and stop when the
corresponding value is found
Set compP = pointer.Offset(0, 1)
```

```
While (C > compP.Value) And Not (IsEmpty(compP.End(xlDown)))
   Set compP = compP.End(xlDown)
Wend


'Go through each value on the Pressure column in the corresponding composition section
' and stop when the corresponding pressure value is found
Set presP = compP.Offset(0, 1)
safetyCounter = 0
While (P > presP.Value) And (safetyCounter < 19)
   Set presP = presP.Offset(1, 0)
   safetyCounter = safetyCounter + 1
Wend


'3)
'soluIPCC => Solubility at input pressure and Current Pointer Composition
soluIPCC = ((P - presP.Offset(-1, 0).Value) / (presP.Value - presP.Offset(-1, 0).Value) *
(presP.Offset(0, 1).Value - presP.Offset(-1, 1).Value)) + presP.Offset(-1, 1).Value

'soluIPPrevC => Solubility at input pressure and at previous Pointer Composition
soluIPPrevC = ((P - presP.Offset(-11, 0).Value) / (presP.Value - presP.Offset(-11,
0).Value) * (presP.Offset(-10, 1).Value - presP.Offset(-11, 1).Value)) + presP.Offset(-
11, 1).Value

'solu => Output
solu = ((C - compP.Offset(-10, 0).Value) / (compP.Value - compP.Offset(-10, 0).Value))
* (soluIPCC - soluIPPrevC) + soluIPPrevC

Setiawan = solu

End Function
```

VBA for water density:

```
Sub main()
Dim penunjuk As Range
Dim t As Double
Dim P As Double
Dim C As Double
Dim i As Integer

'Set worksheet
```

```
Dim ws As Worksheet
Set ws = Sheets("Convection Diffusion")
ws.Select

Set penunjuk = Range("R4")

t = 200
i = 0

While i < 11

While Not (IsEmpty(penunjuk.Value))
P = penunjuk.Offset(0, -3 - i).Value
C = penunjuk.Value
penunjuk.Offset(0, 11).Value = Setiawan(t, P, C)
Set penunjuk = penunjuk.Offset(1, 0)
Wend
Set ws = Sheets("Convection Diffusion")
ws.Select
Set penunjuk = Range("R4").Offset(0, i + 1)
i = i + 1

Wend
ws.Select


End Sub


Function Setiawan(t As Double, P As Double, C As Double) As Double

'1) Gather data
'2) Navigate to the correct cell based on user input
'3) Calculate the appropriate density

'Dim temp As Double
'Dim pressure As Double
'Dim composition As Double

Dim result As Double

Dim pointer As Range
Dim presP As Range
Dim compP As Range
```

```
Dim densityIPCC As Double
Dim densityIPPrevC As Double
Dim density As Double

Dim safetyCounter As Integer

'Set worksheet ke Sheet2 tempat datanya
Dim ws As Worksheet

Set ws = Sheets("Sheet2")
ws.Select
'1)

temp = pointer.Offset(0, 1).Value
pressure = pointer.Offset(1, 1).Value
composition = pointer.Offset(2, 1).Value

'2)
Set pointer = Range("A1").Offset(1, 0)

While t > pointer.Value
   Set pointer = pointer.Offset(0, 5)
Wend

If (t <> pointer.Value) Then
   MsgBox ("We can't seem to find the exact temperature for your input: " & temp &
vbNewLine & "We are showing results from temperature of " & pointer.Value & "
instead.")
End If

'If we reached the correct Temp table, we can go through the corresponding pressure and
composition

'Go through each value on the composition (CO2) column and stop when the
corresponding value is found
Set compP = pointer.Offset(0, 1)

While (C >= compP.Value) And Not (IsEmpty(compP.End(xlDown)))
   Set compP = compP.End(xlDown)
Wend


'Go through each value on the Pressure column in the corresponding composition section
```

```
' and stop when the corresponding pressure value is found
Set presP = compP.Offset(0, 1)
safetyCounter = 0
While (P > presP.Value) And (safetyCounter < 10)
   Set presP = presP.Offset(1, 0)
   safetyCounter = safetyCounter + 1
Wend


'3)
'densityIPCC => Density at input pressure and Current Pointer Composition
densityIPCC = ((P - presP.Offset(-1, 0).Value) / (presP.Value - presP.Offset(-1,
0).Value) * (presP.Offset(0, 1).Value - presP.Offset(-1, 1).Value)) + presP.Offset(-1,
1).Value

'densityIPPrevC => Density at input pressure and at previous Pointer Composition
densityIPPrevC = ((P - presP.Offset(-11, 0).Value) / (presP.Value - presP.Offset(-11,
0).Value) * (presP.Offset(-10, 1).Value - presP.Offset(-11, 1).Value)) + presP.Offset(-
11, 1).Value

'density => Output
density = ((C - compP.Offset(-10, 0).Value) / (compP.Value - compP.Offset(-10,
0).Value)) * (densityIPCC - densityIPPrevC) + densityIPPrevC

Setiawan = density

End Function
```

VBA code for water density and viscosity:

```
Sub main()
Dim penunjuk As Range
Dim t As Double
Dim P As Double
Dim C As Double
Dim solu As Double
Dim i As Integer

'Set worksheet
Dim ws As Worksheet
Set ws = Sheets("Convection Diffusion")
ws.Select
```

```
Set penunjuk = Range("R4")

t = 200
i = 0

While i < 11

While Not (IsEmpty(penunjuk.Value))
P = penunjuk.Offset(0, -3 - i).Value
C = penunjuk.Value
solu = penunjuk.Offset(0, -2 - i).Value
penunjuk.Offset(0, 11).Value = Setiawan(t, P, C)
penunjuk.Offset(0, 22).Value = viscosity(P, C, solu)
Set penunjuk = penunjuk.Offset(1, 0)
Wend
Set ws = Sheets("Convection Diffusion")
ws.Select
Set penunjuk = Range("R4").Offset(0, i + 1)
i = i + 1

Wend
ws.Select

End Sub

Function Setiawan(t As Double, P As Double, C As Double) As Double
'command yang gk perlu gw jadiin comment

'1) Gather data
'2) Navigate to the correct cell based on user input
'3) Calculate the appropriate density

'Dim temp As Double
'Dim pressure As Double
'Dim composition As Double

Dim result As Double

Dim pointer As Range
Dim presP As Range
Dim compP As Range

Dim densityIPCC As Double
Dim densityIPPrevC As Double
```

```
Dim density As Double

Dim safetyCounter As Integer

'Set worksheet ke Sheet2 tempat datanya
Dim ws As Worksheet

Set ws = Sheets("Sheet2")
ws.Select
'1)

'Pasang pointer ke cell yang contain word "Temperature"
'Set pointer = Range("A1").EntireColumn.Find("Temperature")

'temp = pointer.Offset(0, 1).Value
'pressure = pointer.Offset(1, 1).Value
'composition = pointer.Offset(2, 1).Value

'2)
Set pointer = Range("A1").Offset(1, 0)

While t > pointer.Value
   Set pointer = pointer.Offset(0, 5)
Wend

If (t <> pointer.Value) Then
   MsgBox ("We can't seem to find the exact temperature for your input: " & temp &
vbNewLine & "We are showing results from temperature of " & pointer.Value & "
instead.")
End If

'If we reached the correct Temp table, we can go through the corresponding pressure and
composition

'Go through each value on the composition (CO2) column and stop when the
corresponding value is found
Set compP = pointer.Offset(0, 1)

While (C >= compP.Value) And Not (IsEmpty(compP.End(xlDown)))
   Set compP = compP.End(xlDown)
Wend


'Go through each value on the Pressure column in the corresponding composition section
```

```
' and stop when the corresponding pressure value is found
Set presP = compP.Offset(0, 1)
safetyCounter = 0
While (P > presP.Value) And (safetyCounter < 10)
   Set presP = presP.Offset(1, 0)
   safetyCounter = safetyCounter + 1
Wend


'3)
'densityIPCC => Density at input pressure and Current Pointer Composition
densityIPCC = ((P - presP.Offset(-1, 0).Value) / (presP.Value - presP.Offset(-1,
0).Value) * (presP.Offset(0, 1).Value - presP.Offset(-1, 1).Value)) + presP.Offset(-1,
1).Value

'densityIPPrevC => Density at input pressure and at previous Pointer Composition
densityIPPrevC = ((P - presP.Offset(-11, 0).Value) / (presP.Value - presP.Offset(-11,
0).Value) * (presP.Offset(-10, 1).Value - presP.Offset(-11, 1).Value)) + presP.Offset(-
11, 1).Value

'density => Output
density = ((C - compP.Offset(-10, 0).Value) / (compP.Value - compP.Offset(-10,
0).Value)) * (densityIPCC - densityIPPrevC) + densityIPPrevC

'Show the resulting density to the cell
'Set pointer = Range("A1").EntireColumn.Find("Density:").Offset(0, 1)
'pointer.Value = density

Setiawan = density

End Function

Function viscosity(P As Double, C As Double, solu As Double) As Double

'Dim temp As Double
'Dim pressure As Double
'Dim composition As Double

'Dim result As Double

Dim pointer As Range
Dim presP As Range
Dim compP As Range
```

```
Dim visc0 As Double

Dim safetyCounter As Integer

'Set worksheet ke Sheet2 tempat datanya
Dim ws As Worksheet

Set ws = Sheets("Sheet3")
ws.Select
'1)

Set pointer = Range("A1").Offset(1, 1)

'Go through each value on the Pressure column in the corresponding composition section
' and stop when the corresponding pressure value is found
Set presP = pointer
While (P > presP.Value)
   Set presP = presP.Offset(1, 0)
Wend


'2)
'Calculate viscosity at 0 CO2
visc0 = ((P - presP.Offset(-1, 0).Value) / (presP.Value - presP.Offset(-1, 0).Value) *
(presP.Offset(0, 1).Value - presP.Offset(-1, 1).Value)) + presP.Offset(-1, 1).Value

'Calculate viscosity at desired CO2 comp
If (solu = 0) Then
visc = visc0
Else
visc = visc0 * (1 + ((-4.069 / 1000 * 30 + 0.2531) * C / solu))
End If
viscosity = visc


End Function
```

Table B-1 Calculation Results for Base Case

	Conventional Material Balance					Iteration 1		Iteration 2		Iteration 3		
Year	P (psia)	Gp (MMSCF)	Ginj (MMSCF)	We (MMSTB	Sw	P (psia)	We (MMSTB)	P (psia)	We (MMSTB)	P (psia)	We (MMSTB)	Sw
0.00	3000	0	0	0	0.2							
0.25	2958.17	1365	0	0.104	0.20							
0.50	2920.07	2730	0	0.319	0.20							
0.75	2884.54	4095	0	0.616	0.21							
1.00	2851.01	5460	0	0.979	0.21							
1.25	2819.05	6825	0	1.397	0.21							
1.49	2788.33	8190	0	1.860	0.22							
1.74	2758.57	9555	0	2.361	0.22							
1.99	2729.56	10920	0	2.895	0.22							
2.24	2701.12	12285	0	3.456	0.23							
2.49	2673.12	13650	0	4.040	0.23							
2.74	2645.43	15015	0	4.644	0.24							
2.99	2617.95	16380	0	5.266	0.25							
3.24	2590.62	17745	0	5.903	0.25							
3.49	2563.35	19110	0	6.553	0.26							
3.74	2536.09	20475	0	7.215	0.26							
3.99	2508.81	21840	0	7.889	0.27							
4.24	2481.44	23205	0	8.572	0.27							
4.48	2453.97	24570	0	9.265	0.28							
4.73	2426.36	25935	0	9.967	0.29							
4.98	2398.59	27300	0	10.677	0.29							
5.23	2370.62	28665	0	11.395	0.30							

Table B-1 Continued

	Conventional Material Balance					Iteration 1		Iteration 2		Iteration 3		
Year	P (psia)	Gp (MMSCF)	Ginj (MMSCF)	We (MMSTB	Sw	P (psia)	We (MMSTB)	P (psia)	We (MMSTB)	P (psia)	We (MMSTB)	Sw
5.48	2342.45	30030	0	12.120	0.30							
5.73	2314.04	31395	0	12.854	0.31							
5.98	2285.38	32760	0	13.595	0.32							
6.23	2256.46	34125	0	14.343	0.32							
6.48	2227.25	35490	0	15.099	0.33							
6.73	2197.74	36855	0	15.863	0.34							
6.98	2167.92	38220	0	16.634	0.34							
7.23	2137.76	39585	0	17.414	0.35							
7.47	2107.24	40950	0	18.201	0.36							
7.72	2076.36	42315	0	18.997	0.36							
7.97	2045.09	43680	0	19.801	0.37							
8.22	2013.42	45045	0	20.615	0.38							
8.47	1981.32	46410	0	21.437	0.38							
8.72	1948.77	47775	0	22.269	0.39							
8.97	1915.75	49140	0	23.110	0.40							
9.22	1882.23	50505	0	23.962	0.41							
9.47	1848.2	51870	0	24.824	0.41							
9.72	1813.62	53235	0	25.698	0.42							
9.97	1778.45	54600	0	26.583	0.43							
10.21	1742.68	55965	0	27.480	0.44							
10.46	1706.26	57330	0	28.390	0.44							

Table B-1 Continued

	Conventional Material Balance					Iteration 1		Iteration 2		Iteration 3		
Year	P (psia)	Gp (MMSCF)	Ginj (MMSCF)	We (MMSTB	Sw	P (psia)	We (MMSTB)	P (psia)	We (MMSTB)	P (psia)	We (MMSTB)	Sw
10.71	1669.16	58695	0	29.313	0.45							
10.96	1631.33	60060	0	30.250	0.46							
11.21	1592.73	61425	0	31.201	0.47							
11.46	1553.3	62790	0	32.169	0.48							
11.71	1512.99	64155	0	33.153	0.49							
11.96	1471.74	65520	0	34.154	0.49							
12.21	1429.48	66885	0	35.173	0.50							
12.46	1386.12	68250	0	36.212	0.51							
12.71	1341.59	69615	0	37.273	0.52							
12.96	1295.78	70980	0	38.355	0.53							
13.20	1248.57	72345	0	39.461	0.54							
13.45	1199.84	73710	0	40.594	0.55							
13.70	1149.44	75075	0	41.754	0.56							
13.95	1097.2	76440	0	42.944	0.57							
14.20	1042.9	77805	0	44.166	0.58							
14.45	986.315	79170	0	45.425	0.59							
14.70	927.151	80535	0	46.723	0.60							
14.95	865.056	81900	0	48.064	0.62							
15.20	799.607	83265	0	49.453	0.63							
15.45	730.27	84630	0	50.897	0.64							
15.70	656.369	85995	0	52.401	0.65							

Table B-1 Continued

	Conventional Material Balance					Iteration 1		Iteration 2		Iteration 3		
Year	P (psia)	Gp (MMSCF)	Ginj (MMSCF)	We (MMSTB	Sw	P (psia)	We (MMSTB)	P (psia)	We (MMSTB)	P (psia)	We (MMSTB)	Sw
15.95	577.027	87360	0	53.975	0.67							
16.19	697.902	87360	1365	55.165	0.68							
16.44	810.676	87360	2730	55.852	0.68							
16.69	914.075	87360	4095	56.167	0.69							
16.94	1007.33	87360	5460	56.183	0.69	1007.330	56.183	1007.330	56.183	1007.330	56.183	0.69
17.19	1090.53	87360	6825	55.959	0.68	1081.202	55.964	1081.322	55.964	1081.360	55.964	0.68
17.44	1164.37	87360	8190	55.548	0.68	1148.639	55.580	1148.844	55.580	1148.909	55.580	0.68
17.69	1229.87	87360	9555	54.991	0.67	1210.201	55.070	1210.460	55.069	1210.539	55.070	0.68
17.94	1288.14	87360	10920	54.325	0.67	1266.571	54.463	1266.890	54.462	1266.979	54.461	0.67
18.19	1340.27	87360	12285	53.577	0.66	1318.411	53.784	1318.750	53.782	1318.849	53.781	0.66
18.44	1387.26	87360	13650	52.771	0.66	1366.251	53.054	1366.600	53.051	1366.709	53.050	0.66
18.69	1429.96	87360	15015	51.925	0.65	1410.661	52.289	1411.000	52.285	1411.099	52.283	0.65
18.93	1469.09	87360	16380	51.053	0.64	1452.111	51.501	1452.430	51.496	1452.519	51.494	0.64
19.18	1505.26	87360	17745	50.166	0.63	1491.021	50.702	1491.310	50.694	1491.389	50.692	0.64
19.43	1538.97	87360	19110	49.272	0.62	1527.741	49.897	1527.990	49.888	1528.069	49.886	0.63
19.68	1570.6	87360	20475	48.379	0.62	1562.571	49.094	1562.780	49.083	1562.839	49.081	0.62
19.93	1600.5	87360	21840	47.490	0.61	1595.741	48.297	1595.910	48.285	1595.969	48.282	0.62
20.18	1628.91	87360	23205	46.611	0.60	1627.491	47.509	1627.620	47.496	1627.659	47.492	0.61
20.43	1656.07	87360	24570	45.743	0.59	1657.971	46.734	1658.050	46.718	1658.079	46.714	0.60
20.68	1682.14	87360	25935	44.889	0.59	1687.321	45.972	1687.370	45.954	1687.389	45.950	0.60
20.93	1707.26	87360	27300	44.049	0.58	1715.691	45.224	1715.680	45.205	1715.689	45.200	0.59

Table B-1 Continued

	Conventional Material Balance					Iteration 1		Iteration 2		Iteration 3		
Year	P (psia)	Gp (MMSCF)	Ginj (MMSCF)	We (MMSTB	Sw	P (psia)	We (MMSTB)	P (psia)	We (MMSTB)	P (psia)	We (MMSTB)	Sw
21.18	1731.56	87360	28665	43.224	0.57	1743.161	44.491	1743.110	44.471	1743.099	44.465	0.58
21.43	1755.13	87360	30030	42.416	0.57	1769.821	43.774	1769.730	43.752	1769.709	43.747	0.58
21.68	1778.05	87360	31395	41.625	0.56	1795.751	43.074	1795.620	43.050	1795.589	43.044	0.57
21.92	1800.4	87360	32760	40.849	0.55	1821.011	42.388	1820.840	42.364	1820.799	42.357	0.56
22.17	1822.22	87360	34125	40.090	0.55	1845.661	41.719	1845.450	41.692	1845.399	41.685	0.56
22.42	1843.58	87360	35490	39.346	0.54	1869.741	41.065	1869.490	41.037	1869.429	41.029	0.55
22.67	1864.51	87360	36855	38.618	0.53	1893.311	40.425	1893.020	40.396	1892.949	40.388	0.55
22.92	1885.05	87360	38220	37.905	0.53	1916.391	39.800	1916.060	39.769	1915.979	39.761	0.54
23.17	1905.23	87360	39585	37.206	0.52	1939.021	39.189	1938.660	39.156	1938.569	39.147	0.54
23.42	1925.08	87360	40950	36.522	0.51	1961.231	38.591	1960.840	38.557	1960.739	38.548	0.53
23.67	1944.62	87360	42315	35.851	0.51	1983.051	38.006	1982.630	37.970	1982.519	37.961	0.53
23.92	1963.89	87360	43680	35.192	0.50	2004.511	37.433	2004.050	37.396	2003.929	37.386	0.52
24.17	1982.9	87360	45045	34.546	0.50	2025.621	36.871	2025.140	36.833	2025.009	36.823	0.52
24.42	2001.68	87360	46410	33.912	0.49	2046.411	36.321	2045.900	36.282	2045.769	36.271	0.51
24.67	2020.23	87360	47775	33.289	0.49	2066.911	35.781	2066.370	35.741	2066.229	35.729	0.51
24.91	2038.58	87360	49140	32.676	0.48	2087.131	35.252	2086.560	35.209	2086.409	35.198	0.50
25.16	2056.74	87360	50505	32.074	0.48	2107.081	34.732	2106.490	34.688	2106.329	34.676	0.50
25.41	2074.74	87360	51870	31.481	0.47	2126.791	34.220	2126.170	34.175	2126.009	34.163	0.49
25.66	2092.58	87360	53235	30.897	0.47	2146.281	33.718	2145.640	33.672	2145.459	33.659	0.49
25.91	2110.28	87360	54600	30.322	0.46	2165.561	33.223	2164.890	33.176	2164.709	33.163	0.49
26.16	2127.86	87360	55965	29.754	0.46	2184.641	32.736	2183.950	32.688	2183.769	32.675	0.48

Table B-1 Continued

	Conventional Material Balance					Iteration 1		Iteration 2		Iteration 3		
Year	P (psia)	Gp (MMSCF)	Ginj (MMSCF)	We (MMSTB	Sw	P (psia)	We (MMSTB)	P (psia)	We (MMSTB)	P (psia)	We (MMSTB)	Sw
26.41	2145.34	87360	57330	29.194	0.45	2203.551	32.257	2202.840	32.207	2202.649	32.193	0.48
26.66	2162.71	87360	58695	28.641	0.45	2222.301	31.784	2221.570	31.733	2221.369	31.719	0.47
26.91	2180.01	87360	60060	28.095	0.44	2240.901	31.317	2240.150	31.265	2239.949	31.250	0.47
27.16	2197.25	87360	61425	27.554	0.44	2259.371	30.856	2258.600	30.803	2258.399	30.788	0.46
27.41	2214.44	87360	62790	27.020	0.43	2277.731	30.401	2276.950	30.346	2276.739	30.331	0.46
27.66	2231.61	87360	64155	26.490	0.43	2296.001	29.951	2295.190	29.895	2294.979	29.880	0.46
27.90	2248.76	87360	65520	25.964	0.42	2314.181	29.505	2313.360	29.448	2313.139	29.433	0.45
28.15	2265.91	87360	66885	25.443	0.42	2332.301	29.064	2331.460	29.006	2331.239	28.990	0.45
28.40	2283.09	87360	68250	24.926	0.41	2350.371	28.627	2349.520	28.567	2349.299	28.551	0.45
28.65	2300.32	87360	69615	24.411	0.41	2368.421	28.193	2367.560	28.132	2367.329	28.115	0.44
28.90	2305.91	87360	70980	23.924	0.41	2386.461	27.761	2385.590	27.699	2385.349	27.682	0.44
29.15	2307.91	87360	72345	23.486	0.40	2404.511	27.332	2403.630	27.269	2403.389	27.251	0.43
29.40	2325.29	87360	73710	23.050	0.40	2422.611	26.906	2421.710	26.841	2421.469	26.824	0.43
29.65	2342.24	87360	75075	22.606	0.39	2440.761	26.482	2439.860	26.416	2439.619	26.398	0.43
29.90	2358.92	87360	76440	22.159	0.39	2459.001	26.059	2458.090	25.992	2457.849	25.973	0.42
30.15	2375.37	87360	77805	21.709	0.39	2461.021	25.672	2458.920	25.608	2458.349	25.590	0.42
30.40	2391.61	87360	79170	21.259	0.38	2468.011	25.329	2467.040	25.263	2466.779	25.245	0.42
30.64	2407.67	87360	80535	20.808	0.38	2486.051	24.974	2485.050	24.906	2484.779	24.888	0.41
30.89	2423.58	87360	81900	20.357	0.37	2503.771	24.612	2502.750	24.543	2502.469	24.524	0.41
31.14	2439.34	87360	83265	19.907	0.37	2521.241	24.246	2520.200	24.175	2519.919	24.156	0.41
31.39	2454.97	87360	84630	19.457	0.37	2538.501	23.876	2537.440	23.804	2537.149	23.785	0.40

Table B-1 Continued

	Conventional Material Balance					Iteration 1		Iteration 2		Iteration 3		
Year	P (psia)	Gp (MMSCF)	Ginj (MMSCF)	We (MMSTB	Sw	P (psia)	We (MMSTB)	P (psia)	We (MMSTB)	P (psia)	We (MMSTB)	Sw
31.64	2470.48	87360	85995	19.009	0.36	2555.581	23.504	2554.490	23.431	2554.199	23.411	0.40
31.89	2485.89	87360	87360	18.562	0.36	2572.491	23.130	2571.390	23.056	2571.089	23.036	0.40
32.14	2501.21	87360	88725	18.116	0.36	2589.271	22.756	2588.140	22.681	2587.839	22.660	0.39
32.39	2516.43	87360	90090	17.672	0.35	2605.921	22.380	2604.780	22.305	2604.469	22.284	0.39
32.64	2531.58	87360	91455	17.229	0.35	2622.461	22.005	2621.300	21.929	2620.989	21.908	0.39
32.89	2546.66	87360	92820	16.788	0.34	2638.911	21.630	2637.720	21.553	2637.409	21.531	0.39
33.14	2561.66	87360	94185	16.349	0.34	2655.261	21.256	2654.060	21.177	2653.739	21.155	0.38
33.39	2576.61	87360	95550	15.911	0.34	2671.551	20.881	2670.330	20.802	2669.999	20.780	0.38
33.63	2591.49	87360	96915	15.475	0.33	2687.761	20.508	2686.520	20.428	2686.189	20.406	0.38
33.88	2606.32	87360	98280	15.041	0.33	2703.911	20.135	2702.650	20.054	2702.309	20.032	0.37
34.13	2621.1	87360	99645	14.608	0.33	2720.001	19.764	2718.720	19.681	2718.379	19.659	0.37
34.38	2635.84	87360	101010	14.176	0.32	2736.041	19.393	2734.750	19.310	2734.399	19.287	0.37
34.63	2650.53	87360	102375	13.747	0.32	2752.031	19.023	2750.720	18.939	2750.369	18.916	0.36
34.88	2665.18	87360	103740	13.318	0.31	2767.991	18.654	2766.660	18.568	2766.299	18.545	0.36
35.13	2679.79	87360	105105	12.892	0.31	2783.901	18.285	2782.550	18.199	2782.189	18.176	0.36
35.38	2694.37	87360	106470	12.466	0.31	2799.781	17.918	2798.420	17.831	2798.049	17.807	0.35
35.63	2708.91	87360	107835	12.042	0.30	2815.631	17.551	2814.250	17.464	2813.869	17.440	0.35
35.88	2723.42	87360	109200	11.620	0.30	2831.461	17.186	2830.050	17.097	2829.669	17.073	0.35
36.13	2737.9	87360	110565	11.198	0.30	2847.251	16.821	2845.830	16.731	2845.439	16.707	0.34
36.38	2752.35	87360	111930	10.778	0.29	2863.021	16.457	2861.580	16.366	2861.189	16.341	0.34
36.62	2766.77	87360	113295	10.359	0.29	2878.771	16.093	2877.310	16.002	2876.919	15.977	0.34

Table B-1 Continued

	Conventional Material Balance					Iteration 1		Iteration 2		Iteration 3		
Year	P (psia)	Gp (MMSCF)	Ginj (MMSCF)	We (MMSTB	Sw	P (psia)	We (MMSTB)	P (psia)	We (MMSTB)	P (psia)	We (MMSTB)	Sw
36.87	2781.17	87360	114660	9.941	0.29	2894.511	15.730	2893.030	15.638	2892.629	15.613	0.33
37.12	2795.55	87360	116025	9.524	0.28	2910.221	15.368	2908.720	15.275	2908.319	15.250	0.33
37.37	2809.9	87360	117390	9.108	0.28	2925.921	15.007	2924.400	14.913	2923.989	14.887	0.33
37.62	2824.23	87360	118755	8.693	0.27	2941.611	14.646	2940.070	14.551	2939.659	14.525	0.32
37.87	2838.55	87360	120120	8.279	0.27	2957.291	14.285	2955.730	14.190	2955.309	14.164	0.32
38.12	2852.84	87360	121485	7.866	0.27	2972.961	13.925	2971.380	13.829	2970.949	13.803	0.32
38.37	2867.12	87360	122850	7.454	0.26	2988.621	13.566	2987.010	13.469	2986.579	13.442	0.32
38.62	2881.38	87360	124215	7.042	0.26	3004.271	13.206	3002.650	13.109	3002.209	13.082	0.31
38.87	2895.63	87360	125580	6.631	0.26							
39.12	2909.86	87360	126945	6.221	0.25							
39.36	2924.08	87360	128310	5.812	0.25							
39.61	2938.29	87360	129675	5.403	0.25							
39.86	2952.49	87360	131040	4.995	0.24							
40.11	2966.67	87360	132405	4.588	0.24							
40.36	2980.85	87360	133770	4.181	0.24							
40.61	2995.02	87360	135135	3.774	0.23							
40.86	3009.18	87360	136500	3.368	0.23							

Table B-2 Calculation Results for Base Case with Changing Viscosity

	Conventional Material Balance					Iteration 1		Iteration 2		Iteration 3		
Year	P (psia)	Gp (MMSCF)	Ginj (MMSCF)	We (MMSTB)	Sw	P (psia)	We (MMSTB)	P (psia)	We (MMSTB)	P (psia)	We (MMSTB)	Sw
0.00	3000	0	0	0.000	0.20							
0.25	2958.17	1365	0	0.104	0.20							
0.50	2920.07	2730	0	0.319	0.20							
0.75	2884.54	4095	0	0.616	0.21							
1.00	2851.01	5460	0	0.979	0.21							
1.25	2819.05	6825	0	1.397	0.21							
1.49	2788.33	8190	0	1.860	0.22							
1.74	2758.57	9555	0	2.361	0.22							
1.99	2729.56	10920	0	2.895	0.22							
2.24	2701.12	12285	0	3.456	0.23							
2.49	2673.12	13650	0	4.040	0.23							
2.74	2645.43	15015	0	4.644	0.24							
2.99	2617.95	16380	0	5.266	0.25							
3.24	2590.62	17745	0	5.903	0.25							
3.49	2563.35	19110	0	6.553	0.26							
3.74	2536.09	20475	0	7.215	0.26							
3.99	2508.81	21840	0	7.889	0.27							
4.24	2481.44	23205	0	8.572	0.27							
4.48	2453.97	24570	0	9.265	0.28							
4.73	2426.36	25935	0	9.967	0.29							
4.98	2398.59	27300	0	10.677	0.29							
5.23	2370.62	28665	0	11.395	0.30							
5.48	2342.45	30030	0	12.120	0.30							
5.73	2314.04	31395	0	12.854	0.31							
5.98	2285.38	32760	0	13.595	0.32							
6.23	2256.46	34125	0	14.343	0.32							
6.48	2227.25	35490	0	15.099	0.33							
6.73	2197.74	36855	0	15.863	0.34							
6.98	2167.92	38220	0	16.634	0.34							

Table B-2 Continued

	Conventional Material Balance					Iteration 1		Iteration 2		Iteration 3		
Year	P (psia)	Gp (MMSCF)	Ginj (MMSCF)	We (MMSTB)	Sw	P (psia)	We (MMSTB)	P (psia)	We (MMSTB)	P (psia)	We (MMSTB)	Sw
7.23	2137.76	39585	0	17.414	0.35							
7.47	2107.24	40950	0	18.201	0.36							
7.72	2076.36	42315	0	18.997	0.36							
7.97	2045.09	43680	0	19.801	0.37							
8.22	2013.42	45045	0	20.615	0.38							
8.47	1981.32	46410	0	21.437	0.38							
8.72	1948.77	47775	0	22.269	0.39							
8.97	1915.75	49140	0	23.110	0.40							
9.22	1882.23	50505	0	23.962	0.41							
9.47	1848.2	51870	0	24.824	0.41							
9.72	1813.62	53235	0	25.698	0.42							
9.97	1778.45	54600	0	26.583	0.43							
10.21	1742.68	55965	0	27.480	0.44							
10.46	1706.26	57330	0	28.390	0.44							
10.71	1669.16	58695	0	29.313	0.45							
10.96	1631.33	60060	0	30.250	0.46							
11.21	1592.73	61425	0	31.201	0.47							
11.46	1553.3	62790	0	32.169	0.48							
11.71	1512.99	64155	0	33.153	0.49							
11.96	1471.74	65520	0	34.154	0.49							
12.21	1429.48	66885	0	35.173	0.50							
12.46	1386.12	68250	0	36.212	0.51							
12.71	1341.59	69615	0	37.273	0.52							
12.96	1295.78	70980	0	38.355	0.53							
13.20	1248.57	72345	0	39.461	0.54							
13.45	1199.84	73710	0	40.594	0.55							
13.70	1149.44	75075	0	41.754	0.56							
13.95	1097.2	76440	0	42.944	0.57							

Table B-2 Continued

	Conventional Material Balance					Iteration 1		Iteration 2		Iteration 3		
Year	P (psia)	Gp (MMSCF)	Ginj (MMSCF)	We (MMSTB)	Sw	P (psia)	We (MMSTB)	P (psia)	We (MMSTB)	P (psia)	We (MMSTB)	Sw
13.95	1097.2	76440	0	42.944	0.57							
14.20	1042.9	77805	0	44.166	0.58							
14.45	986.315	79170	0	45.425	0.59							
14.70	927.151	80535	0	46.723	0.60							
14.95	865.056	81900	0	48.064	0.62							
15.20	799.607	83265	0	49.453	0.63							
15.45	730.27	84630	0	50.897	0.64							
15.70	656.369	85995	0	52.401	0.65							
15.95	577.027	87360	0	53.975	0.67							
16.19	697.902	87360	1365	55.165	0.68							
16.44	810.676	87360	2730	55.852	0.68							
16.69	914.075	87360	4095	56.167	0.69							
16.94	1007.33	87360	5460	56.183	0.69	1007.33	56.183	1007.33	56.183	1007.33	56.183	0.69
17.19	1090.53	87360	6825	55.959	0.68	1081.374	55.976	1081.452	55.977	1081.36	55.964	0.68
17.44	1164.37	87360	8190	55.548	0.68	1149.028	55.606	1149.159	55.606	1148.909	55.580	0.68
17.69	1229.87	87360	9555	54.991	0.67	1210.824	55.108	1210.988	55.108	1210.539	55.070	0.68
17.94	1288.14	87360	10920	54.325	0.67	1267.424	54.513	1267.638	54.512	1266.979	54.461	0.67
18.19	1340.27	87360	12285	53.577	0.66	1319.494	53.844	1319.728	53.843	1318.849	53.781	0.66
18.44	1387.26	87360	13650	52.771	0.66	1367.554	53.124	1367.788	53.122	1366.709	53.050	0.66
18.69	1429.96	87360	15015	51.925	0.65	1412.154	52.367	1412.378	52.364	1411.099	52.283	0.65
18.93	1469.09	87360	16380	51.053	0.64	1453.774	51.587	1453.978	51.583	1452.519	51.494	0.64
19.18	1505.26	87360	17745	50.166	0.63	1492.814	50.793	1493.008	50.788	1491.389	50.692	0.64
19.43	1538.97	87360	19110	49.272	0.62	1529.654	49.994	1529.828	49.988	1528.069	49.886	0.63
19.68	1570.6	87360	20475	48.379	0.62	1564.574	49.195	1564.718	49.188	1562.839	49.081	0.62
19.93	1600.5	87360	21840	47.490	0.61	1597.824	48.402	1597.948	48.394	1595.969	48.282	0.62
20.18	1628.91	87360	23205	46.611	0.60	1629.634	47.616	1629.718	47.608	1627.659	47.492	0.61
20.43	1656.07	87360	24570	45.743	0.59	1660.154	46.843	1660.208	46.833	1658.079	46.714	0.60
20.68	1682.14	87360	25935	44.889	0.59	1689.544	46.082	1689.578	46.071	1687.389	45.950	0.60

Table B-2 Continued

	Conventional Material Balance					Iteration 1		Iteration 2		Iteration 3		
Year	P (psia)	Gp (MMSCF)	Ginj (MMSCF)	We (MMSTB)	Sw	P (psia)	We (MMSTB)	P (psia)	We (MMSTB)	P (psia)	We (MMSTB)	Sw
20.93	1707.26	87360	27300	44.049	0.58	1717.934	45.336	1717.928	45.323	1715.689	45.200	0.59
21.18	1731.56	87360	28665	43.224	0.57	1745.414	44.604	1745.388	44.591	1743.099	44.465	0.58
21.43	1755.13	87360	30030	42.416	0.57	1772.074	43.888	1772.028	43.873	1769.709	43.747	0.58
21.68	1778.05	87360	31395	41.625	0.56	1798.004	43.187	1797.928	43.172	1795.589	43.044	0.57
21.92	1800.4	87360	32760	40.849	0.55	1823.264	42.502	1823.158	42.486	1820.799	42.357	0.56
22.17	1822.22	87360	34125	40.090	0.55	1847.904	41.832	1847.768	41.815	1845.399	41.685	0.56
22.42	1843.58	87360	35490	39.346	0.54	1871.974	41.177	1871.818	41.159	1869.429	41.029	0.55
22.67	1864.51	87360	36855	38.618	0.53	1895.534	40.538	1895.338	40.518	1892.949	40.388	0.55
22.92	1885.05	87360	38220	37.905	0.53	1918.594	39.912	1918.378	39.892	1915.979	39.761	0.54
23.17	1905.23	87360	39585	37.206	0.52	1941.214	39.300	1940.968	39.279	1938.569	39.147	0.54
23.42	1925.08	87360	40950	36.522	0.51	1963.404	38.701	1963.148	38.679	1960.739	38.548	0.53
23.67	1944.62	87360	42315	35.851	0.51	1985.214	38.115	1984.928	38.092	1982.519	37.961	0.53
23.92	1963.89	87360	43680	35.192	0.50	2006.644	37.542	2006.348	37.517	2003.929	37.386	0.52
24.17	1982.9	87360	45045	34.546	0.50	2027.744	36.980	2027.418	36.954	2025.009	36.823	0.52
24.42	2001.68	87360	46410	33.912	0.49	2048.524	36.428	2048.178	36.402	2045.769	36.271	0.51
24.67	2020.23	87360	47775	33.289	0.49	2069.004	35.888	2068.638	35.861	2066.229	35.729	0.51
24.91	2038.58	87360	49140	32.676	0.48	2089.204	35.357	2088.818	35.329	2086.409	35.198	0.50
25.16	2056.74	87360	50505	32.074	0.48	2109.144	34.837	2108.738	34.808	2106.329	34.676	0.50
25.41	2074.74	87360	51870	31.481	0.47	2128.834	34.325	2128.418	34.294	2126.009	34.163	0.49
25.66	2092.58	87360	53235	30.897	0.47	2148.314	33.821	2147.878	33.790	2145.459	33.659	0.49
25.91	2110.28	87360	54600	30.322	0.46	2167.574	33.326	2167.128	33.295	2164.709	33.163	0.49
26.16	2127.86	87360	55965	29.754	0.46	2186.644	32.839	2186.178	32.806	2183.769	32.675	0.48
26.41	2145.34	87360	57330	29.194	0.45	2205.544	32.358	2205.068	32.325	2202.649	32.193	0.48
26.66	2162.71	87360	58695	28.641	0.45	2224.284	31.885	2223.788	31.850	2221.369	31.719	0.47
26.91	2180.01	87360	60060	28.095	0.44	2242.874	31.417	2242.368	31.382	2239.949	31.250	0.47
27.16	2197.25	87360	61425	27.554	0.44	2261.334	30.956	2260.818	30.920	2258.399	30.788	0.46
27.41	2214.44	87360	62790	27.020	0.43	2279.694	30.500	2279.158	30.463	2276.739	30.331	0.46
27.66	2231.61	87360	64155	26.490	0.43	2297.944	30.049	2297.408	30.012	2294.979	29.880	0.46

Table B-2 Continued

	Conventional Material Balance					Iteration 1		Iteration 2		Iteration 3		
Year	P (psia)	Gp (MMSCF)	Ginj (MMSCF)	We (MMSTB)	Sw	P (psia)	We (MMSTB)	P (psia)	We (MMSTB)	P (psia)	We (MMSTB)	Sw
27.90	2248.76	87360	65520	25.964	0.42	2316.124	29.603	2315.568	29.565	2313.139	29.433	0.45
28.15	2265.91	87360	66885	25.443	0.42	2334.234	29.161	2333.678	29.122	2331.239	28.990	0.45
28.40	2283.09	87360	68250	24.926	0.41	2352.304	28.724	2351.738	28.684	2349.299	28.551	0.45
28.65	2300.32	87360	69615	24.411	0.41	2370.354	28.289	2369.778	28.248	2367.329	28.115	0.44
28.90	2305.91	87360	70980	23.924	0.41	2388.394	27.857	2387.808	27.815	2385.349	27.682	0.44
29.15	2307.91	87360	72345	23.486	0.40	2406.454	27.427	2405.858	27.385	2403.389	27.251	0.43
29.40	2325.29	87360	73710	23.050	0.40	2424.544	27.001	2423.938	26.957	2421.469	26.824	0.43
29.65	2342.24	87360	75075	22.606	0.39	2442.704	26.576	2442.088	26.532	2439.619	26.398	0.43
29.90	2358.92	87360	76440	22.159	0.39	2460.944	26.153	2460.338	26.108	2457.849	25.973	0.42
30.15	2375.37	87360	77805	21.709	0.39	2462.174	25.768	2460.748	25.725	2458.349	25.590	0.42
30.40	2391.61	87360	79170	21.259	0.38	2469.904	25.423	2469.258	25.379	2466.779	25.245	0.42
30.64	2407.67	87360	80535	20.808	0.38	2487.924	25.067	2487.248	25.022	2484.779	24.888	0.41
30.89	2423.58	87360	81900	20.357	0.37	2505.634	24.704	2504.938	24.658	2502.469	24.524	0.41
31.14	2439.34	87360	83265	19.907	0.37	2523.094	24.337	2522.388	24.290	2519.919	24.156	0.41
31.39	2454.97	87360	84630	19.457	0.37	2540.344	23.967	2539.628	23.919	2537.149	23.785	0.40
31.64	2470.48	87360	85995	19.009	0.36	2557.414	23.595	2556.678	23.546	2554.199	23.411	0.40
31.89	2485.89	87360	87360	18.562	0.36	2574.334	23.220	2573.578	23.171	2571.089	23.036	0.40
32.14	2501.21	87360	88725	18.116	0.36	2591.104	22.846	2590.338	22.796	2587.839	22.660	0.39
32.39	2516.43	87360	90090	17.672	0.35	2607.754	22.471	2606.978	22.420	2604.469	22.284	0.39
32.64	2531.58	87360	91455	17.229	0.35	2624.294	22.095	2623.508	22.044	2620.989	21.908	0.39
32.89	2546.66	87360	92820	16.788	0.34	2640.744	21.720	2639.938	21.668	2637.409	21.531	0.39
33.14	2561.66	87360	94185	16.349	0.34	2657.094	21.345	2656.288	21.292	2653.739	21.155	0.38
33.39	2576.61	87360	95550	15.911	0.34	2673.384	20.971	2672.558	20.917	2669.999	20.780	0.38
33.63	2591.49	87360	96915	15.475	0.33	2689.594	20.597	2688.758	20.543	2686.189	20.406	0.38
33.88	2606.32	87360	98280	15.041	0.33	2705.744	20.225	2704.898	20.170	2702.309	20.032	0.37
34.13	2621.1	87360	99645	14.608	0.33	2721.834	19.853	2720.978	19.797	2718.379	19.659	0.37
34.38	2635.84	87360	101010	14.176	0.32	2737.884	19.482	2737.008	19.426	2734.399	19.287	0.37
34.63	2650.53	87360	102375	13.747	0.32	2753.874	19.112	2752.988	19.055	2750.369	18.916	0.36

Table B-2 Continued

	Conventional Material Balance					Iteration 1		Iteration 2		Iteration 3		
Year	P (psia)	Gp (MMSCF)	Ginj (MMSCF)	We (MMSTB)	Sw	P (psia)	We (MMSTB)	P (psia)	We (MMSTB)	P (psia)	We (MMSTB)	Sw
34.88	2665.18	87360	103740	13.318	0.31	2769.834	18.742	2768.928	18.685	2766.299	18.545	0.36
35.13	2679.79	87360	105105	12.892	0.31	2785.744	18.374	2784.838	18.316	2782.189	18.176	0.36
35.38	2694.37	87360	106470	12.466	0.31	2801.634	18.006	2800.708	17.948	2798.049	17.807	0.35
35.63	2708.91	87360	107835	12.042	0.30	2817.484	17.640	2816.548	17.580	2813.869	17.440	0.35
35.88	2723.42	87360	109200	11.620	0.30	2833.304	17.274	2832.358	17.214	2829.669	17.073	0.35
36.13	2737.9	87360	110565	11.198	0.30	2849.104	16.909	2848.138	16.848	2845.439	16.707	0.34
36.38	2752.35	87360	111930	10.778	0.29	2864.874	16.544	2863.898	16.483	2861.189	16.341	0.34
36.62	2766.77	87360	113295	10.359	0.29	2880.634	16.181	2879.638	16.119	2876.919	15.977	0.34
36.87	2781.17	87360	114660	9.941	0.29	2896.364	15.818	2895.358	15.756	2892.629	15.613	0.33
37.12	2795.55	87360	116025	9.524	0.28	2912.084	15.456	2911.068	15.393	2908.319	15.250	0.33
37.37	2809.9	87360	117390	9.108	0.28	2927.784	15.094	2926.758	15.031	2923.989	14.887	0.33
37.62	2824.23	87360	118755	8.693	0.27	2943.474	14.733	2942.428	14.669	2939.659	14.525	0.32
37.87	2838.55	87360	120120	8.279	0.27	2959.154	14.372	2958.098	14.308	2955.309	14.164	0.32
38.12	2852.84	87360	121485	7.866	0.27	2974.824	14.012	2973.758	13.947	2970.949	13.803	0.32
38.37	2867.12	87360	122850	7.454	0.26	2990.484	13.652	2989.398	13.587	2986.579	13.442	0.32
38.62	2881.38	87360	124215	7.042	0.26	3006.144	13.293	3005.038	13.227	3002.209	13.082	0.31
38.87	2895.63	87360	125580	6.631	0.26							
39.12	2909.86	87360	126945	6.221	0.25							
39.36	2924.08	87360	128310	5.812	0.25							
39.61	2938.29	87360	129675	5.403	0.25							
39.86	2952.49	87360	131040	4.995	0.24							
40.11	2966.67	87360	132405	4.588	0.24							
40.36	2980.85	87360	133770	4.181	0.24							
40.61	2995.02	87360	135135	3.774	0.23							
40.86	3009.18	87360	136500	3.368	0.23							